

UPWATER

UNDERSTANDING GROUNDWATER POLLUTION TO PROTECT AND
ENHANCE WATER QUALITY

DELIVERABLE D5.2

FINAL REPORT ON GROUNDWATER RISK ASSESSMENT



Funded by
the European Union

| | |
|--------------------------------------|--|
| Dissemination level | Public |
| Issued by | Ineris |
| Contributing project partners | Ineris – AU – IDAEA– NTUA |
| Author(s) | Michel-Malfait, J., Bour, O., Thaysen, E.M. |
| Reviewed by | Domènech, C. Thaysen, E.M., Offermann, M., Bester, K. |
| Keywords | Groundwater vulnerability, intrinsic vulnerability, specific vulnerability, pesticides, PFAS, pollutant mobility, EU priority list recommendation, groundwater risk assessment |
| Number of pages | 109 |
| Number of annexes | 4 |
| Date: | 2026-01-29 |
| Version: | V 1 |
| Deliverable number | D5.2 |
| Work Package number: | WP5 |
| Status: | Delivered |
| Approved by coordinator | 2026-01-29 |

COPYRIGHT NOTICES

© 2026 UPWATER Consortium Partners. All rights reserved. UPWATER is funded under the European Union, Grant agreement No 101081807. For more information on the project, its partners, and contributors please see www.upwater.eu. You are permitted to copy and distribute verbatim copies of this document, containing this copyright notice, but modifying this document is not allowed. All contents are reserved by default and may not be disclosed to third parties without the written consent of the UPWATER partners, except as mandated by the European Commission contract, for reviewing and dissemination purposes. All trademarks and other rights on third party products mentioned in this document are acknowledged and owned by the respective holders.

The information contained in this document represents the views of UPWATER members as of the date they are published. The UPWATER consortium does not guarantee that any information contained herein is error-free, or up to date, nor makes warranties, express, implied, or statutory, by publishing this document. The information in this document is provided as is and no guarantee or warranty is given that the information is fit for any particular purpose. The user thereof uses the information at its sole risk and liability.

Funded by the European Union. Views and opinions expressed are however those of the author(s) only and do not necessarily reflect those of the European Union or the granting authority European Research Executive Agency (REA). Neither the European Union nor the granting authority can be held responsible for them.

HOW TO CITE THIS DOCUMENT

Michel, J., Bour, O., Thaysen, E.M., 2026: D5.2 – Final report on groundwater risk assessment. 109 p, UPWATER project funded by the European Union – No 101081807

REVISION HISTORY

| Version | Reason for changes | Name | Date |
|---------|------------------------|--------|-----------|
| 1 | Original release to EU | Ineris | 29.1.2026 |
| | | | |
| | | | |
| | | | |
| | | | |

CONTENT

| | | |
|-------|---|----|
| 1 | Context and aim of the groundwater risk assessment | 10 |
| 1.1 | EU Project UPWATER | 10 |
| 1.2 | Objectives | 10 |
| 1.3 | Groundwater risk assessment | 11 |
| 1.4 | Pollutant priority list | 12 |
| 2 | Groundwater risk assessment methodology | 13 |
| 3 | Groundwater risk assessment in relation to the Stengården case study | 15 |
| 3.1 | Intrinsic vulnerability | 15 |
| 3.2 | Specific vulnerability | 15 |
| 3.2.1 | Pollutants considered in the frame of the groundwater risk assessment | 15 |
| 3.2.2 | Material and methods | 16 |
| 3.2.3 | Results | 20 |
| 3.3 | Conclusion on the groundwater risk assessment at the Stengården case study | 31 |
| 4 | Groundwater risk assessment in relation to the Besòs case study | 32 |
| 4.1 | Intrinsic vulnerability | 32 |
| 4.2 | Specific vulnerability | 32 |
| 4.2.1 | Pollutants considered in the frame of the groundwater risk assessment | 32 |
| 4.2.2 | Material and methods | 33 |
| 4.2.3 | Results of the specific vulnerability assessment | 44 |
| 4.3 | Conclusion on the groundwater risk assessment at the Besòs case study | 53 |
| 5 | Groundwater risk assessment in relation to the Athens case study | 54 |
| 5.1 | Intrinsic vulnerability | 54 |
| 5.2 | Specific vulnerability | 56 |
| 5.2.1 | Pollutants considered in the frame of the groundwater risk assessment | 56 |
| 5.2.2 | Material and methods | 57 |
| 5.2.3 | Results | 61 |
| 5.3 | Conclusion on the groundwater risk assessment at the Athens case study | 72 |
| 6 | Pollutant priority lists | 73 |
| 6.1 | Confirmation of current priority list (IDAEA, IWW-FO) | 73 |
| 6.2 | Recommendation for uptake into the current priority list (IDAEA, IWW-FO) | 76 |
| 6.3 | Recommendation for further research into chemical PMT properties (IDAEA, IWW-FO) | 78 |
| 6.4 | Potential pollution sources (IDAEA, IWW-FO, AU) | 84 |
| 7 | Identification of risk mitigation measures to meet targeted ecological environmental protection goals (IDAEA) | 85 |

| | | |
|---|----------------------------------|----|
| 8 | Conclusion and perspectives..... | 86 |
| 9 | References | 88 |

LIST OF ABBREVIATIONS

| Abbreviation | Definition |
|--------------|--|
| AU | Aarhus university |
| DCPP | Dichlorprop |
| HCS | Hydrogeological complex and settings |
| GVA | Groundwater vulnerability assessment |
| GW | Groundwater |
| IDAEA | Institute of Environmental Assessment and Water Research |
| Ineris | French national institute for industrial environment and risks |
| IWW-FO | Institut für Wasserforschung gemeinnützige GmbH |
| K_D | partition coefficient |
| MCPP | Mecoprop |
| MCPP_sulf | Mecoprop sulphate |
| MS | Matrix systems |
| NTUA | National technical university of Athens |
| N,N-DMSF | N,N-Dimethylsulfamide |
| PCSM | Point count system models |
| PFAS | Per- and polyfluoroalkyl substances |
| PFBA | Perfluoro-n-butanoic acid |
| PFBS | Perfluorobutane sulfonic acid |
| PFCA | Perfluoroalkyl carboxylic acids |
| PFDA | Perfluoro-n-decanoic acid |
| PFDoA | Perfluoro-n-dodecanoic acid |
| PFDoDS | Perfluorododecane sulfonic acid |
| PFDS | Perfluorodecane sulfonic acid |
| PFHpA | Perfluoro-n-heptanoic acid |
| PFHxA | Perfluoro-n-hexanoic acid |
| PFHxS | Perfluorohexane sulfonic acid |
| PFHpS | Perfluoroheptane sulfonic acid |
| PFNA | Perfluoro-n-nonanoic acid |
| PFNS | Perfluorononane sulfonic acid |
| PFOA | Perfluoro-n-octanoic acid |
| PFOS | Perfluorooctane sulfonic acid |
| PFPeA | Perfluoro-n-pentanoic acid |
| PFPeS | Perfluoropentane sulfonic acid |

| | |
|----------|---|
| PFSA | Perfluoroalkyl sulfonic acids |
| PFTTrDA | Perfluoro-n-tridecanoic acid |
| PFTTrDS | Perfluorotridecane sulfonic acid |
| PFUnDA | Perfluoro-n-undecanoic acid |
| PFUnDS | Perfluoroundecane sulfonic acid |
| PMT | Persistent, mobile, and toxic |
| PS | Parametric system |
| RS | Rating systems |
| UBA | German Environment Agency |
| US EPA | United States Environmental Protection Agency |
| vPvM | Very persistent, very mobile |
| WWTP | Waste water treatment plant |
| 2-CPP | 2-(2-chlorophenoxy) propionic acid |
| 2-MPP | 2-(2-methylphenoxy)propanoic acid |
| 2,4-DCP | 2,4-dichlorophenol |
| 2,6-DCBZ | 2,6-Dichlorobenzamide |
| 3-MeCat | 3-methyl catechol |
| 4-CICat | 4-chloro catechol |
| 4-CICr | 4-chloro-o-cresol |
| 4CIPh | 4-Chlorophenol |
| 4-CPP | 2-(4-chlorophenoxy) propionic acid |

EXECUTIVE SUMMARY

The following deliverable D5.2 describes the groundwater risk assessment developed in task T5.2 within the UPWATER project (Understanding groundwater Pollution to protect and enhance WATER quality, Horizon Europe project No 101081807). It also features a list of chemicals to be taken up into the EU chemical priority list.

The groundwater risk assessment combined **intrinsic** and **specific vulnerabilities** of groundwater:

- **intrinsic vulnerability** was evaluated using the **DRASTIC method**, providing a general view of groundwater susceptibility for the three case studies (Stengården, Besòs, Athens). The detailed methodology was presented in D5.5,
- **specific vulnerability** accounted for pollutant properties. Key parameters include the **attenuation capability of the soil-rock-groundwater system** with respect to individual pollutant properties and the **pollutant travel time** through the unsaturated zone. The attenuation capability of the soil-rock-groundwater system was evaluated by means of laboratory experiments, allowing the calculation of a partitioning coefficient (K_D), specific for each soil and each selected pollutant. The travel time of the selected pollutants from the surface to the first aquifer was simulated using the HYDRUS 1D model.

Case Study Highlights:

- **Stengården case study:** the **groundwater intrinsic vulnerability** was assessed as **moderate**. At this case study, groundwater is mainly impacted by **pesticides and their metabolites**, which were assessed to be **mobile to very mobile**. Therefore, **there is a high risk that pesticides and pesticide metabolites reach groundwater**. The modeling indicated pollutant travel times in the range of 96 to 143 days from the old waste deposits to the first aquifer. Nevertheless, this travel time, estimated under worst-case conditions leaves sufficient time to adjust remediation solutions in case of an extreme rain event (more pumping at the wells/hydraulic trap, for example),
- **Besòs case study:** the **groundwater intrinsic vulnerability** fell within the upper range of the **moderate** classification. The study focused on **PFAS** due to their environmental persistence, toxicity, and high mobility. Laboratory tests confirmed that PFAS were **mobile to very mobile**. **It can be concluded that there is a high risk at this case study that PFAS reach groundwater**. The modeling indicated PFAS travel times in the range of 5 hours to 13 days. These travel times are fast and leave few possibilities of remediation after a storm event: it will be necessary to reduce the anthropogenic water infiltrations in the contaminated area, to reduce the risk of PFAS migration in soils and groundwater,
- **Athens case study:** the groundwater intrinsic vulnerability varied from low to high, depending on the area. PFAS were considered in the frame of the groundwater risk assessment and were found to be mobile to very mobile. At this case study, **there is a high risk that PFAS reach groundwater**. The modeling indicated PFAS travel times in the range of 2 to 15 days. As in the Besòs case study, travel times to the first aquifer are short (less than 15 days). However, in Athens, it occurs even in a natural area. This highlights the need for particular attention to both natural and anthropogenic areas.

PFAS Behavior Insights:

Mobility decreases with longer carbon chains, but long-chain PFAS remain capable of forming extensive plumes. Soil organic matter significantly influences retention of long-chain PFAS, while short-chain PFAS are mainly unaffected. Further studies are needed to clarify the factors controlling PFAS retention in soils.

1 Context and aim of the groundwater risk assessment

1.1 EU Project UPWATER

Groundwater (GW) is crucial for water supplies and livelihoods, serving as a strategic resource. Agriculture, particularly through nitrates and pesticides, poses a significant threat to GW quality. The UPWATER project aims to evaluate preventive measures to minimize chemical releases at the source, necessitating advancements in scientific understanding, the development of cost-efficient sampling methods, and modeling tools for scenario simulations and risk assessments. Additionally, bio-based treatment systems were developed and validated to mitigate GW pollution. Three case studies supported the validation of these solutions across different socio-economic and environmental contexts.

Outcomes of the UPWATER project include:

- recommendations to update the EU chemical priority lists,
- scale up the pilot bio-based solutions to demonstration scale,
- the adoption of preventive measures in the case studies,
- the close-to-market development of passive sampling devices for organic contaminants and pathogens.

The project consortium possesses diverse expertise and was guided by global authorities in science-to-policy translation and water governance, including collaboration with Australian partners on GW management and water policies.

1.2 Objectives

Within the UPWATER project, the work package (WP) 5 deals with environmental risk and impact assessment.

The objectives of WP5 were to:

1. Identify pollution sources, pathways, and impacts following a structured approach.
2. Assess the impact of selected risk reduction measures and treatment solutions.
3. Provide decision support for risk reduction and mitigation measures.
4. Provide up-scaling.

In this context, four tasks (T) were defined to achieve these objectives:

- T5.1: Assessment framework for analyzing pollution pathways, and assessing related risks and impacts of mitigation measures,
- T5.2: Environmental risk assessment,
- T5.3: Performance of monitoring tools and mitigation solutions,
- T5.4: Simulating/Assessing the large-scale impacts of mitigation solutions.

This document represents the public deliverable D5.2, which describes the final report on groundwater risk assessment developed in task T5.2 within the UPWATER project. This task also features a list of chemicals to be taken up into the EU chemical priority list.

1.3 Groundwater risk assessment

In many European countries, groundwater is the primary resource for irrigation and drinking. In Denmark and Holland for example, all drinking water comes from groundwater, while in Germany about 70% of all drinking water is sourced from the subsurface. However, due to urbanization, agricultural practices, and industrial activities, groundwater is increasingly at risk of pollution. As a result, its protection against pollution is a key issue, and methods to evaluate this risk of pollution are applied to manage it. Risk assessment can be defined as the process of estimating the possibility that a particular event may occur under a given set of circumstances (Finizio and Villa, 2002).

Specifically, the **risk of groundwater to be polluted** was first assessed with its **vulnerability** (Taghavi et al., 2022; Gogu and Dassargues, 2000) and was first defined in literature as the exposure of the water table to surface pollution (Albinet and Margat, 1970). Since then, other definitions have been published, such as:

- the tendency of or likelihood for pollutants to reach a specified position in the groundwater system after introduction at some location above the uppermost aquifer (National_Research_Council, 1993),
- an intrinsic property of a groundwater system, depending on the sensitivity of that system to human and/or natural impacts (Vrba and Zaporozec, 1994),
- the probability of pollutant migration from the ground surface into the groundwater system (Machiwal et al., 2018).

While there is no universally accepted definition of the risk of groundwater to be polluted in literature (Taghavi et al., 2022), all these definitions are consistent with the general definition of **risk**, which is a **combination of hazard and vulnerability** (Varnes et al., 1984). **Vulnerability** corresponds to the degree of **intrinsic weakness** of the investigated natural system, and **hazard** is the **probability** that a detrimental event will occur in a given area in a period of time (Passarella et al., 2022). Therefore, the **vulnerability of aquifers**, corresponding to their degree of **intrinsic weakness**, is tied to the aquifer characteristics, which do not change over time (Uricchio et al., 2004). This is called the **intrinsic vulnerability** of the aquifer (Schnebelen et al., 2002; Vrba and Zaporozec, 1994). Applied to groundwater, the **hazard** is the probability that a specific pollutant will **leach** along the soil and reach groundwater (Uricchio et al., 2004). This is called the **specific vulnerability** (Schnebelen et al., 2002).

Therefore, in the frame of T5.2 “Environmental risk assessment” of the UPWATER project, which has the global aim of evaluating the risk of groundwater to be polluted by specific pollutants at each case study, **the combination of both intrinsic vulnerability and specific vulnerability of the aquifers** was assessed at each case study level. This is in alignment with the published definitions presented above.

This deliverable presents in detail the methods used by Ineris for groundwater risk assessment, by means of intrinsic and specific vulnerabilities. Results obtained by Ineris at each case study level are then presented. In addition, in alignment with the results of the groundwater vulnerability to pollutants and monitoring campaigns, pollutant priority lists were established.

1.4 Pollutant priority list

Based on the results from the UPWATER monitoring campaigns, a prioritized ranking list of chemicals and pathogens was elaborated by the Institute of Environmental Assessment and Water Research (IDAEA) and Institut für Wasserforschung gemeinnützige GmbH (IWW-FO) for each UPWATER case study, following the steps listed below:

1. Collection of all available monitoring data (IDAEA partner). Where available, grab sampling data were prioritized over passive sampling data due to a higher measurement uncertainty of passive sampling for some organic compounds (ceramic passive samplers; CPS) and the fact that the deployed metal passive samplers, i.e. the diffusive gradients in thin films (DGT), only measure bioavailable metals in water.
2. Identification of compounds detected at high frequency and at high concentrations (IDAEA partner).
3. Collection of available persistent, mobile, and toxic (PMT) data from the German Department of Environment (Umweltbundesamt, UBA) (IWW-FO partner).
4. Alignment of compounds identified under point 2) with compounds on the current published priority list (EC, 2022) to confirm the current priority list (IDAEA partner).
5. Definition of which compounds of those identified under 2) are PMT compounds but are NOT already included in the current priority list, forming the base for a recommendation for uptake into the current priority list (IDAEA partner).

2 Groundwater risk assessment methodology

As stated in section 1.3, the risk for groundwater to be polluted is a combination of groundwater intrinsic and specific vulnerabilities. Methods for evaluating the groundwater intrinsic vulnerability have already been detailed in UPWATER deliverable D5.5, along with the method chosen in the frame of the UPWATER project (DRASTIC method, Aller et al., 1987). This can be found in Annex 1 of this report. The method used by Ineris to evaluate the specific vulnerability is detailed in this chapter.

The groundwater specific vulnerability represents the vulnerability of groundwater to a specific type of pollutant or group of pollutants, taking into account its properties such as biogeochemical attenuation processes and their relationship with various elements of intrinsic vulnerability (Taghavi et al., 2022). Key parameters in the specific vulnerability assessment include the **attenuation capability of the soil-rock-groundwater system** regarding the properties of individual pollutants and the **pollutant travel time** through the unsaturated zone (Gogu and Dassargues, 2000). The travel time of a pollutant through the unsaturated zone can be estimated by analytical advective-dispersive transport models (Connell and Daele, 2003), finite element models (Fusco et al., 2020), or type transfer functions (Bancheri et al., 2021).

The attenuation capability of the soil-rock-groundwater system was evaluated by means of laboratory experiments for each case study, allowing the calculation of a partitioning coefficient (K_D), specific to each soil and each selected pollutant. The experiments, specifically designed for each case study, are presented in chapters 0, 4, and 5.

In the frame of the UPWATER project, the travel time calculation of the selected pollutants from the surface to the first aquifer was assessed using the HYDRUS 1D model (Šimůnek et al., 1998). HYDRUS 1D has been widely used to simulate reactive solute transport processes in soils, especially when the more dominant process is sorption.

Solute transport can be described by the convection-dispersion equation (CDE). For reactive solute transport, the HYDRUS-1D model solves the CDE, incorporating both sorption and degradation processes (Equation 1).

$$\frac{\partial C}{\partial t} + \rho \frac{\partial (S)}{\partial t} = D \frac{\partial^2 C}{\partial x^2} - v \frac{\partial C}{\partial x} - \mu_1 C - \frac{\rho}{\theta} \mu_s S \quad \text{Equation 1}$$

In this equation, C ($M L^{-3}$) is the volume-averaged solution concentration, θ ($L^3 L^{-3}$) is the volumetric water content, ρ ($M L^{-3}$) is the solid bulk density, S ($M M^{-1}$) is the sorbed concentration, D ($L^2 T^{-1}$) is the dispersion coefficient in the liquid phase, v ($L T^{-1}$) is the water velocity, μ_1 (T^{-1}) is the first order degradation rate constant for the liquid phase, μ_2 (T^{-1}) is the first order degradation rate constant for the sorbed phase and t (T) is the time.

To take into account the specific vulnerability, equilibrium reactions between the solid and liquid phases were considered, using the K_D parameter for linear equilibrium. Results of laboratory experiments (batch and column experiments) were used: the partitioning coefficients were used as input data for the model. In addition, the calibrated hydraulic parameters from the D3.7 UPWATER report (Athens and Besòs case studies) and from a specific report on the Stengården site characterization (Overheu et al., 2015) were used.

This modeling phase focused on the travel time to the first aquifer under simplified saturated conditions to simulate adverse conditions. It allowed for the comparison of parameters without the influence of varying meteorological conditions. Saturated conditions also correspond to all experiments done at the laboratory scale (batch and column experiments) for the determination of pollutant-specific parameters, such as sorption, and, when applicable, desorption or degradation.

Two hydraulic conductivities can be used to model a soil column, representing both worst-case and average conditions of water flow from either the surface or subsurface. In the first scenario, the lowest hydraulic conductivities of the soil layers were used to simulate a potential water flow. This scenario is more critical than using the mean annual recharge, as it reflects a more important potential infiltration. The typical occurrence of this situation is a stormwater event that could lead to a larger recharge of the first aquifer, which may become more common in the future climate. This study refers to this first scenario as “worst-case conditions”. The second scenario was more conventional. It considered an average annual recharge and was only conducted for comparison purposes, using a non-reactive tracer. This study refers to this second scenario as “average scenario”.

A constant input of pollutants was considered to represent a steady state source of pollutants. The results were interpreted based on achieving a concentration of 50 % of the input source ($C/C_0 = 0.5$) for the travel time to the first aquifer. An arbitrary concentration of 5×10^{-5} mol/L was used for the source modeling to estimate the travel times and the equivalent retardation factors of the studied compounds.

A longitudinal dispersivity equal to one-tenth of the travel length (the column soil length) was selected, as commonly used (Frippiat and Holeyman, 2008). Diffusion was not considered in the frame of this study, as worst-case conditions are essentially convective and dispersive.

For each case study, a sensitivity analysis was conducted by modifying the sorption parameters or introducing degradation. Finally, the combination of the equivalent retardation factor and travel time for a non-reactive tracer allowed us to estimate the variation in travel times for each case study.

3 Groundwater risk assessment in relation to the Stengården case study

The Stengården case study has been polluted by dumping residues of a pesticide production plant together with household waste into a pit without separation from the deep soil/GW. The site nowadays is a testing facility that is owned and operated by the local authority 'Region Sjælland'.

3.1 Intrinsic vulnerability

The detailed intrinsic vulnerability assessment for the Stengården case study was presented in the UPWATER deliverable D5.5. Parameters and their corresponding ratings are presented in Annex 2 of this report.

3.2 Specific vulnerability

3.2.1 Pollutants considered in the frame of the groundwater risk assessment

At Stengården, the aquifer is primarily polluted by pesticides, specifically MCP and DCP, along with their respective metabolites. The concentrations of these contaminants in groundwater significantly exceed the EU drinking water limits. The polluted water of the site is affecting groundwater several kilometers away, moving towards drinking water abstraction sites for the city of Copenhagen and the town of Roskilde.

Based on the historical use of the site and the results of the groundwater analysis, pesticides and their metabolites are the pollutants of concern addressed in the frame of the groundwater risk assessment of the UPWATER project. The project focused on the pesticides MCP, DCP, and their metabolites (see Table 1). A specific vulnerability analysis was conducted to identify if these pollutants can lead to a risk of groundwater pollution at this site.

Table 1: Pesticides and metabolites addressed in the frame of the UPWATER project – Stengården case study

| Compound | CAS no. |
|--|--------------|
| Mecoprop (MCP) | 93-65-2 |
| Dichlorprop (DCP) | 120-36-5 |
| 2,4-dichlorophenol (2,4-DCP) | 120-83-2 |
| 2-(2-methylphenoxy)propanoic acid (2-MPP) | 7345-21-3 |
| 4-Chlorophenol (4CIPh) | 106-48-9 |
| 2-(2-chlorophenoxy) propionic acid (2-CPP) | 25140-86-7 |
| 2-(4-chlorophenoxy) propionic acid (4-CPP) | 3307-39-9 |
| Mecoprop sulphate (MCP_sulf) | 2801487-84-1 |
| 4-chloro-o-cresol (4-CICr) | 1570-64-5 |

3.2.2 Material and methods

As stated in chapter 2, the specific vulnerability analysis was based on the travel time calculation of the selected pollutants from the surface to the first aquifer, along with the attenuation capability of the soil-rock-groundwater system. The travel time was calculated by Ineris using the HYDRUS-1D model. In this model, equilibrium reactions between the solid and liquid phases were considered. They are described by the soil-water partitioning coefficients (K_D) of the pollutants of interest, which were assessed in the laboratory by Ineris, by means of batch and column experiments on the Stengården soil.

Additionally, the degradation was assessed by Ineris via the half-life of the pesticide parent compounds (DCPP and MCP) through batch experiments. This data was also used as input for the model, in the frame of a sensitivity analysis.

3.2.2.1 Soil sampling and characterization

Soil was sampled at a depth of 3 m at the Stengården case study in August 2023 by AU. Before conducting any experiment or characterization, the soil was air-dried at room temperature and then sieved through a 2 mm stainless-steel mesh.

The soil was characterized in the frame of the UPWATER project by Ineris. Its physical and chemical characteristics are presented in Table 2. This soil has a basic pH of 9.1. It is mainly composed of coarse sand (78 wt.%) and has a low clay and silt content. The organic carbon content is very low (0.425 %).

Table 2: Soil physical and chemical characteristics – Stengården soil

| Granulometry (g kg ⁻¹) | | | | | |
|---|----------------|---------------------------------------|-------------------------------|-----------------------|---------------------------|
| Parameter | Clay (< 2 µm) | Fine silt (2/20 µm) | Coarse silt (20/50 µm) | Fine sand (50/200 µm) | Coarse sand (200/2000 µm) |
| Value | 19 | 22 | 19 | 160 | 780 |
| Organic carbon and total nitrogen (g kg ⁻¹) | | | | | |
| Parameter | Organic carbon | Total nitrogen | Total carbon | C/N | Organic matter |
| Value | 2.46 | 0.157 | 37.9 | 15.6 | 4.25 |
| Parameter | pH (water) | Total limestone (g kg ⁻¹) | CEC (cmol+ kg ⁻¹) | | |
| Value | 9.1 | 295 | 2.11 | | |

Pesticides and pesticide metabolites were analyzed in this soil by AU and the concentrations were too low to be quantified. Therefore, to assess the soil-water partitioning coefficients of pesticides and their metabolites in this soil, sorption experiments were conducted (see below).

3.2.2.2 Sorption experiments

Sorption experiments were conducted by Ineris to calculate a soil-water partitioning coefficient (K_D) for each compound. Stock solutions of each pesticide and pesticide metabolite presented in Table 1 were prepared in methanol at a concentration of 0.5 g/L. Then, from these stock solutions, aqueous solutions containing a mixture of all the pesticides and pesticide metabolites were prepared at the desired concentrations (see below) with calcium chloride dihydrate ($\text{CaCl}_2 \cdot 2\text{H}_2\text{O}$) at a concentration of 5×10^{-3} mol/L and sodium azide (NaN_3) at a concentration of 0.2 g/L (“mixed compound solution”). Calcium chloride was used to create an ionic strength in all the solutions and, therefore, stabilize clays in the soil. This concentration was chosen to mimic the calcium concentration in groundwater at the Stengården case study. Sodium azide was used to inhibit microbial activity.

3.2.2.2.1 Batch sorption experiments (Ineris)

First, sorption of the mixed compound solution was performed using the batch equilibrium technique by Ineris. This method is an effective approach to gaining a comprehensive understanding of the interactions between the studied compounds and the soil (OECD, 2000). Experiments were conducted in triplicate in 50 mL polypropylene centrifuge tubes at a temperature of 21 ± 2 °C.

A quantity of 15 g of soil was introduced into the vials, and 20 mL of solution was added in two steps. First, a conditioning step of the soil was performed: 10 mL of an aqueous solution containing $\text{CaCl}_2 \cdot 2\text{H}_2\text{O}$ (5×10^{-3} mol/L) and NaN_3 (0.2 g/L) was added to the soil and shaken for 1 h at 250 rpm in an orbital shaker, to moisten the dry soil and avoid experimental artifacts. Then, 10 mL of the mixed compound solution at a concentration of 50 µg/L were added to the vial and shaken on an orbital shaker in order to reach the equilibrium time. The mixture was then centrifuged at 3,000 G for 30 min, and 10 mL of the supernatant were sampled and stored in the freezer in glass vials pending analyses by AU.

Control vials containing the mixed compound solution without soil and blank vials containing soil and an aqueous solution of $\text{CaCl}_2 \cdot 2\text{H}_2\text{O}$ (5×10^{-3} mol/L) and NaN_3 (0.2 g/L) underwent the same procedure to account for potential losses or wall adsorption during the experiment and to evaluate the potential release of compounds from the soil.

The amounts of sorbed compounds were calculated using the following equation:

$$q_t = \frac{V}{M} (C_0 - C_t) \quad \text{Equation 2}$$

where q_t (µg/kg) is the mass concentration of sorbed solute at time t , V (L) the volume of solution, M (kg) the mass of soil, C_0 (µg/L) the initial solute concentration of the mixed compound solution and C_t (µg/L) the solute concentration at time t , t being the equilibrium time.

The liquid-to-solid ratio was optimized before conducting the experiments based on two criteria: first, there should be a significant difference in solution concentrations at equilibrium, and second, the solution concentration at equilibrium should be above the quantification limit.

The equilibrium time was assessed through a kinetics study, consisting of monitoring the pesticide and pesticide metabolite solution concentrations throughout the experiment (up to 72 h). Polypropylene vials were filled with 15 g of soil and 20 mL of the mixed compound solution at a concentration of 50 µg/L. The procedure described earlier was then applied. Pesticide and pesticide metabolite solution concentrations were measured at several time points: 1 h, 8 h, 16 h, 24 h, 48 h, and 72 h. Equilibrium time was assumed to be reached when the percentage of sorption achieved was constant. This kinetics study showed that equilibrium was achieved before 24 h, which is why a shaking duration of 24 h was selected for the sorption assessment.

Then, the K_D (L/kg) was calculated using the following equation:

$$K_D = \frac{q_{24h}}{C_{24h}} \quad \text{Equation 3}$$

where q_{24h} (µg/kg) is the mass concentration of sorbed solute at equilibrium (24 h) and C_{24h} (µg/L) the solute concentration in solution at equilibrium, corresponding to the difference between the concentration measured in solution at equilibrium and the concentration measured in the blank samples at equilibrium.

The mass concentration of sorbed solute at equilibrium q_{24h} (µg/kg) was calculated using the following equation:

$$q_{24h} = \frac{(C_0 - C_{eq}) \times 0.02}{m_{soil}} \quad \text{Equation 4}$$

where C_0 (µg L⁻¹) is the initial concentration, corresponding to the concentration measured in the control samples, to account for wall adsorption on the vials, C_{eq} (µg L⁻¹) is the concentration measured in solution after equilibrium, and m_{soil} (kg) is the soil mass introduced in the vials (0.015 kg).

3.2.2.2.2 Column experiments (Ineris)

To confirm soil-water partitioning coefficients derived from batch sorption experiments, column experiments were conducted. These experiments can simulate further field conditions by adding a flow component. Discrepancies between results obtained from batch and column may arise due to the different experimental procedures used. Batch experiments are conducted under static conditions, while column experiments are performed under dynamic conditions, which may more accurately reflect field scenarios (Yang et al., 2013). In batch experiments, the ratio of the soil mass to solution volume is typically lower, and the contact time between the two phases is longer compared to column experiments. Additionally, batch experiments may lead to particle attrition and desegregation, which render them less representative of field conditions compared to column experiments.

Column experiments were conducted by Ineris using a glass column with an internal diameter of 1.6 cm, packed with approximately 42 g of soil and 1 g of sand at the top. A peristaltic pump was used to inject the solution into the column in an up-flow mode. The experiments were carried out at room temperature (21 ± 2 °C) and with the natural pH of solutions.

The columns were saturated upwards with a background solution appropriate for the experiment (see below), using a low flow rate of 0.15 mL min^{-1} as a preconditioning procedure and conditioned at a flow rate of 1 mL min^{-1} with the same solution for 72 h. Then, columns were fed with the same solution, but this time containing the studied compounds (see Table 1) at a concentration of $50 \text{ }\mu\text{g/L}$, until the outlet concentrations of the pollutants reached their respective inlet concentrations (sorption step). Desorption was then initiated by injecting the background solution appropriate for the experiment (see below) until the pollutants were no longer detected at the column outlet. Samples were collected from the column outlet at various time intervals. Pesticide and pesticide metabolite concentrations in these samples were analysed by AU.

In the frame of the UPWATER project, two sorption/desorption experiments were performed, each with a fresh soil sample:

- sorption/desorption of the mixed compound solution. For this experiment, the background solution was prepared with CaCl_2 at a concentration of $5 \times 10^{-3} \text{ mol/L}$ and NaN_3 at a concentration of 0.2 g/L
- sorption/desorption of a DCP and MCP mixture. In this case, the background solution was prepared with CaCl_2 at a concentration of $5 \times 10^{-3} \text{ mol/L}$. No bacterial inhibitor was added in order to evaluate the DCP and MCP degradation over the course of the experiment.

The results are presented as breakthrough curves, which show the normalized concentration, defined as the ratio of the effluent concentration (C) to the inlet concentration (C_0), as a function of normalized volume. The normalized volume is the ratio of the total volume at time t (V) to the column pore volume (V_p). The column pore volume was determined experimentally through a tracer experiment.

In addition, the K_D (L/kg) was calculated using the following equation:

$$K_D = \frac{q}{C} \quad \text{Equation 5}$$

where q ($\mu\text{g kg}^{-1}$) is the mass concentration of sorbed solute at the end of the sorption step and C ($\mu\text{g L}^{-1}$) the inlet solution concentration of the studied compound ($50 \text{ }\mu\text{g/L}$).

The mass concentration of sorbed solute at the end of the sorption step (q , $\mu\text{g kg}^{-1}$) was calculated using the following equation:

$$q = m_{\text{fix}} / m_{\text{soil}} \quad \text{Equation 6}$$

with m_{fix} (M) the pollutant mass fixed in the column, and m_{soil} (M) the soil mass in the column.

During column experiments, 2,4-DCP was not quantified because of a crosstalk with MCP.

3.2.2.3 Degradation experiments (Ineris)

Batch degradation experiments were carried out in triplicate by Ineris under aerobic conditions in order to evaluate the half-life of the pesticide parent compounds (MCPP and DCPP). They were conducted in 1 L glass bottles, with each bottle containing 90 g of soil and 900 mL of solution. The solution was a mixture of DCPP and MCPP at a concentration of 50 µg/L, prepared in a CaCl₂ solution at a concentration of 5 x10⁻³ mol/L. Additionally, a control batch was prepared, which included the same soil-solution mixture, but with NaN₃ added at a concentration of 0.2 g/L to inhibit microbial activity. To enhance the sorption process in the soil, these soil-solution mixtures were shaken in an orbital shaker for 72 h. In this scenario, any decrease in the concentration of DCPP or MCPP in the solution after 72 h can be attributed solely to degradation, since sorption equilibrium was reached by 24 h, as outlined in the earlier description of the sorption kinetics experiments.

At predetermined time intervals (days 0, 3, 16, 62, 113, 129, 167, 190, 216, 234, 317, 354, and 380), a 2 mL aliquot was sampled from each bottle, centrifuged at 3,000 G for 30 min, and stored in the freezer until pesticide and pesticide metabolite analysis.

3.2.2.4 Analysis (AU)

The analysis of pesticides and their metabolites using UPLC-MS/MS was conducted by AU.

3.2.3 Results

3.2.3.1 Batch experiments

Pesticide and pesticide metabolite concentrations in solution measured at equilibrium under exclusion of microbial degradation allowed us to calculate the soil-water partitioning coefficients (K_D), presented in Table 3.

Table 3 shows that the sorption of pesticides and pesticide metabolites onto this soil was very low. Soil-water partitioning coefficients are in the range of 1.3 L/kg for 4-CPP to 3.2 L/kg for MCPP-sulfate. In this table, log K_{OC} is calculated. K_{OC} is the soil organic carbon – water partitioning coefficient, which helps to classify a pollutant as mobile or very mobile, thanks to the German environmental agency, UBA. When log K_{OC} is below 4, the substance is considered mobile, whereas when it is below 3, the substance is considered very mobile, according to the UBA PMT classification (UBA, 2019). Therefore, according to the log K_{OC} presented in Table 3, all pollutants studied in the Stengården case study can be considered very mobile, except MCPP-sulf, which is considered mobile. Therefore, it can be expected that they reach groundwater easily and form extended pollution plumes.

Table 3: Soil-water partitioning coefficients (K_D) calculated after batch experiments

| Pollutant | MCPP | DCPP | 4-CPP | 2-CPP | 4-CIPh | 2-MPP | 2,4 DCP | 4-CICr | MCPP-sulf |
|-----------------------|------|------|-------|-------|--------|-------|------------|--------|-----------|
| K _D (L/kg) | 1.9 | 1.4 | 1.3 | 1.7 | 1.8 | 1.9 | 1.9 | 1.9 | 3.2 |
| Log K _{OC} | 2.9 | 2.8 | 2.7 | 2.8 | 2.9 | 2.9 | 2.9 | 2.9 | 3.1 |

A low sorption of pesticides has been found by other authors when conducting sorption experiments with the batch technique. For example, the following results have been found:

- for MCP, log K_{oc} of 1.5 and 1.6 were found with 2 soils exhibiting an organic carbon content of 3.6 and 3.9% (Piwowarczyk and Holden, 2013),
- for DCP, log K_{oc} values were in the range from 1.7 to 2.1 when characterizing its sorption onto 5 soils containing between 1.4 and 30.4% of organic carbon (Riise and Salbu, 1992),
- for 2,4-D, log K_{oc} values were between 0.4 and 2.7 on soils with organic carbon content of 0.23 to 8.68% (Ololade et al., 2018; Kim et al., 2012; Shan et al., 2011; Liu et al., 2008).

All these results showed that these three pesticides were considered very mobile as well, with regard to the UBA PMT criteria.

3.2.3.2 Column experiments (Ineris)

The breakthrough curves of the 8 pollutants quantified during the sorption/desorption of the mixed compound solution are presented in Figure 1. Error bars correspond to the analytical uncertainty.

All breakthrough curves exhibited the same shape. A rapid breakthrough was observed for all compounds, with an outlet concentration reaching the inlet concentration after injecting 1.4 pore volumes, except for 4-CIPh, for which the breakthrough was longer (injection of 2.6 pore volumes to reach the inlet concentration at the outlet of the column).

The desorption of all compounds was a rapid process as well. It needed the injection of 2.3 to 2.4 pore volumes for all compounds to be completed, except for 4-CICr and 4-CIPh, for which it needed 12 and 3.7 pore volumes, respectively. Other authors showed a rapid, complete breakthrough of DCP between 2 and 3 pore volumes in column experiments on a sandy loam soil (Wu et al., 2025).

For each pollutant studied, Table 4 shows the pollutant mass sorbed onto the soil during the sorption step (m_{sorbed}), the pollutant mass desorbed from the soil during the desorption step ($m_{desorbed}$), and the percentage of sorption irreversibility ($\%_{irr}$). Note that for some compounds, the desorbed mass was higher than the sorbed mass. This is an artifact due to the measurement uncertainties, which may be quite high for these small mass values. The sorption of these pollutants was mainly a reversible process. For DCP, 2-MPP, 4-CIPh, 4-CPP, and 4-CICr, the desorption step allowed the desorption of all the pollutant mass that was sorbed during the sorption step. For the other pollutants studied (2-CPP, MCP-sulf, and MCP), the sorption irreversibility was 5, 10, and 25%, respectively. This low sorption reversibility shows the weak affinity of the soil for these pollutants.

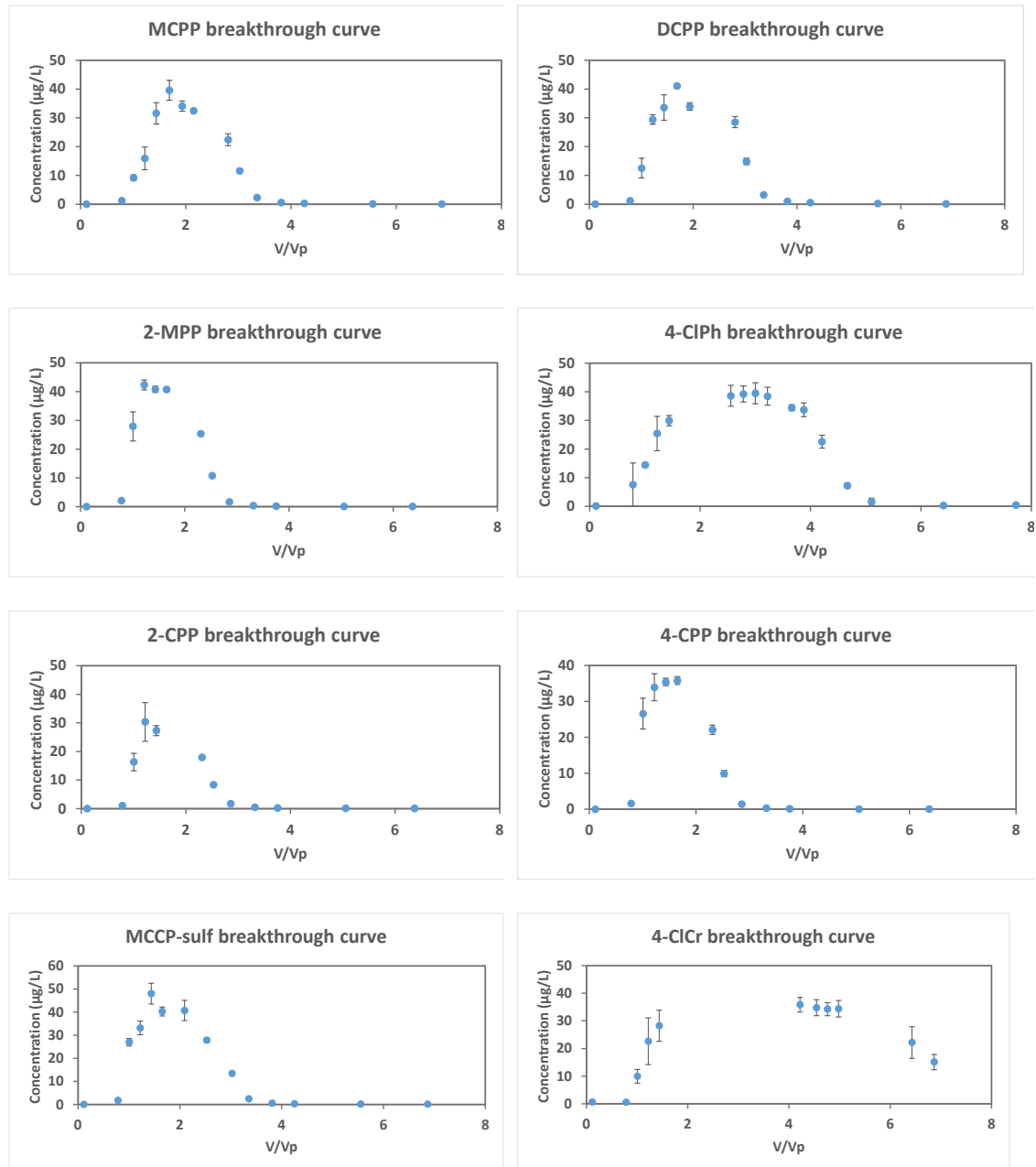


Figure 1: Breakthrough curve of the studied pollutants (sorption/desorption of the mixed compound solution)

Table 4 shows that the K_D values calculated after column experiments were lower than the ones calculated after batch experiments, meaning that the soil uptake capacity was higher in batch experiments.

Table 4: Irreversibility of the sorption (sorption/desorption of the mixed compound solution) and comparison of K_D from batch and column experiments

| Pollutant | MCPP | DCPP | 2-MPP | 4-CIPh | 2-CPP | 4-CPP | MCPP-sulf | 4-CICr |
|--|------|------|-------|--------|-------|-------|-----------|--------|
| m_{sorbed} (μg) | 0.67 | 0.44 | 0.55 | 0.62 | 0.41 | 0.43 | 0.69 | 0.71 |
| m_{desorbed} (μg) | 0.50 | 0.56 | 0.57 | 0.94 | 0.39 | 0.50 | 0.62 | 1.32 |
| %irr | 25 | 0 | 0 | 0 | 5 | 0 | 10 | 0 |
| K_D column (L/kg) | 0.39 | 0.25 | 0.30 | 0.37 | 0.31 | 0.30 | 0.33 | 0.46 |
| Log K_{oc} | 2.2 | 2 | 2.1 | 2.2 | 2.1 | 2.1 | 2.1 | 2.3 |
| K_D batch (L/kg) | 1.9 | 1.4 | 1.9 | 1.8 | 1.7 | 1.3 | 3.2 | 1.9 |

Using these two different experimental procedures to evaluate the sorption of pollutants onto soil could lead to differing results, depending on the contact mode between soil and solution (Naboulsi et al., 2024; Barna et al., 2007). Experiments conducted under static conditions used high liquid-to-solid ratios and involved long contact times between the soil and solution. This allowed the system to reach equilibrium. Dynamic conditions had lower instantaneous liquid-to-solid ratios, resulting in higher concentration of sorption sites, which allowed for quantification of weaker soil/solution interactions (Delolme et al., 2004). Therefore, in batch experiments, the sorbent performance depended only on the soil uptake capacity, whereas in column experiments, it depended both on sorption kinetics and uptake capacity (Shimabuku et al., 2023).

In addition, the key distinction between static and dynamic approaches is the management of reaction products. Under dynamic conditions, they are continuously removed from the system, unlike in static conditions, where they remain present throughout the experiment.

Table 4 shows that the log K_{oc} calculated after column experiments for the 8 pollutants studied were below 3, confirming their classification into the “very mobile” category of the PMT classification from UBA.

The breakthrough curves of MCPP and DCPP during the sorption/desorption of a DCPP and MCPP mixture are presented in Figure 2. Error bars correspond to the analytical uncertainty. In this case, no bacterial inhibitor was added to evaluate the DCPP and MCPP degradation over the course of the experiment. These curves are compared to the ones obtained when injecting the mixed compound solution containing the 9 studied pesticides and a bacterial inhibitor.

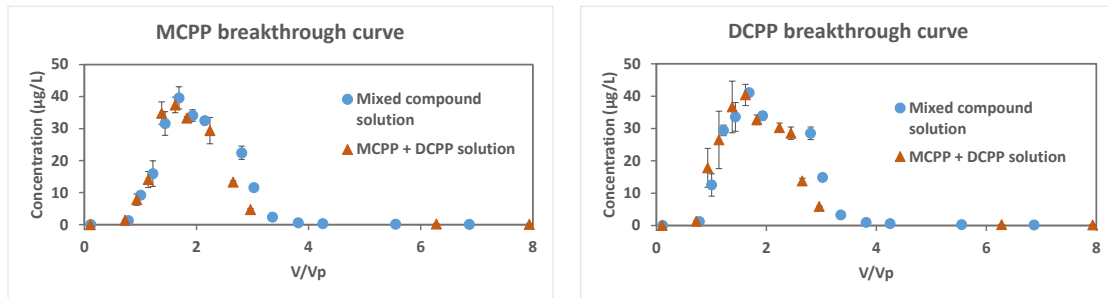


Figure 2: MCPP and DCPD breakthrough curves (sorption/desorption of the solution containing MCPP and DCPD)

At the outlet of the column, no other pesticides were quantified, showing that no degradation occurred in the frame of this experiment. This was expected given the relatively short time of this test (between 6 and 7 hours).

Breakthrough curves of MCPP and DCPD, when these compounds were injected together in the column, exhibited the same shape compared to the ones when they were injected in the mixed compound solution, that is to say, with 7 other pesticides. This suggests that no competing effect occurred during the sorption of these compounds onto the soil. Sorption sites were present in excess.

The pesticide sorbed masses during the sorption step were very close for both experiments (see Table 5). This leads to similar K_D and, therefore, to similar $\log K_{OC}$ for both experiments, confirming the “very mobile” classification of both compounds. The desorbed masses were in the same order of magnitude, leading to reversible sorption in both cases.

Table 5: Comparison of the sorbed/desorbed mass of MCPP and DCPD in the frame of the 2 column experiments

| Pollutant | MCPP | | DCPD | |
|----------------|-------------------------|----------------------|-------------------------|----------------------|
| | Mixed compound solution | MCPP + DCPD solution | Mixed compound solution | MCPP + DCPD solution |
| msorbed (µg) | 0.67 | 0.53 | 0.44 | 0.49 |
| mdesorbed (µg) | 0.50 | 0.61 | 0.56 | 0.70 |
| %irr | 25 | 0 | 0 | 0 |
| K_D (L/kg) | 0.39 | 0.35 | 0.25 | 0.31 |

Results from batch and column experiments are consistent and show that the studied pesticides and pesticide metabolites are mobile to very mobile in this soil. Therefore, given the results of the intrinsic vulnerability analysis at this case study, showing that groundwater was moderately vulnerable to surface pollution, **it can be considered that there is a high risk at this case study that pesticides and pesticide metabolites reach groundwater.**

At this stage, as pesticides and pesticide metabolites are measured in groundwater, it is essential to implement both mitigation and preventive measures to avoid further groundwater pollution.

3.2.3.3 Degradation experiments (Ineris)

The evolution of the MCPP and DCPD concentrations during the degradation experiment is presented in Figure 3. A two step process is observed. The first one, with a fast decrease in concentration over 3 days, corresponds to the MCPP and DCPD sorption onto this soil. The second step, where the MCPP and DCPD concentrations decrease, is the degradation of MCPP and DCPD.

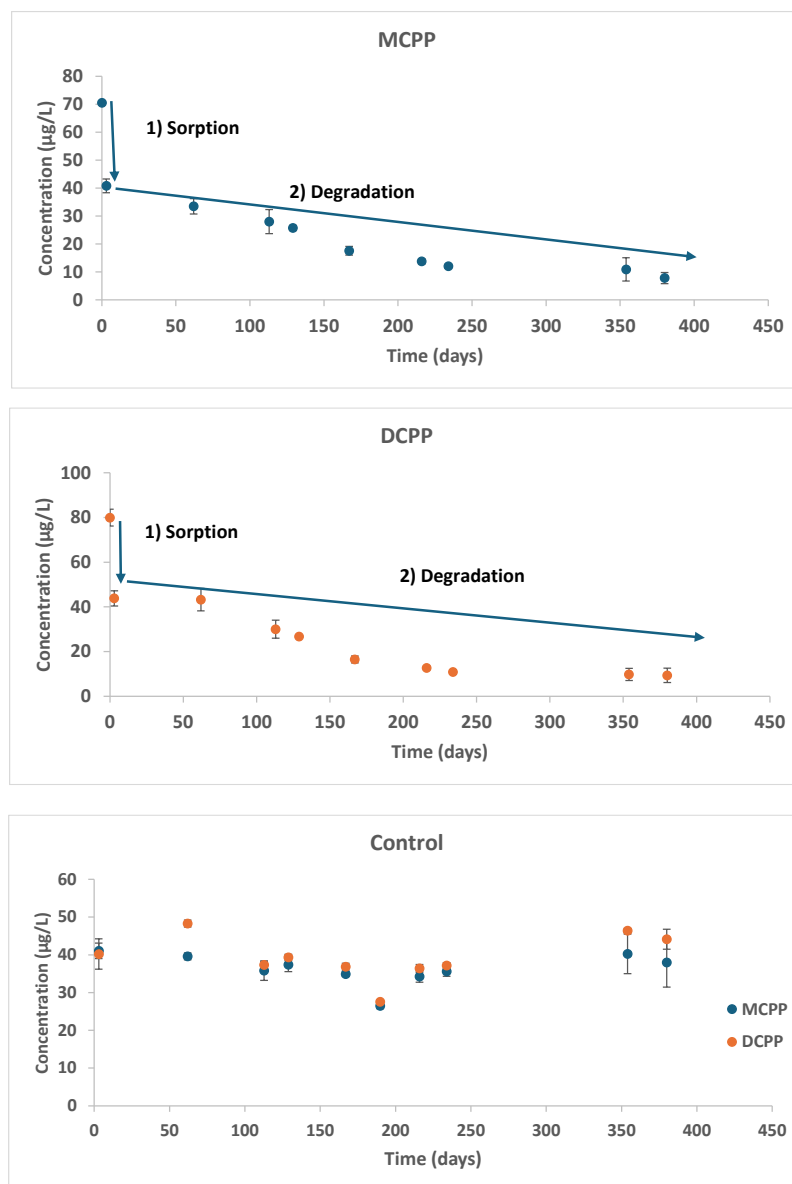


Figure 3: Degradation of MCPP and DCPD

MCPP and DCPD concentrations in the control during the experiment are presented in Figure 3 as well. MCPP and DCPD concentrations in the control were stable, except at a contact time of 190 days between the soil and the solution. After 190 days, as MCPP and DCPD concentrations were similar to the ones measured at the beginning of the experiment, these lower values were considered non-significant and attributed to an analytical problem. Therefore, no sorption of MCPP or DCPD was observed on the glass bottles used for the experiment. The decrease in MCPP and DCPD concentrations during the experiments can therefore be attributed to degradation only.

MCPP and DCPD degradation was modeled according to first-order kinetics, following Equation 7:

$$q_t = q_e (1 - e^{-k_1 t}) \quad \text{Equation 7}$$

where q_e is the amount of solute adsorbed per unit of adsorbent mass (mg g^{-1}), q_t is the amount of solute adsorbed per unit of adsorbent mass (mg g^{-1}) at time t (min); k_1 is the kinetic constant of pseudo-first order (min^{-1}). The slope of the straight-line plot of $\ln (q_e - q_t)$ against t allowed us to calculate k_1 and the half-life time ($t_{1/2}$) of MCPP and DCPD, according to Equation 8, for a first-order kinetics degradation:

$$t_{1/2} = \frac{\ln 2}{k_1} \quad \text{Equation 8}$$

Table 6 presents the MCPP and DCPD half-life times and the correlation coefficients of the plot $\ln (q_e - q_t)$ against t .

Table 6: MCPP and DCPD half-lives under aerobic conditions

| MCPP | | DCPD | |
|---------------|--------|---------------|--------|
| $t_{1/2}$ (d) | r^2 | $t_{1/2}$ (d) | r^2 |
| 98 | 0.9294 | 53 | 0.9381 |

Other authors have modeled MCPP degradation with first-order kinetics (Frková et al., 2016). In literature, MCPP half-lives varied between 12 and 84 days (Bollmann et al., 2017; Rodríguez-Cruz et al., 2010; Romero et al., 2001). They were found to be dependent on the soil structure and on the soil depth: the MCPP half-life increased with an increase in soil depth, being measured at a value of 84 days at a depth between 70 and 80 cm (Rodríguez-Cruz et al., 2010). For DCPD, the half-lives have been calculated between 9 and 98 days depending on the soil structure, the half-life being higher in a clay loam soil (Romero et al., 2001).

These values are in the order of magnitude of the half-lives of MCPP and DCPD found at the Stengården case study in the frame of the UPWATER project.

In addition, a decrease of DCPD concentration was confirmed on streamlines of the groundwater flow model built in a specific report on the Stengården site characterization (Overheu et al., 2015). Nevertheless, it was not confirmed in the case of MCPD, even if the hypothesis was not discarded: this report also indicated some hints of degradation of MCPD, but it concluded that Monitored Natural Attenuation (MNA) could not be used for this site. Our microcosms were also not controlled to reflect degradation in groundwater, but the possibility of degradation.

3.2.3.4 Pesticide and pesticide metabolite travel time calculation (Ineris)

The time needed for these pollutants to reach groundwater was calculated using the HYDRUS-1D model by Ineris. Parameters used to build the conceptual model were extracted from a specific report on the Stengården site characterization (Overheu et al., 2015) and were based on the intrinsic and specific vulnerability assessment presented in the previous paragraphs.

3.2.3.4.1 Intrinsic vulnerability parameters considered

- Soil column and water table depth

On this site, the soil is composed of two main layers: a waste and clay layer (moraine), on top of a sand layer (Kilstrup sand). The thickness of the waste and clay layer ranges between 5 and 10 m. Since the clay layer slows down the movement of contaminants, a thickness of 5 m for the waste and clay layer was considered to model unfavorable conditions. Buried waste in moraine represents the pesticide pollution source. In this model, the pesticide pollution source was located at 3.25 m from the ground surface.

The second layer, represented by Kilstrup sand, is connected to the first aquifer. In the Stengården case study, the water table level is 16 to 19 m below ground level. To model worst-case conditions corresponding to the fastest transfer, the water table level was set at 16 m below the ground level.

This conceptual model is presented in Figure 4.

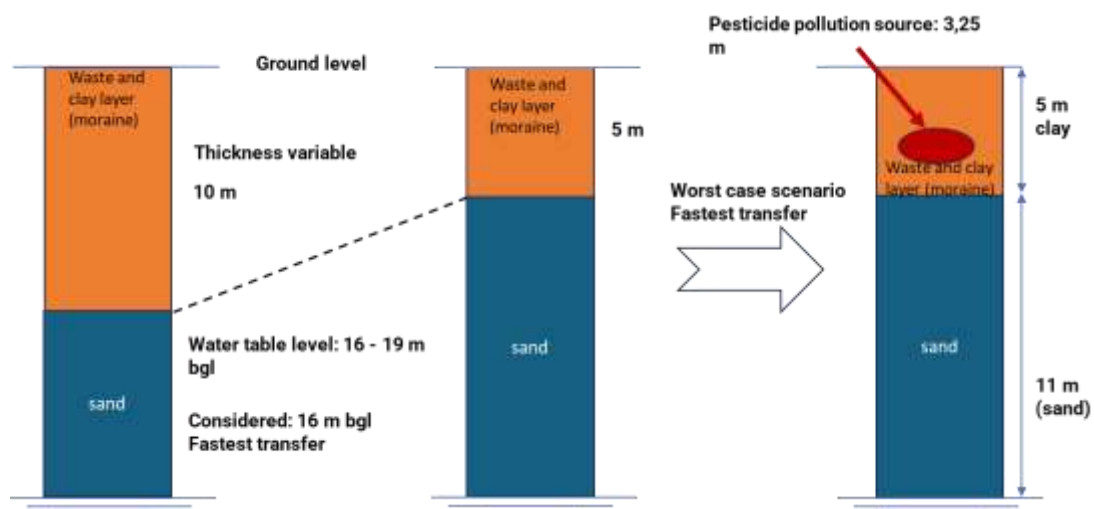


Figure 4: Conceptual model for pesticide transport modeling from pollution source to the first aquifer at the landfill scale (Stengården case study)

➤ Permeability and porosity of the soil column

The hydraulic conductivity (10^{-6} m/s) and porosity (0.25) of the first layer were extracted from a specific report on the Stengården site characterization (Overheu et al., 2015). This corresponds to the “HK 100” zone of the model developed in this report. The hydraulic conductivity of Kilstrup sand varies among 3 values (10^{-4} , 10^{-3} , and 2.5×10^{-3} m/s), with a geometric mean of 6×10^{-4} m/s. Parameters coming from the “HK200” zone of the model developed in the previously cited report (hydraulic conductivity: 10^{-3} m/s, porosity: 0.3) were used to compare the pore velocities. In this model, the hydraulic conductivity of the soil column under saturated conditions is governed by the lowest conductivity, which is that of the clay layer (10^{-6} m/s). With this scenario, water infiltrations reach the mean groundwater annual recharge in only 3.5 days.

3.2.3.4.2 Specific vulnerability parameters considered

➤ Sorption

In the frame of this study, partitioning coefficients were obtained for 9 compounds (pesticides and pesticide metabolites) using both batch and column experiments. K_D values derived from column experiments were used for the modeling, as they are considered more representative of the field conditions (see Table 4). In addition, K_D values obtained after column experiments were lower than those obtained after batch experiments. This is in alignment with the modeling strategy, intended to consider worst-case conditions.

In column experiments, 2,4 DCP was not detected due to analytical problems. Hence the K_D value used for this compound was an average value of the K_D calculated from batch experiments for MCP and 2-MPP, which coincided with the K_D value for 2,4 DCP in batch experiments (0.35 L/kg).

In the frame of a sensitivity analysis, the use of batch-derived K_D values was studied.

➤ Degradation

In order to conduct the modeling phase under worst-case conditions, the model did not take into account the MCP and DCP degradation in this scenario. Nevertheless, the possibility of degradation was studied as a sensitivity analysis, since the degradation experiments conducted at the laboratory scale showed a degradation of both molecules, with a half-life of 98 and 53 days for MCP and DCP, respectively under aerobic conditions.

3.2.3.4.3 Results of the modeling phase

Simulated breakthrough curves for each pesticide and pesticide metabolite are presented in Figure 5. These breakthrough curves were obtained using K_D values derived from column experiments. The travel times calculated with these curves (time to reach a ratio of 0.5 between the concentration at the outlet of the soil column and the injected concentration) are in the range of 96 days (DCP) to 143 days (4-CICr). These travel times are imposed by the lower permeability of the first layer (10^{-6} m/s) and the partitioning coefficients, K_D . Travel times and the associated retardation factors are presented in Table 7.

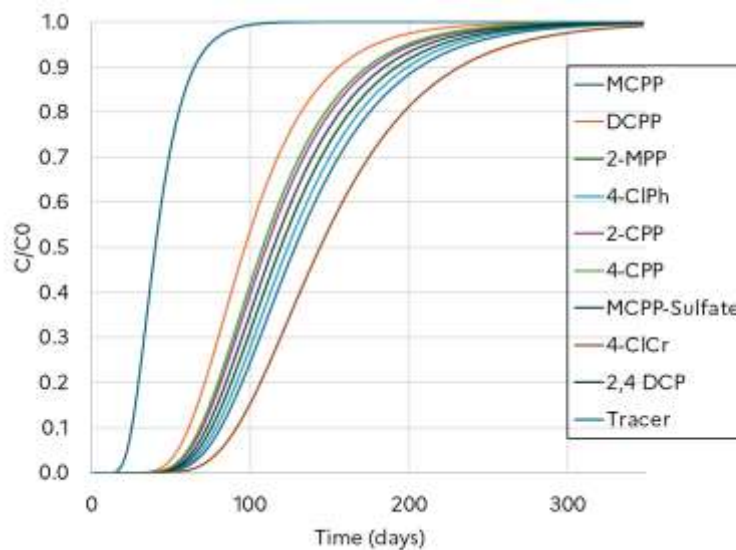


Figure 5: Simulated breakthrough curves for pesticides and pesticide metabolites (Stengården case study, K_D derived from column experiments)

Parameters considered in the modeling yielded an average travel time of 40 days for a non-reactive tracer (worst-case conditions). This travel time reached 11 years for the average scenario, considering the annual groundwater recharge limiting the water flow. For example, in this case, the travel time T_{ti} of a chemical i with a retardation factor R_i of 3 will be 33 years ($T_{ti} = T_t \text{ tracer} * R_i$).

Table 7: Retardation factors and travel times for the pesticides and pesticide metabolites studied

| Pollutant | MCPP | DCPP | 2-MPP | 4-CIPh | 2-CPP | 4-CPP | MCPP-S | 4-CICr | 2,4DCP | Tracer |
|--------------------|------|------|-------|--------|-------|-------|--------|--------|--------|--------|
| R (-) | 3.2 | 2.4 | 2.7 | 3.1 | 2.7 | 2.7 | 2.9 | 3.6 | 3.0 | 1.0 |
| Travel time (days) | 128 | 96 | 108 | 124 | 108 | 108 | 116 | 143 | 120 | 40 |

➤ Sensitivity analysis

The use of partitioning coefficients (K_D) derived from batch experiments, instead of column experiments, increased travel times, as presented in Figure 6. The ratios of the retardation factors derived from batch experiments to the ones derived from column experiments ranged between 3.1 (4-CPP) and 6.7 (MCCP-sulfate).

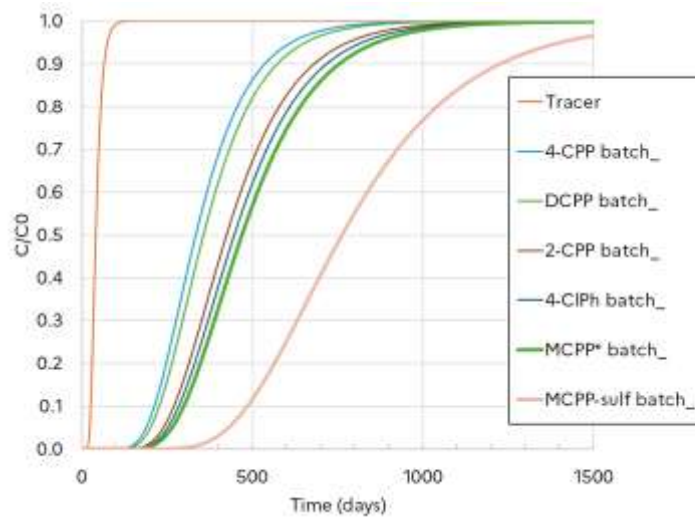


Figure 6: Simulated breakthrough curves for pesticides and pesticide metabolites (Stengården case study, KD derived from batch experiments)

In the frame of the sensitivity analysis, a scenario considering the degradation of MCPP and DCPD was considered. In this case, the retardation factors were higher (

Figure 7). They increased from 3.2 to 3.6 for MCPP and from 2.4 to 3.3 for DCPD. In addition, concentrations of MCPP and DCPD reached, respectively, 75% and 60% of the injected concentration in the time frame considered (1,500 days). Therefore, the addition of degradation increased the observed retardation factors, but limited the concentrations of MCPP and DCPD coming from the first layer. The effect of biodegradation would be higher with a lower average flow (annual recharge), which allows more time for pesticide degradation to take place.

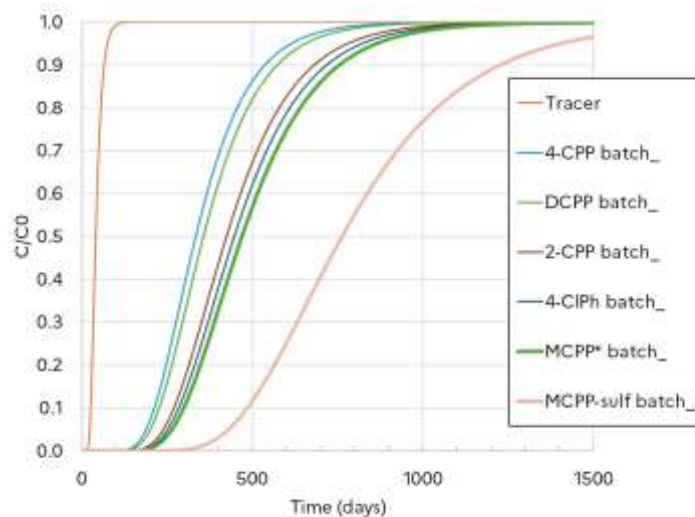


Figure 7: Effect of degradation on the breakthrough curves of MCPP and DCPD (Stengården case study, KD derived from column experiments)

These results emphasize the importance of combining degradation processes and partitioning coefficients (K_D) when studying pollutant behavior in soils. K_D values were low and could reach even lower values for deeper soil horizons. Therefore, assuming no sorption or considering the molecule as a non-reactive tracer can be relevant in worst-case scenario assessment. Concerning degradation kinetics, assumptions of the specific K_D of the soil must be considered with caution.

In this case, metabolites may be present in the pesticide product itself as impurities from production. Contaminant plumes are composed of a mix of parent products (DCPP and MCP), impurities, known metabolites (4-CPP), and other metabolites. On this site, it was reported that 4-CPP degradation was slower than DCPP degradation, but the degradation kinetics of 4-CPP are not known (Overheu et al., 2015). Therefore, travel times coming from concentration measurements in groundwater samples could hardly be used with this complex mixture of pesticides and probable degradation of parent and daughter products.

In this study, the travel time was approximately 3 to 5 months for these pesticides. This travel time from waste buried in the first aquifer, estimated under unfavorable conditions, leaves sufficient time to adjust remediation solutions in case of a storm event (more pumping at the wells/hydraulic trap, for example).

3.3 Conclusion on the groundwater risk assessment at the Stengården case study

For the **Stengården case study**, the **groundwater intrinsic vulnerability** was assessed as **moderate**. The **pollutants of concern** (pesticides and their metabolites) were found to be **mobile to very mobile** substances according to the PMT (persistent, mobile, and toxic) classification by the German environmental agency, UBA. Therefore, **there is a high risk that pesticides and pesticide metabolites reach groundwater beyond the actual site**. The modeling indicated pollutant travel times of 96 to 143 days. Nevertheless, these travel times from waste buried in the clay layer to the first aquifer, estimated under worst-case conditions, leave sufficient time to adjust remediation solutions in case of a storm event (more pumping at the wells/hydraulic trap already in place to treat the pesticides in groundwater, for example).

4 Groundwater risk assessment in relation to the Besòs case study

In the Besòs basin, groundwater pollution problems are associated with various pollution sources, including landfill leaching, agricultural activities, industrial discharges, wastewater (wastewater treatment plant and sewage leaks), polluted soils, saline intrusion in the vicinity of the coast, among others.

4.1 Intrinsic vulnerability

The detailed intrinsic vulnerability assessment for the Besòs case study was presented in the UPWATER deliverable D5.5. Parameters and their corresponding ratings are presented in Annex 3 of this report.

4.2 Specific vulnerability

4.2.1 Pollutants considered in the frame of the groundwater risk assessment

Various pollution sources are present in the Besòs case study. In the frame of the UPWATER project, to produce new and innovative knowledge, the groundwater risk assessment focused on an emerging pollutant family that has not yet been considered in the different studies carried out in the area, but could contribute to the global environmental and health risk. This strategy will further allow for improving groundwater risk assessment by considering a more complete set of pollutants and, even if it is not directly planned in this task of the project, to carry out human health risk assessment in a more comprehensive way in future studies. This will help to strengthen the understanding of groundwater pollution. With regards to the industrial activities in the area, it has been decided to focus the study of the groundwater specific vulnerability on per- and polyfluoroalkyl substances (PFAS). This decision was also driven by the rising international concerns about these substances, due to their persistence in the environment, their toxicity, and their mobility in soils. In theory, this means that they can easily reach groundwater.

PFAS are a group of more than 12.000 synthetic fluorinated aliphatic compounds, made of carbon chains of different lengths and hydrophilic functional groups. These compounds are hydrophobic, thanks to their carbon chain, hydrophilic due to their functional group, and very stable due to their strong C-F bond, which is why they have been widely used in consumer products around the world since about the 1950s. They can be found in various everyday products, such as food packaging, or cookware to keep food from sticking, clothes and carpet to make them resistant to stains, as well as in firefighting foams (Cui et al., 2020; Buck et al., 2011). Nevertheless, these properties, coupled with their physical, chemical, and biological degradation resistance, lead to a high persistence in the environment, their bioaccumulation, and their ubiquitous presence in the environment (Sima and Jaffé, 2021; Ochoa-Herrera et al., 2016; Gyllenhammar et al., 2015; Ahrens, 2011). In addition, PFAS exhibit toxic effects. For example, PFOA (perfluorooctanoic acid) can lead to kidney or testicle cancer, a high cholesterol rate, or thyroid diseases (Winquist and Steenland, 2014b; 2014a; Barry et al., 2013). In general, PFAS are associated with endocrine disruptions, developmental abnormalities, and aggravated cancer risk (Cousins et al., 2020).

To date, no consensus has been found in literature on the influence of physical and chemical soil properties on the fate of PFAS in this environmental medium. PFAS behavior in soils will be different from other persistent organic pollutant behavior due to their combined hydrophilic and hydrophobic nature (Campos Pereira et al., 2018). Therefore, there is a need for data concerning PFAS fate and transport in soils, particularly from laboratory experiments conducted on real polluted soil samples. In addition, whereas PFOA and PFOS are the most studied PFAS in literature, other PFAS, such as fluorotelomer sulfonates, are not documented. That is why, in this study, up to 59 PFAS were investigated in soils, and up to 30 PFAS were analyzed in water.

A specific vulnerability analysis was conducted to identify if these pollutants can lead to a risk of groundwater pollution at this site.

4.2.2 Material and methods

4.2.2.1 Soil sampling (IDAEA)

At the Besòs case study, two soils were sampled by IDAEA in the frame of the UPWATER project: a non-polluted soil and a PFAS-polluted soil.

The non-polluted soil was sampled by IDAEA at the uppermost soil horizon (at a depth between 25 and 50 cm) at the end of September 2023. This sample is called “BCN soil sample” in this report. A soil cross-section at this location is presented in Figure 4. In this area, the superficial aquifer is composed of alluvial materials, primarily gravel and sand. The aquitard is made of silt and clay.

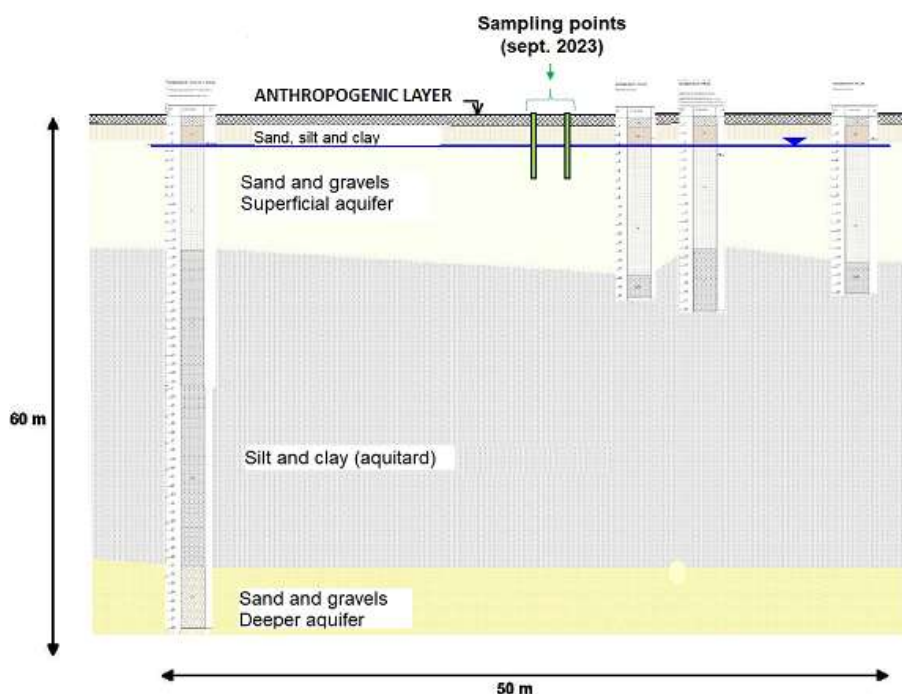


Figure 8: Soil cross-section (sampling location of BCN soil sample in Sept. 2023)

The PFAS-polluted soil was sampled by IDAEA at the end of January 2024, in an area where firefighting occurred. This activity is known to be one of the major PFAS soil pollution sources (Milley et al., 2018; Ahrens et al., 2015; Baduel et al., 2015; Filipovic et al., 2015). Three different depths were sampled: 2.3 to 2.5 m (sample S1) / 2.5 to 3.6 m (sample S2), and 6 to 6.5 m (sample S3). The lithology at the sampling location is the same as that presented in Figure 8.

Before conducting any experiments, all soil samples were air-dried at room temperature and sieved at 2 mm.

4.2.2.2 PFAS analyses in soil samples (Ineris)

In order to verify the PFAS content of these samples (BCN, S1, S2, and S3), PFAS were analyzed by Ineris in the fraction sieved at 2 mm. This soil fraction is the one commonly used in the frame of laboratory experiments for pollutant behavior assessment in soils. PFAS analyses were conducted in 2 steps on these samples. First, 22 PFAS were analyzed in these 4 samples (the 20 PFAS of the drinking water directive, as well as PFOSA and 10:2 FTS, see Table 8).

This first step was conducted to confirm the presence or absence of PFAS in the soil samples. When the presence of PFAS was confirmed, the second step of the soil PFAS analysis was carried out. This second step aimed to target more PFAS in polluted soil samples. As the supposed PFAS-polluted soil was sampled in an area where aqueous film-forming foams were used to extinguish fires, it was expected to find other PFAS, in addition to the 20 PFAS of the drinking water directive. Therefore, a total of 59 PFAS were analyzed in these samples.

Table 8: PFAS analysed in a first step in the Besòs soil samples

| Compound | Abbreviation | CAS no. | PFAS family |
|----------------------------------|--------------|-------------|-------------|
| Perfluorobutanoic acid | PFBA | 375-22-4 | PFCA |
| Perfluoropentanoic acid | PFPeA | 2706-90-3 | |
| Perfluorohexanoic acid | PFHxA | 307-24-4 | |
| Perfluoroheptanoic acid | PFHpA | 375-85-9 | |
| Perfluorooctanoic acid | PFOA | 335-67-1 | |
| Perfluorononanoic acid | PFNA | 375-95-1 | |
| Perfluorodecanoic acid | PFDA | 335-76-2 | |
| Perfluoroundecanoic acid | PFUnDA | 2058-94-8 | |
| Perfluorododecanoic acid | PFDoA | 307-55-1 | |
| Perfluorotridecanoic acid | PFTTrDA | 72629-94-8 | |
| Perfluorobutane sulfonic acid | PFBS | 375-73-5 | |
| Perfluoropentane sulfonic acid | PFPeS | 2706-91-4 | |
| Perfluorohexane sulfonic acid | PFHxS | 355-46-4 | |
| Perfluoroheptane sulfonic acid | PFHpS | 375-92-8 | |
| Perfluorooctane sulfonic acid | PFOS | 1763-23-1 | |
| Perfluorononane sulfonic acid | PFNS | 98789-57-2 | |
| Perfluorodecane sulfonic acid | PFDS | 335-77-3 | |
| Perfluoroundecane sulfonic acid | PFUnDS | 749786-16-1 | |
| Perfluorododecane sulfonic acid | PFDoDS | 79780-39-5 | |
| Perfluorotridecane sulfonic acid | PFTTrDS | 791563-89-8 | |
| Perfluorooctane sulfonamide | PFOSA | 754-91-6 | FASA |
| 10:2 fluorotelomer sulfonic acid | 10:2 FTS | 108026-35-3 | FTS |

Concentrations of the 22 PFAS analyzed in the samples in this first step are presented in Table 9.

PFAS content in BCN soil sample was low (1.9 µg/kg for the 22 PFAS analyzed), which confirms that this sample can be considered as a non-polluted soil, as regard to soil PFAS background values found in literature (Tang et al., 2021; Brusseau et al., 2020; Zhang et al., 2019; Meng et al., 2018; Wang et al., 2018; Rankin et al., 2016; Strynar et al., 2012).

Table 9: PFAS content of the Besòs soil samples BCN, S1, S2, and S3 (µg/kg).

| Compound | BCN | S1 | S2 | S2 |
|------------|-------|-------|-------|-------|
| PFBA | 0.3 | 1.4 | 1.1 | 0.5 |
| PFPeA | 0.2 | 4 | 4 | 2.2 |
| PFHxA | <0.1 | 4.6 | 5.4 | 0.9 |
| PFHpA | <0.1 | 2.4 | 3.2 | 0.4 |
| PFOA | 0.37 | 3.1 | 3.7 | <0.1 |
| PFNA | 0.1 | <0.1 | <0.1 | <0.1 |
| PFDA | 0.1 | <0.1 | <0.1 | <0.1 |
| PFUnDA | <0.1 | <0.1 | <0.1 | <0.1 |
| PFDoA | <0.1 | <0.1 | <0.1 | <0.1 |
| PFTTrDA | <0.1 | <0.1 | <0.1 | <0.1 |
| PFBS | <0.1 | 0.3 | 0.3 | <0.1 |
| PFPeS | <0.1 | 0.6 | 0.6 | <0.1 |
| PFHxS | <0.1 | 16.8 | 23 | 0.4 |
| PFHpS | <0.1 | 0.3 | 0.2 | <0.1 |
| PFOS | 0.81 | 3.6 | 5.1 | 1.4 |
| PFNS | <0.1 | <0.1 | <0.1 | <0.1 |
| PFDS | <0.1 | <0.1 | <0.1 | <0.1 |
| PFUnDS | <0.1 | <0.10 | <0.10 | <0.10 |
| PFDoDS | <0.1 | 0.1 | <0.10 | <0.10 |
| PFTTrDS | <0.1 | <0.10 | <0.10 | <0.10 |
| PFOSA | <0.1 | <0.10 | <0.10 | <0.10 |
| 10:2 FTS | <0.10 | <0.10 | 0.2 | <0.10 |
| Total PFAS | 1.9 | 37.2 | 46.8 | 5.8 |

Total PFAS concentrations in samples S1, S2, and S3 are presented in Figure 9. Error bars correspond to the analytical uncertainty.

Total PFAS concentrations are similar in samples S1 and S2, considering the analytical uncertainty (37.2 and 46.8 µg/kg, respectively). As the soil was taken from a firefighting area, PFAS concentrations were expected to be higher. In these soil samples, short-chain PFAS concentrations are slightly lower than long-chain PFAS concentrations. This is in accordance with previously published results, as short-chain PFAS are more mobile in soils than long-chain PFAS, so they should have been quickly transferred to deeper soil horizons (Kabiri and McLaughlin, 2021).

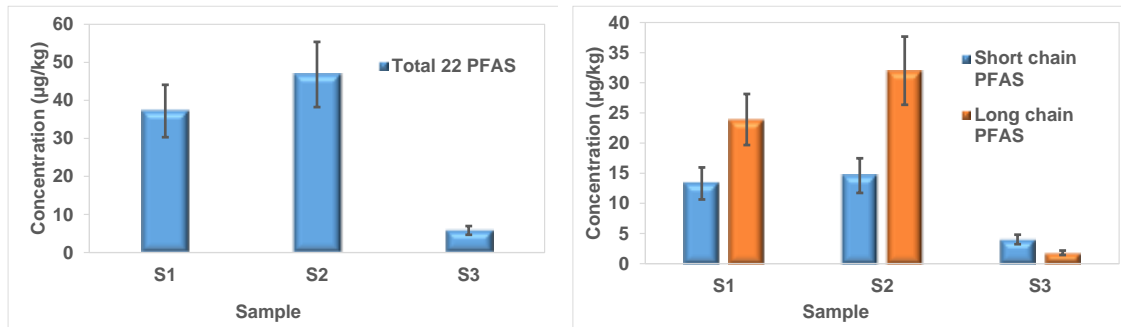


Figure 9: Total PFAS concentrations in the three samples (S1-S3) of the Besòs soil

These concentrations correspond to concentrations generally measured at some distance away from pollution sources (Brusseau et al., 2020). This could be explained by the fact that this pollution may be historic and that PFAS already reached deeper soil horizons. Sample S3 (6 to 6.5 m) exhibits lower pollution, with a total PFAS concentration of 5.8 µg/kg. This sample could be considered as a non-contaminated soil. Therefore, as a PFAS-contaminated soil was expected, only samples S1 (2.3 to 2.5 m) and S2 (2.5 to 3.6 m) will be discussed further and considered in the frame of the groundwater specific vulnerability assessment.

Concentrations of perfluoroalkyl carboxylic acids (PFCA) and perfluoroalkyl sulfonic acids (PFSA) in samples S1 and S2 are presented in Figure 10. Error bars correspond to the analytical uncertainty. In sample S1, PFCA and PFSA concentrations are similar, considering the analytical uncertainty (15.5 and 21.7 µg/kg, respectively). In sample S2, PFSA concentrations are higher than PFCA concentrations (29.2 and 17.4 µg/kg, respectively).

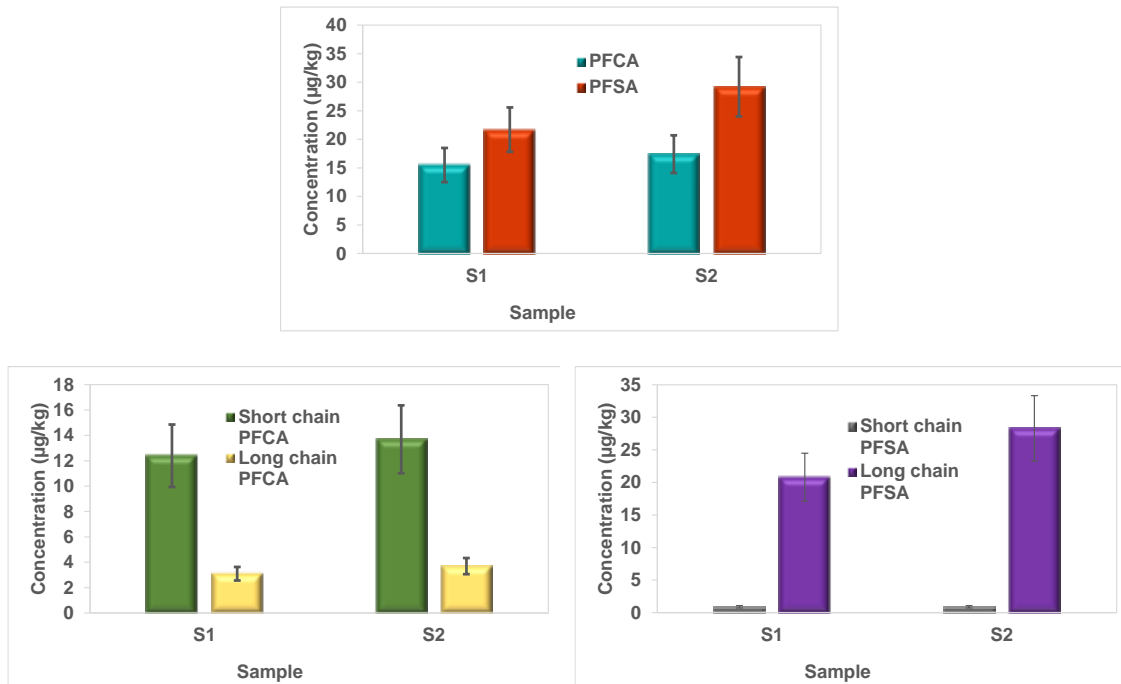


Figure 10: PFCA and PFSA concentrations in samples S1 and S2

In samples S1 and S2, short-chain PFCA concentrations are higher than long-chain PFCA concentrations. The short-chain PFCA correspond to PFBA, PFPeA, PFHxA, and PFHpA. These compounds were quantified in samples S1 and S2. The long-chain PFCA correspond to the other perfluoroalkyl carboxylic acids analysed. Among the long-chain PFCA, only PFOA was quantified in both soil samples.

In samples S1 and S2, the short-chain PFSA concentrations are lower than the long-chain PFSA concentrations. The short-chain PFSA correspond to PFBS and PFPeS. Both compounds were quantified in the soil samples. The long-chain PFSA correspond to the other perfluoroalkyl sulfonic acids analysed. Among the long-chain PFSA, only PFHxS, PFHpS, and PFOS were quantified in both samples. In sample S2, PFDoDS was also quantified at a concentration equal to the limit of quantification (0.1 µg/kg).

PFOSA and 10:2 FTS were not quantified in sample S1. Among these 2 PFAS, only 10:2 FTS was quantified at a concentration of 0.2 µg/kg in sample S2.

Both samples (S1 and S2) were mixed to form a composite sample on which the groundwater risk assessment was conducted. This composite sample will be referred to as “BCN-2” in this report. As explained earlier in this paragraph, a total of 59 PFAS were analyzed on this composite sample, on the soil fraction sieved at 2 mm. These 59 PFAS correspond to the 20 PFAS of the drinking water directive, PFOSA, and 10:2 FTS (presented in Table 8) and 37 other PFAS. These other PFAS are presented in Table 10.

Table 10: Other PFAS measured in BCN-2

| PFAS | Abbreviation | CAS nr | PFAS family |
|--|-----------------|--------------|-------------|
| Perfluorotetradecanoic acid | PFTeDA | 376-06-7 | PFCA |
| Perfluoropentadecanoic acid | PFPeDA | 141074-63-7 | |
| Perfluorohexadecanoic acid | PFHxDA | 67905-19-5 | |
| Perfluorooctadecanoic acid | PFODA | 16517-11-6 | |
| Perfluoro-3,7-dimethyloctanoic acid | 3,7-DMPFOA | 172155-07-6 | |
| 7H-perfluoroheptanoic acid | HPFHpA | 1546-95-8 | |
| 4,8-Dioxa-3H-perfluorononanoic acid | ADONA | 958445-44-8 | PFECA |
| Difluoro-2-[2,2,4,5-tetrafluoro-5-(trifluoromethoxy)-1,3-dioxolan-4-yl]oxyacetic acid | C6O4/F-DIOX | 1190931-41-9 | |
| Perfluoro-2-methoxypropanoic acid | PMPA | 13140-29-9 | |
| Perfluoro-4-oxapentanoic acid | PFMPA | 377-73-1 | |
| 2,3,3,3-tetrafluoro-2-(heptafluoropropoxy)propanoic acid | HFPO-DA / Gen-X | 13252-13-6 | |
| Perfluoro-ethylcyclohexanesulfonic acid | PFECHS | 335-24-0 | PFESA |
| 7H-perfluoro 4-methyl-3,6-dioxaoctanesulfonic acid | NAFION_BP2 | 749836-20-2 | |
| 9-Chlorohexadecafluoro-3-Oxanone-1-Sulfonic Acid | 9Cl-PF3ONS | 73606-19-6 | Cl-PFESA |
| 2-((8-chloro-1,1,2,2,3,3,4,4,5,5,6,6,7,7,8,8-hexadecafluorooctyl)oxy)-1,1,2,2-tetrafluoroethanesulfonic acid | 11Cl-PF3OUdS | 763051-92-9 | |

| PFAS | Abbreviation | CAS nr | PFAS family |
|---|--------------|-------------|-------------|
| Perfluorobutanesulfonamide | PBSA | 30334-69-1 | FASA |
| Perfluorohexanesulfonamide | PFHxSA | 41997-13-1 | |
| Perfluorooctanesulfonamide | PFOSA | 754-91-6 | |
| N-ethyl perfluorooctanesulfonamide | N-EtFOSA | 4151-50-2 | |
| N-methylperfluorobutanesulfonamide | MePFBSA | 68298-12-4 | |
| N-methylperfluorooctanesulfonamide | N-MeFOSA | 31506-32-8 | |
| N-methylperfluorobutane sulfonamide acetic acid | MePFBSAA | 159381-10-9 | FASAA |
| N-methylperfluorooctane sulfonamide acetic acid | N-MeFOSAA | 2355-31-9 | |
| Acide N-éthylperfluorooctanesulfamido acétique* | N-EtFOSAA | 2991-50-6 | |
| 2H,2H,3H,3H-perfluorooctanoic acid | 5:3 FTCA | 914637-49-3 | FTCA |
| 3-perfluoroheptylpropanoic acid | 7:3 FTCA | 812-70-4 | |
| 2H,2H-perfluorodecanoic acid | 8:2 FTCA | 27854-31-5 | |
| 2H,2H,3H,3H-perfluoroundecanoic acid | 8 :3 FTCA | 34598-33-9 | |
| 2H-perfluoro-2-octenoic acid | 6:2 FTUCA | 70887-88-6 | FTUCA |
| 2H-perfluoro-2-decenoic acid | 8:2 FTUCA | 70887-84-2 | |
| Ethylperfluorooctanesulfonamidoethanol | EtFOSE | 1691-99-2 | FOSE |
| Methylperfluorooctanesulfonamidoethanol | MePFOSE | 24448-09-7 | |
| 4:2 Fluorotelomer sulfonic acid | 4:2 FTS | 757124-72-4 | FTS |
| 6:2 Fluorotelomer sulfonic acid | 6:2 FTS | 27619-97-2 | |
| 8:2 Fluorotelomer sulfonic acid | 8:2 FTS | 39108-34-4 | |
| 6:2 polyfluoroalkylphosphate diester | 6:2 diPAP | 57677-95-9 | PAP |
| 6:2 fluorotelomer sulfonamide alkylbetaine | 6:2 FTAB | 34455-29-3 | FTAB |

PFAS analysis in the composite sample BCN-2 showed the presence of 5 PFAS families in this soil: PFCA, PFSA, FTS, FASA, and FTAB. Figure 11 shows the proportion of these different PFAS families in the soil sample and the concentrations of the PFAS from the drinking water directive (DWD). These PFAS are identified as PFCA DWD and PFSA DWD.

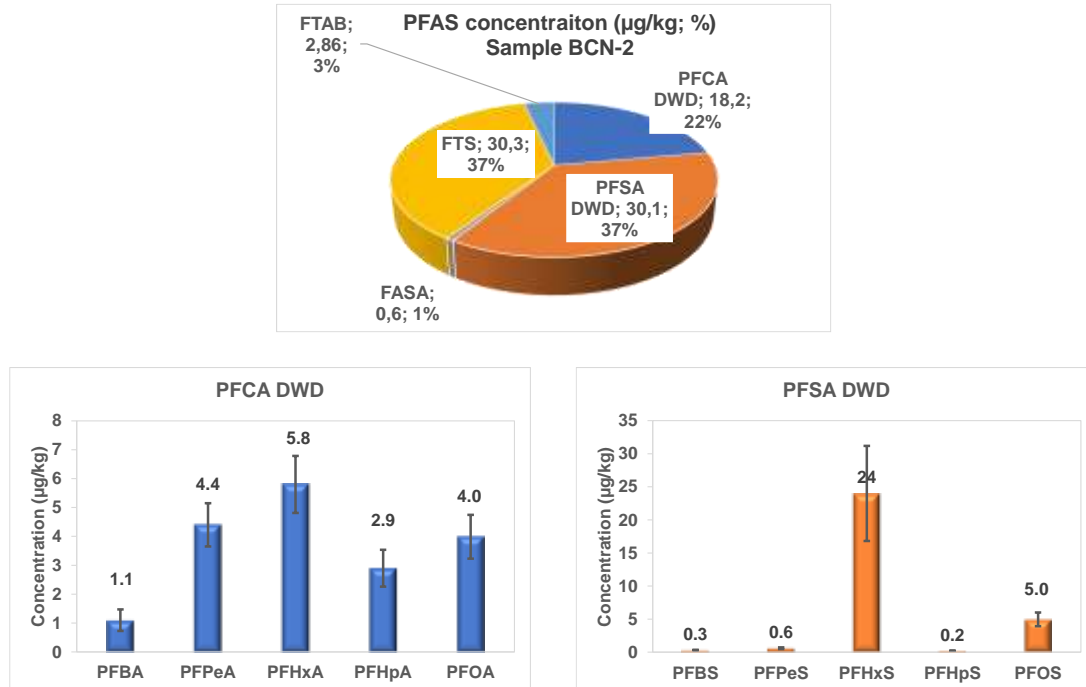


Figure 11: PFAS families quantified in BCN-2 soil sample and concentrations of PFAS from the DWD

In this soil sample, the total concentration of the 20 PFAS from the DWD was 48.3 µg/kg. Total PFSA concentration was higher than total PFCA concentration (30.1 and 18.2 µg/kg, respectively).

Only 5 PFSA were quantified in this soil sample, corresponding to molecules having between 4 and 8 carbon atoms. PFHxS is the main PFSA with a concentration of 24 µg/kg. The other PFSA (PFBS, PFPeS, PFHpS, and PFOS) were measured at lower concentrations (0.3, 0.6, 0.2, and 5 µg/kg, respectively). PFOS and PFHxS are 2 PFSA commonly found in soils where aqueous film-forming foams (AFFF) were used to extinguish fires (Mesfin Tefera et al., 2022).

Only 5 PFCA were quantified in this soil sample, at concentrations between 1.1 and 5.8 µg/kg, corresponding to molecules having between 4 and 8 carbon atoms (PFBA, PFPeA, PFHxA, PFHpA, and PFOA). PFHxA is the main PFCA with a concentration of 5.8 µg/kg. This was also observed by other authors on sites where AFFF were used (Hubert et al., 2023). The presence of PFOA is consistent with the use of AFFF (Mesfin Tefera et al., 2022).

Total PFAS concentration in BCN-2 soil sample was 82 µg/kg, meaning that the 20 PFAS from the DWD represent only 59% of the total PFAS measured in this soil. FTS were measured as well at a concentration of 30.3 µg/kg, representing 37% of the total PFAS concentration. This concentration was similar to the PFSA concentration. Among the FTS, 6:2 FTS was the dominant PFAS with a concentration of 29.3 µg/kg. 8:2 FTS and 10:2 FTS were also quantified, at lower concentrations (0.8 and 0.2 µg/kg). Other authors highlighted the presence of FTS in such soils, in similar proportions compared to PFCA and PFSA (Houtz et al., 2013). These PFAA precursors can represent up to 99% of the detected organofluorine compounds (Glover et al., 2024). FTS were measured in soils and groundwater where AFFF were used, which is consistent with the composition of these foams, containing 6:2 FTS (Battye et al., 2024; Backe et al., 2013; Herzke

et al., 2012). In addition, 6:2 FTS is a degradation product of other PFAS found in AFFF, particularly 6:2 FTAB (6:2 sulfonamidoalkyl betaïne fluorotelomer), which is one of the main compounds of AFFF (Yan et al., 2024; Shaw et al., 2019). In this soil, 6:2 FTAB was measured at a concentration of 2,9 µg/kg, representing 3% of the PFAS measured. The use of 6:2 FTS as a substituent of perfluorinated compounds with a carbon chain containing at least 7 carbon atoms, like PFOS, PFOA, and PFHxS, is increasing in AFFF (Méndez et al., 2022; Hamid et al., 2020).

In this soil sample, 2 FASA (PBSA and PFHxSA) were quantified at concentrations of 0.16 and 0.41 µg/kg, respectively. Their presence in this soil is consistent with literature data, showing that this PFAS family is generally not abundant in soils where AFFF were applied (Hubert et al., 2023).

The results of PFAS analyses in soils showed that, for the Besòs case study, 2 types of soil were sampled: a PFAS-polluted soil and a non-polluted soil. Therefore, the groundwater risk assessment has been done by assessing, on the one hand, PFAS release from the polluted soil and on the other hand, PFAS transfer in the non-polluted soil, representing PFAS migration in soils (saturated and unsaturated zones) after being released from soil pollution sources.

4.2.2.3 Soil physical and chemical characterization (Ineris)

A physical and chemical characterization was conducted by Ineris on both soil samples (BCN and BCN-2). Results are presented in Table 11.

Both soils have a basic pH: 8.5 for BCN and 8 for BCN-2. They are mainly composed of sand (58 wt.% for BCN and 53 wt.% for BCN-2). Nevertheless, the BCN sample is composed of coarser sand than the BCN-2 sample. Both soils have a low organic matter content (0.9% for BCN and 0.2% for BCN-2).

With these characteristics concerning the granulometry and the organic matter content, a low PFAS retention is expected in this soil, meaning that a pollution entering the soil from the unsaturated zone will have a great potency to move toward groundwater and then, move far away from the pollution source. Nevertheless, it is known that PFAS sorption onto soil cannot be predicted from its organic matter content alone (Sharifan et al., 2021; Li et al., 2018). Soil mineral constituents will also play a role, particularly in the sorption of ionic PFAS (Lyu et al., 2020). However, data concerning soil constituents responsible for PFAS sorption in soils in literature do not converge. Some authors showed that PFAS sorption in soils could be predicted by TOC (total organic carbon) and clay content (Hunter Anderson et al., 2019), others by organic carbon content, clay and silt content and pH (Knight et al., 2019) and others by organic carbon content, metal oxides and silt and clay content (Wang et al., 2021). Therefore, trying to predict PFAS release and transfer in the Besòs soil could be a challenging task, and uncertainty in the results could be high. That is why, in the frame of the groundwater risk assessment for the Besòs case study, laboratory experiments were carried out to evaluate the release and transfer potential of PFAS. These experiments are described in the following section of this report.

Table 11: Soil physical and chemical characteristics

| Granulometry (g kg ⁻¹) | | | | | | | | | | |
|---|----------------|-------|---------------------------------------|-------|-------------------------------|-------|-----------------------|-------|---------------------------|-------|
| Parameter | Clay (< 2 µm) | | Fine silt (2/20 µm) | | Coarse silt (20/50 µm) | | Fine sand (50/200 µm) | | Coarse sand (200/2000 µm) | |
| Sample | BCN | BCN-2 | BCN | BCN-2 | BCN | BCN-2 | BCN | BCN-2 | BCN | BCN-2 |
| Value | 126 | 123 | 160 | 178 | 138 | 168 | 178 | 331 | 398 | 200 |
| Organic carbon and total nitrogen (g kg ⁻¹) | | | | | | | | | | |
| Parameter | Organic carbon | | Total nitrogen | | Total carbon | | C/N | | Organic matter | |
| Sample | BCN | BCN-2 | BCN | BCN-2 | BCN | BCN-2 | BCN | BCN-2 | BCN | BCN-2 |
| Value | 5.3 | 1.3 | 0.5 | 0.2 | 20.3 | 1.3 | 10.1 | 5.5 | 9.2 | 2.3 |
| pH and Cation Exchange Capacity | | | | | | | | | | |
| Parameter | pH (water) | | Total limestone (g kg ⁻¹) | | CEC (cmol+ kg ⁻¹) | | | | | |
| Sample | BCN | BCN-2 | BCN | BCN-2 | BCN | BCN-2 | | | | |
| Value | 8.5 | 8 | 125 | <1 | 12.1 | 12.9 | | | | |

4.2.2.4 PFAS release from BCN-2 soil sample (Ineris)

4.2.2.4.1 Laboratory experiments

PFAS release experiments from BCN-2 soil sample were carried out by Ineris in order to evaluate the interactions of the studied PFAS with the soil, by means of batch experiments. In the frame of the groundwater risk assessment, these experiments aimed to evaluate the release potential of PFAS, quantified with a desorption partitioning coefficient (K_{des}).

All experiments were conducted in triplicate in 50 mL polypropylene centrifuge tubes at a temperature of 21 ± 2 °C. A quantity of 15 g of soil was introduced into each vial, and 20 mL of a desorption solution was added to reach an L/S ratio of 1.3. The desorption solution was made of calcium chloride dihydrate ($\text{CaCl}_2 \cdot 2\text{H}_2\text{O}$) at a concentration of 0.5×10^{-3} mol/L and sodium azide (NaN_3) at a concentration of 0.2 g/L. This soil/solution mixture was shaken in an end-over-end shaker. In the frame of other research projects conducted by Ineris, it has been shown that PFAS release from polluted soils was fast and an equilibrium was reached before 24 h. Hence, the shaking time was set to 24 h for these experiments. The soil/solution mixture was then centrifuged at 3,000 G for 30 min, and 10 mL of the supernatant were sampled.

PFAS were then extracted from this solution by adding 10 mL of methanol, as well as mass-labelled internal standards. This solution was then shaken for 15 min and centrifuged at 20,000 G for 20 min. Solutions were stored in the freezer in polypropylene vials and then analyzed by Ineris by LC-MS/MS.

Control vials containing the desorption solution without soil underwent the same procedure to account for potential PFAS pollution during the experiment.

Desorption partitioning coefficients were then calculated following Equation 5.

4.2.2.4.2 Statistical analysis

To identify whether the mean values of PFAS release percentages were significantly different from each other, an analysis of variance (ANOVA) was conducted for each PFAS family with more than 2 PFAS quantified in solution at equilibrium. For PFAS families with only 2 PFAS quantified in solution, a Student's t-test was performed to compare the two means. This test is equivalent to an ANOVA when only two means have to be compared. One-way ANOVA is a statistical method used to compare the means of several groups simultaneously. Unlike running multiple t-tests, which would increase the risk of statistical error, ANOVA provides a single global test to assess whether the assumption that all group means are equal can be rejected. The hypothesis for conducting an ANOVA were verified, particularly the variance homogeneity with a Levene test.

However, ANOVA alone does not identify which specific groups differ. Therefore, an additional *post hoc* test, the Tukey's HSD test, was used to determine the source of the differences.

The Tukey HSD test was used to compare all pairwise differences between means after the ANOVA. Interpretation was based on two equivalent criteria: if the confidence interval for the difference does not include zero, or if the adjusted p-value is below the 0.05 threshold, then the difference between the two groups is considered statistically significant. Conversely, if the interval includes zero or the p-value is greater than 0.05, there is no statistically significant difference between the groups. The Tukey test is widely used in experimental data analysis because it robustly identifies which means truly differ from each other, while controlling the overall risk of false positives.

4.2.2.5 PFAS sorption/desorption isotherms on BCN soil sample (Ineris)

PFAS sorption/desorption experiments were conducted by Ineris on the BCN soil sample. All experiments were conducted in triplicate in 50 mL polypropylene centrifuge tubes at a temperature of 21 ± 2 °C.

4.2.2.5.1 Sorption isotherm determination

For the sorption isotherm determination, 15 g of soil were added to each vial. First, a conditioning step of the soil was performed: 10 mL of the background solution (calcium chloride dihydrate ($\text{CaCl}_2 \cdot 2\text{H}_2\text{O}$) at a concentration of 0.5×10^{-3} mol/L and sodium azide (NaN_3) at a concentration of 0.2 g/L) were added to the soil and shaken for 1 hour in an end-over-end shaker to moisten the dry soil and prevent experimental artifacts. Then, 10 mL of a solution containing a mixture of 30 PFAS prepared in the background solution were added to the vial and mixed in order to reach the equilibrium time using the same apparatus. Initial aqueous concentrations of PFAS were in the range of 50 – 500 ng/L. When the percentage of sorption achieved was constant, equilibrium was reached. The soil/solution mixture was then centrifuged at 3,000 G for 30 min, and 2 mL of the supernatant were sampled. PFAS were then extracted from this solution by adding 8 mL of methanol, as well as mass-labelled internal standards. This solution was then shaken for 15 min and centrifuged at 20,000 G for 20 min. Solutions were stored in the freezer in polypropylene vials, and PFAS in these solutions were analyzed by Ineris by LC-MS/MS. The amounts of sorbed PFAS were calculated according to Equation 2.

Note that the percentage of methanol for PFAS extraction was increased for these experiments, compared to the release experiments. This was in accordance with the evolution of the PFAS analysis protocol, since it has been demonstrated that increasing the methanol percentage could improve the extraction of long-chain PFAS.

Simultaneously, control vials containing the PFAS mixture at the different concentrations tested in the absence of soil and blank vials containing the background solution and soil in the absence of the studied PFAS, underwent the same procedure to account for potential losses due to photolysis or wall adsorption, and to evaluate the potential leaching of PFAS initially present in the dry soil, as a total PFAS concentration of 1.9 µg/kg was measured in this soil.

Preliminary experiments were performed to determine the equilibrium time (sorption kinetic experiments). The study consisted of monitoring the PFAS aqueous phase concentration throughout the experiment (up to 7 days). After the conditioning step presented previously, 10 mL of the 28 PFAS mixture prepared in the background solution at a concentration of 1,000 ng/L were added. These vials underwent the same procedure as described above. The concentrations of PFAS were measured along the sorption experiment at seven different times: 1 h, 6 h, 16 h, 24 h, 3 d, 5 d, and 7 d. The results of the kinetic studies showed that sorption equilibrium was reached after 1 to 6 h, and no variations in concentrations until 7 days were observed. Therefore, a 24 h contact time between the soil and the solution was used.

4.2.2.5.2 Desorption isotherm determination

When the PFAS sorption step on the BCN soil sample was completed and the supernatant collected for analysis, the remaining soil/solution mixture was centrifuged at 3,000 G for 30 min, and the remaining solution was removed. Each vial was placed in an oven at 40 °C for 5 days to dry the soil sample. The soil mass was monitored during this step. Then, the PFAS desorption was carried out with the same procedure as the one described for PFAS release experiments from the BCN-2 soil sample. The PFAS extraction procedure was the same as the one described for the sorption isotherm determination, with 8 mL of methanol added to 2 mL of solution.

As these desorption experiments were carried out on a freshly polluted soil (polluted during the sorption step), preliminary experiments were also performed to determine the equilibrium time (desorption kinetic experiments). The study consisted of monitoring the PFAS aqueous phase concentration throughout the entire experiment (up to 7 days). Vials shaken during 24 h in the sorption step were used for this experiment. A volume of 20 mL of the background solution was added to the vials containing 15 g of soil. These vials underwent the same procedure as described for the desorption isotherm determination. The concentrations of PFAS were measured along the desorption experiment at seven different times: 1 h, 6 h, 16 h, 24 h, 3 d, 5 d, and 7 d. The results of the kinetic studies showed that the desorption equilibrium was reached after 5 days.

4.2.3 Results of the specific vulnerability assessment

4.2.3.1 PFAS release experiments from BCN-2 soil sample

Figure 12 presents the boxplot of the PFAS release percentages from the BCN-2 soil sample. The boxplot shows the distribution of release percentages for each molecule quantified in solution. The box illustrates the interquartile range (50% of the central values), and the horizontal line inside represents the median. Black dots correspond to individual measurements, while the colored symbols represent the mean value for each molecule. Colors highlight the different groups of molecules under comparison (PFCA, PFSA, and FTS). Error bars were calculated to consider a 95% confidence interval, thanks to the following equation:

$$IC_{95\%} = \bar{x} \pm t \frac{s}{\sqrt{n}} \quad \text{Equation 9}$$

With \bar{x} the mean value of the release percentages of the 3 replicates, t the quantile of the Student's t-distribution associated with a 95 % confidence interval (4.303 in this case), s the standard deviation, and n the sample size (3 in this case).

The letters above each box indicate the results of Tukey's HSD test. Two molecules sharing the same letter are not significantly different in terms of release percentages ($p > 0.05$), while different letters indicate a statistically significant difference in release percentages.

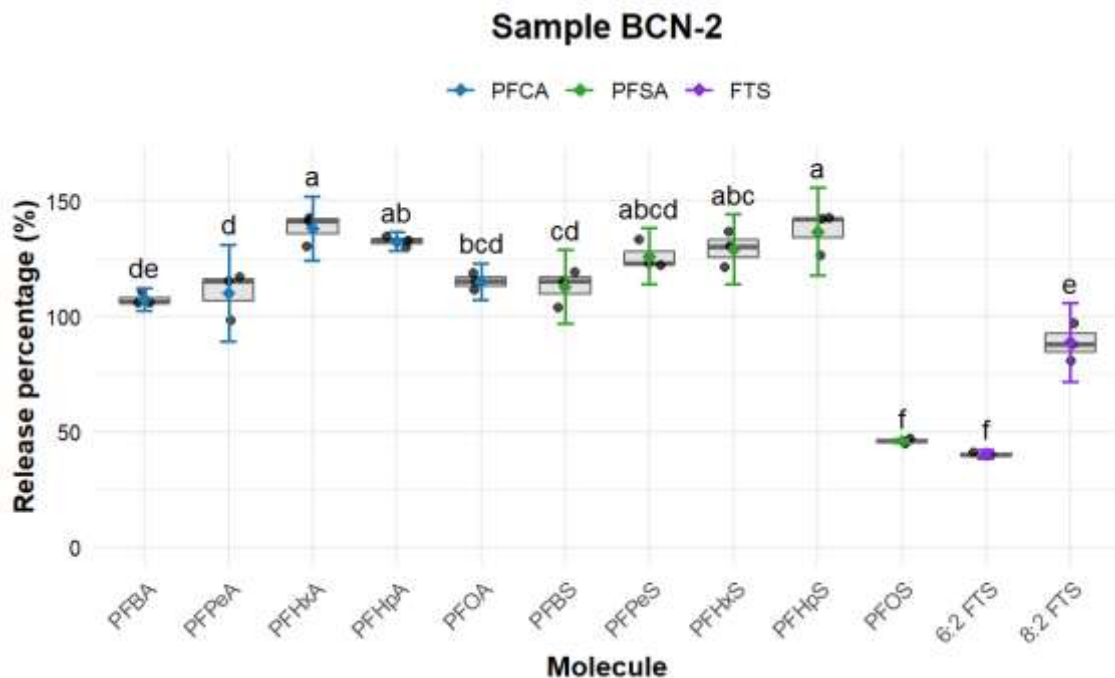


Figure 12: PFAS release from BCN-2 soil sample

At equilibrium (24h), 12 PFAS were quantified in solution. PBSA and PFHxSA were measured in the soil but were not analyzed in the solutions. 10:2 FTS was present as well in the soil, but was below the quantification limit in the solutions.

Except for PFOS, 6:2 FTS, and 8:2 FTS, release percentages were higher than 100%. This is due to both uncertainties in the solution and soil concentrations. Release percentages of these 3 molecules were 46, 40, and 89 %, respectively.

For **short-chain PFSA** (PFBS and PFPeS), the Student's t-test showed that release percentages were not significantly different. The experiment showed that both PFAS were totally released in solution.

For the other PFAS families (PFCA, long chain PFSA, and FTS), the ANOVA and the Student's t-test revealed that within each group, at least one mean value of the release percentages was significantly different than the others.

Among PFCA, Tukey’s test indicated that the release percentage of PFHxA was significantly higher than that of PFBA, PFPeA, and PFOA. Release percentages of these 3 molecules were not significantly different. The release percentage of PFHpA was significantly higher than that of PFBA and PFPeA but was not significantly different than that of PFHxA and PFOA. Therefore, among PFCA, the molecule with 6 carbon atoms is the one that exhibited the highest release.

Among long-chain PFSA, the release percentages of PFHxS and PFHpS were not significantly different. Both molecules exhibited a release percentage significantly higher than that of PFOS (46%). If molecules with the same number of carbon atoms are compared between PFCA and PFSA, release percentages were not significantly different, except for PFOS, exhibiting a significantly lower release percentage than that of PFOA. This confirms that, for molecules with 8 carbon atoms, PFSA shows a higher affinity for the soil matrix than PFCA.

Among FTS, the release percentage of 6:2 FTS was significantly lower than that of 8:2 FTS (40% and 89%, respectively). It was not significantly different than that of PFOS but significantly lower than that of the other molecules, considering all PFAS families. Release percentages of 8:2 FTS and PFBA were comparable.

Even if these experiments carried out at the laboratory scale under controlled conditions can lead to higher release percentages than the ones observed in the field (Mahmood-UI-Hassan et al., 2008; Enell et al., 2004), they can give a good overview of the pollutant behavior and allow for quantifying it. These release percentages have to be compared with those of other organic compounds such as PAHs, generally exhibiting release percentages lower than a few percent (Roskam and Comans, 2009).

Our results indicate that PFAS have a very weak affinity for this soil and that they can easily migrate to groundwater. To quantify the extent of PFAS mobility, soil-water partitioning coefficients during desorption (K_{Des}) and soil organic carbon-water partitioning coefficients (K_{Oc}) were calculated (see Table 12) for PFOS, 6:2 FTS, and 8:2 FTS. As the other PFAS were entirely released from the soil, no K_{Des} can be calculated for these compounds. Therefore, their behavior was similar to a tracer, meaning that they will be very mobile in this soil.

Table 12: Soil-water partitioning coefficients and soil organic carbon-water partitioning coefficients for PFAS released from the BCN-2 soil sample.

| PFAS | PFOS | 6:2 FTS | 8:2 FTS |
|------------------|------|---------|---------|
| K_{Des} (L/kg) | 1.6 | 2 | 0.2 |
| Log K_{Oc} | 3.1 | 3.2 | 2.1 |

As explained in chapter 3.2.3.1, log K_{Oc} was used to rank the mobility of PFOS, 6:2 FTS, and 8:2 FTS according to the German environmental agency, UBA. PFOS and 6:2 FTS were classified as “mobile” because the log K_{Oc} was below 4, and 8:2 FTS was classified as “very mobile” because the log K_{Oc} was below 3.

Therefore, given the results of the intrinsic vulnerability analysis at this case study, showing that groundwater was moderately vulnerable to surface pollution, it can be considered that there is a high risk at this case study that PFAS reach groundwater.

4.2.3.2 PFAS sorption/desorption isotherms on BCN soil sample

The specific vulnerability of groundwater in this case study was further addressed by working on a non-polluted soil. This situation is representative of the PFAS migration in a non-polluted soil, after being released from the pollution sources.

In the experiments concerning the BCN soil sample, it was possible to plot sorption isotherms for 10 PFAS out of the 30 PFAS analyzed in water, allowing to calculate a soil-water partitioning coefficient (K_D). These 10 PFAS were PFBA, PFHxA, PFHpA, PFOA, PFNA, PFBS, PFHxS, PFHpS, PFOS, and FOSA. These isotherms are presented in Annex 4 of this report. An example for PFNA, PFHxS, PFHpS, and FOSA is presented in Figure 13. Error bars were calculated to consider a 95% confidence interval when two or three out of the three replicates showed consistency. If only one replicate was deemed consistent, the error bars were calculated to represent the global uncertainty.

For 7 PFAS (PFPeS, 4:2 FTS, 6:2 FTS, 8:2 FTS, ADONA, HFPO-DA, and 9CI-PF3ONS), it was not possible to plot the isotherm because only 2 concentrations were consistent. Nevertheless, it was possible to calculate a K_D for these 7 molecules as well, using Equation 5 for each concentration. The mean value of the K_D calculated for each concentration was considered.

For 1 PFAS (PFPeA), the concentrations measured in solution after the sorption experiment were similar to those introduced in the spiked solution. This means that no sorption could be observed for this compound. Its behavior can therefore be compared to that of a tracer.

The other 12 PFAS were not quantified in solution after the sorption experiment, meaning that all the PFAS mass introduced in the soil-solution system was sorbed onto the soil. This does not mean that these PFAS will not be mobile at all in soils. In the experimental conditions, these PFAS were found to be less mobile than the others. With less soil or with a higher concentration of these PFAS in the soil-solution system, the sorption could be precisely quantified. These PFAS are PFNS, PFDS, PFUnDS, PFDoDS, PFTrDS, PFDA, PFUnDA, PFDoDA, PFTrDA, PFTeDA, PFODA, and 10 :2 FTS. They correspond to PFSA from 9 to 13 carbon atoms, PFCA from 10 to 14 and 18 carbon atoms, and a FTS with 10 perfluorinated carbon atoms. These molecules are the ones with the longest carbon chain length among the PFAS analyzed in these PFAS families. This is consistent with literature, indicating that long-chain PFAS have a greater affinity for the soil matrix than shorter-chain PFAS, due to the increased hydrophobicity of the longer carbon chains (Kleja et al., 2025).

Sorption isotherms were found to be linear in the experimental conditions, following the equation:

$$q_e = K_D C_e \quad \text{Equation 10}$$

In this equation, q_e (ng/kg) is the amount of sorbed PFAS per mass of soil, C_e (ng/L) is the PFAS equilibrium aqueous concentration, K_D (L/kg) is the soil-water partitioning coefficient for the linear model calculated from the slope of the isotherm plot.

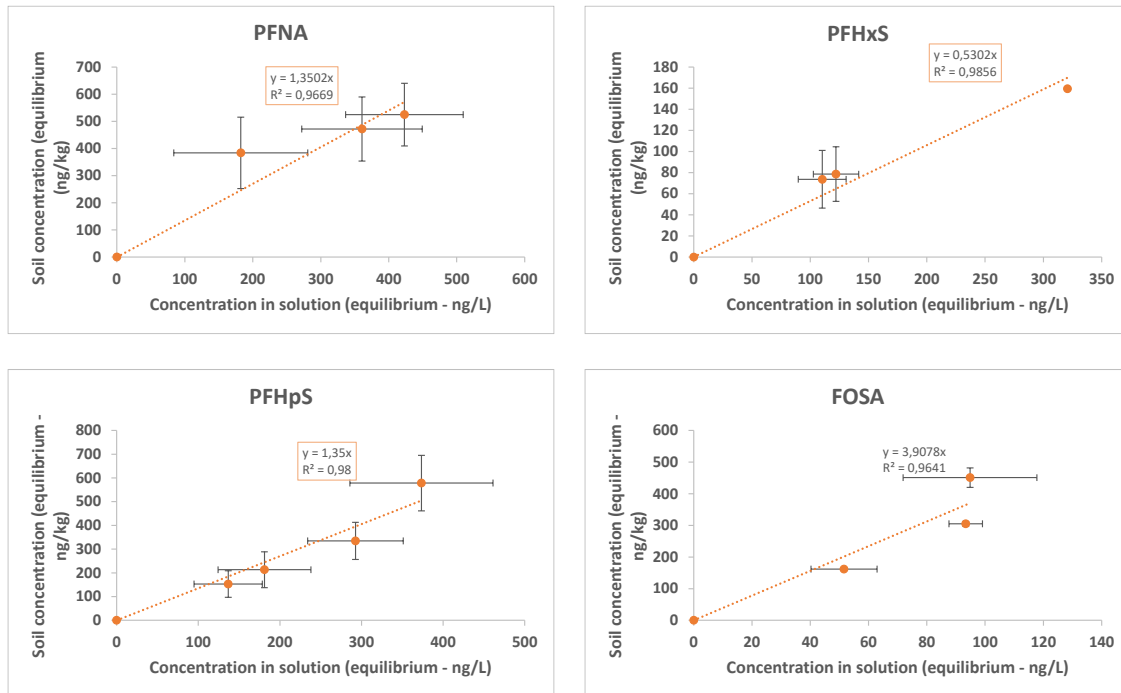


Figure 13: PFAS sorption isotherms on BCN soil sample

The soil-water partitioning coefficients calculated for the Besòs case study are presented in Table 13.

Table 13: Soil-water partitioning coefficients for the Besos case study

| PFAS | PFBA | PFPeA | PFHxA | PFHpA | PFOA | PFNA | PFBS | PFPeS | PFHxS |
|-----------------------|-------|-------|---------|---------|---------|---------|------------|-------|-------|
| K _D (L/kg) | 0.39 | 0 | 0.19 | 0.36 | 0.63 | 1.35 | 0.47 | 0.35 | 0.53 |
| K _{oc} | 74 | - | 36 | 68 | 118 | 255 | 89 | 65 | 100 |
| log K _{oc} | 1.9 | - | 1.6 | 1.8 | 2.1 | 2.4 | 2.0 | 1.8 | 2.0 |
| PFAS | PFHpS | PFOS | 4:2 FTS | 6:2 FTS | 8:2 FTS | HFPO-DA | 9Cl-PF3ONS | ADONA | PFOSA |
| K _D (L/kg) | 1.35 | 5.88 | 0.47 | 0.42 | 6.13 | 0.27 | 14.33 | 0.18 | 3.91 |
| K _{oc} | 255 | 1 112 | 89 | 79 | 1 159 | 51 | 2 709 | 34 | 739 |
| log K _{oc} | 2.4 | 3.0 | 1.9 | 1.9 | 3.1 | 1.7 | 3.4 | 1.5 | 2.9 |

Regarding the uncertainties associated with the K_D calculation, it can be considered that K_D below 1L/kg are not significantly different, denoting very mobile compounds. This corresponds to PFCA containing up to 8 carbon atoms (PFBA, PFPeA, PFHxA, PFHpA, and PFOA) and PFSA with up to 6 carbon atoms (PFBS, PFPeS, and PFHxS). This is confirmed by their log K_{OC} values, which are below 3, showing that these PFAS are very mobile in soils. As explained in chapter 3.2.3.1, log K_{OC} was used to rank the mobility of these PFAS according to the German environmental agency, UBA. Then, for the longer chain PFCA and PFSA, the K_D increased with an increasing carbon chain length. This was observed for PFNA, PFHpS, and PFOS. Nevertheless, according to the UBA classification, they can still be considered as very mobile substances.

For 4:2 and 6:2 FTS, K_D are not significantly different. Then, for 8:2 FTS, the K_D value is higher, denoting a higher sorption of longer chain FTS.

HFPO-DA and ADONA are used as PFOA substituents in fluoropolymer synthesis. They contain 6 and 7 carbon atoms, respectively. These molecules have a K_D of the same order of magnitude as the PFAS with the lower observed sorption, meaning that they are very mobile in soils. In particular, their K_D is not significantly different from the one calculated for the molecule they substitute. Nevertheless, another substituent (9CI-PF3ONS) showed the highest K_D in this study, being still classified as a mobile molecule thanks to the UBA classification. This is an important finding, showing that **substituents may not necessarily be a good alternative in terms of environmental behavior**.

PFOSA is a PFOS precursor, containing 8 carbon atoms. Its K_D is lower than the one calculated for PFOS, classifying it as a very mobile substance.

In addition, these results confirm that, for molecules with the same number of carbon atoms, PFSA sorption in soils is higher than PFCA sorption.

In addition, the desorption experiments allowed us to calculate a desorption soil-water partitioning coefficient K_{Des} for 9 PFAS out of the 17 PFAS for which the retention onto the soil during the sorption experiments could be quantified (PFBS, PFHxS, PFHpS, PFOS, PFOA, PFNA, FOSA, 6:2 FTS, and 8:2 FTS). It was not possible to plot desorption isotherms because only 1 or 2 concentrations were suitable for evaluation. K_{Des} for these 9 molecules were calculated using Equation 5 for each concentration. The mean value of the K_{Des} calculated for each concentration is presented in Table 14.

Table 14: Soil-water partitioning coefficients for the Besòs case study

| PFAS | PFBS | PFHxS | PFHpS | PFOS | PFOA | PFNA | FOSA | 6:2 FTS | 8:2 FTS |
|------------------|------|-------|-------|------|------|------|------|---------|---------|
| K_{Des} (L/kg) | 0.35 | 0.68 | 1.14 | 3.42 | 0.15 | 0.69 | 4.43 | 0.08 | 5.28 |

For the other 8 PFAS showing retention onto the soil during the sorption experiments (PFBA, PFHxA, PFHpA, PFPeS, 4:2 FTS, ADONA, HFPO-DA, and 9CI-PF3ONS), it was not possible to calculate a K_{Des} for two reasons: concentrations were below the quantification limit, or when the molecule was quantified, initial and final concentrations were too close to allow a robust calculation.

For the other 12 PFAS that were not quantified in solution after the sorption experiment (PFNS, PFDS, PFUnDS, PFDoDS, PFTrDS, PFDA, PFUnDA, PFDoDA, PFTrDA, PFTeDA, PFODA, and 10 :2 FTS), they were not quantified after the desorption experiment, denoting their stronger affinity for the soil matrix again.

Therefore, given the results of the intrinsic vulnerability analysis at this case study, showing that groundwater was moderately vulnerable to surface pollution, and the results of the specific vulnerability, showing that PFAS are mobile to very mobile substances, **it can be considered that there is a high risk at this case study that PFAS reach groundwater.**

4.2.3.3 PFAS travel time calculation (Ineris)

The time needed for these pollutants to reach groundwater was calculated using the HYDRUS-1D model by Ineris. Parameters used to build the conceptual model were extracted from the UPWATER D3.7 report and were based on the intrinsic and specific vulnerability assessment presented in the previous paragraphs.

4.2.3.3.1 Specificity of the Besòs case study

In the Besòs case study, it was assumed that the PFAS pollution of subsurface water and groundwater was originating from contaminations of anthropogenic soil by firefighting and past industrial activities. Urban groundwater recharge was specially studied in the area of the Besòs delta. Many recharge and pumping systems existing in that area were studied (Tubau et al., 2017; Vazquez-Sune, 2003). These works concerned the assessment of groundwater recharge quantification in urban environments, in which paved areas and sewage leaks should be taken into account. Therefore, natural rainfall infiltrations will constitute a small fraction of the total recharge. For the modeling phase, the scenario conducted under worst-case conditions took into account the lowest hydraulic conductivities of the soil layers, allowing more infiltration. For the average scenario, the natural recharge was used. Stormwater is also a major contributor to diffuse urban pollution.

4.2.3.3.2 Intrinsic vulnerability parameters considered

- Soil column and water table depth

In the Besòs case study, the topsoil layer could be divided into 2 sublayers. The first one is related to anthropogenic works done in the historical part of the Besòs delta. In the frame of the modeling phase, the anthropogenic topsoil layer is not relevant as infiltration occurred in very specific areas with a probable bypass of the first-level topsoil. The first layer considered in the modeling was therefore the superficial subsoil located between 1 and 2 m below ground level. The PFAS pollution source in the conceptual model was located at the top of this layer. Parameters associated with this superficial subsoil were derived from those of the stratified unit described as unit F in a previous hydrogeological model built in this area (Vázquez-Suñé et al., 2016). Parameters of unit F were used for the lower layer. This soil layer is composed of a mixture of sand, gravel, and clay. It is located below the superficial subsoil.

The depth of the soil column was determined based on the groundwater level at the nearest location to the non-polluted soil sampling point. For this assessment, the highest recorded groundwater level from 2010 to 2023, which is 4.10 m, was considered. The choices and assumptions made in the Besòs conceptual model are illustrated in Figure 14.

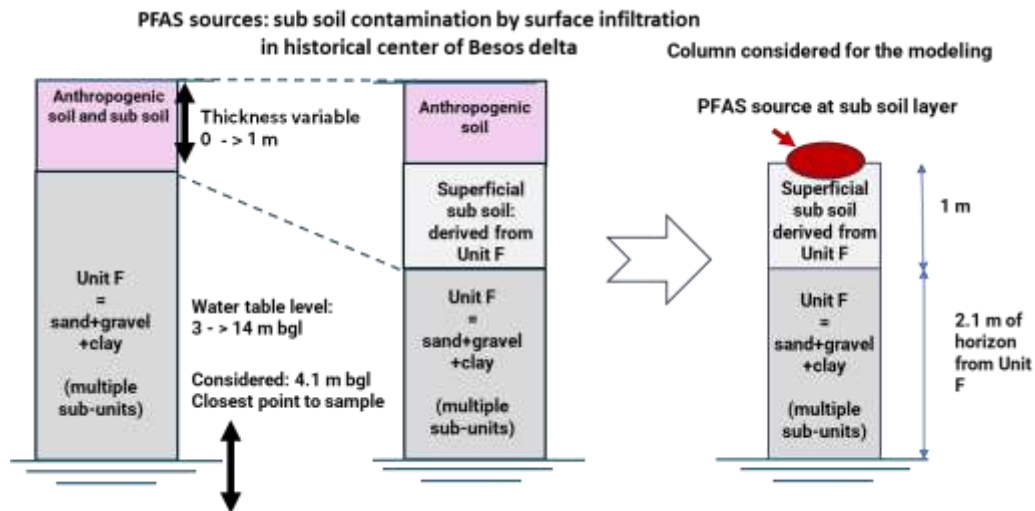


Figure 14: Conceptual model for PFAS transport modeling from pollution source to the first aquifer (Besòs case study)

➤ Hydraulic Conductivity and porosity of the soil column

Studies on the Besòs delta gave access to a set of more than 300 hydraulic conductivity values (Vázquez-Suñé et al., 2016). In the area where the non-polluted soil was sampled, a subset of 63 values was available. The 95th percentile (6.3 m/day and 7.3×10^{-5} m/s for unit F and the subsoil, respectively) and the 75th percentile (5.1 m/day and 5.9×10^{-5} m/s for unit F and the subsoil, respectively) of this subset were calculated. The lowest conductivity of 5.9×10^{-5} m/s was used in order to simulate the potential water flow. Infiltration reaches the annual recharge (250 mm) in only 1.2 hours with this unfavorable scenario. A porosity of 0.40 was used for the two layers, considering the mixture of sand, gravel, and clay.

4.2.3.3.3 Specific vulnerability parameters considered

Partitioning coefficients calculated for 18 PFAS with batch experiments were used. They are presented in Table 13.

4.2.3.3.4 Results of the modeling phase

Variations ranging between 5 hours and 13 days for travel times were observed for the different PFAS, even if time is rather compressed with a low travel distance (3.1 m) to the water table (Figure 15).

Due to the high hydraulic conductivity (5.9×10^{-5} m/s), the travel time of a non-reactive tracer is very short under these unfavorable conditions, reaching only 5 hours. It was found after the experiments that PFPeA exhibited a tracer-like behaviour. In this case, it will be challenging to adjust the remediation solution during a storm event, for example. This non-reactive tracer travel time reaches 4.5 years in the average scenario (if only the annual rainfall recharge flow is considered), which is not relevant in this case, due to large impermeable areas in this urban environment. Soil sealing is indeed a problem for the mitigation of polluted soil in cities. A variation of more than three orders of magnitude would be used for the water flow in the worst-case scenario, whereas in this case, anthropogenic infiltrations drive pollutant migration.

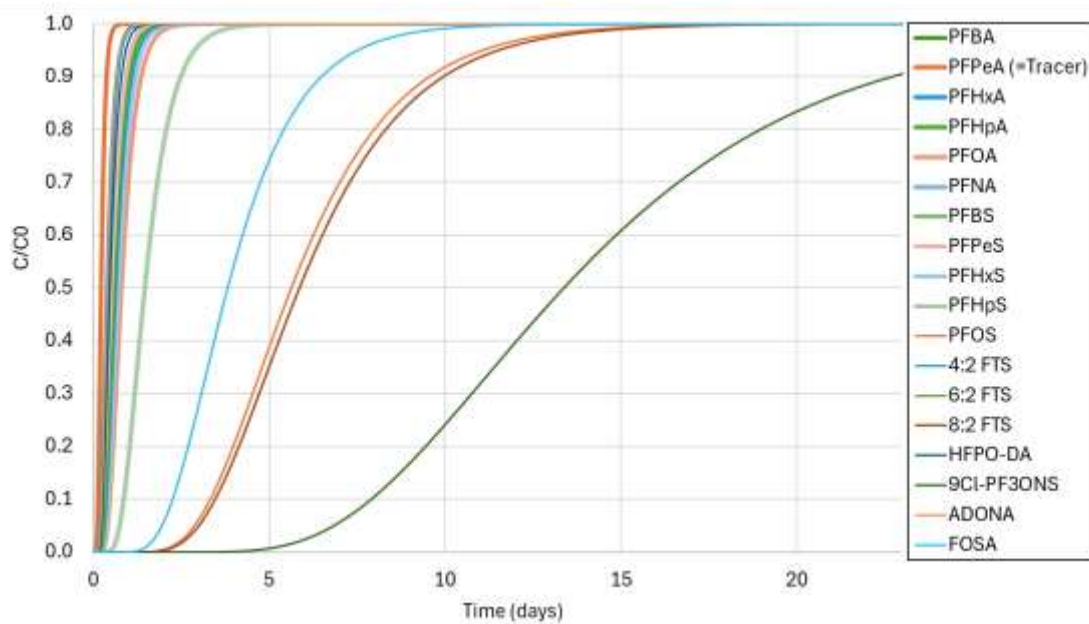


Figure 15: Simulated breakthrough curves of the PFAS studied (Besòs case Study - K_D from batch sorption)

The retardation factors for the different PFAS considered in the Besòs case study are presented in Table 15, along with their travel times.

Table 15: Retardation factors of the 18 PFAS studied in the Besòs case study

| PFAS | PFBA | PFPeA | PFHxA | PFHpA | PFOA | PFNA | PFBS | PFPeS | PFHxS |
|-----------------|-------|-------------|---------|---------|-------------|---------|--------------|-------|------------|
| R (-) | 2.6 | 1 | 1.8 | 2.5 | 3.6 | 6.6 | 2.9 | 2.4 | 3.2 |
| Travel time (h) | 13 | 5 | 9 | 12.5 | 18 | 33 | 14.5 | 12 | 16 |
| PFAS | PFHpS | PFOS | 4:2 FTS | 6:2 FTS | 8:2 FTS | HFPO-DA | 9Cl-PF3ONS | ADONA | PFOSA |
| R (-) | 6.6 | 25.3 | 2.9 | 2.7 | 26.3 | 2.1 | 60.1 | 1.7 | 17.1 |
| Travel time (h) | 33 | 126.5 (5 d) | 14.5 | 13.5 | 131.5 (6 d) | 10.5 | 300.5 (13 d) | 8.5 | 85.5 (4 d) |

➤ Sensitivity analysis

A sensitivity analysis was conducted using the partitioning coefficients derived from desorption experiments. Desorption partitioning coefficients were calculated for a subset of 3 PFAS, for which a difference of more than 0.5 unit between sorption and desorption partitioning coefficients was observed: PFNA, PFOS, and 8:2 FTS. Breakthrough curves are presented in Figure 16.

Sorption partitioning coefficients were similar for 8:2 FTS (6.13 L/kg) and PFOS (5.78 L/kg), but the differences were more pronounced between the desorption partitioning coefficients of both molecules (5.28 and 3.12 L/kg for 8:2 FTS and PFOS, respectively).

PFAS travel times were fast (less than 15 days) and leave few possibilities of remediation after an extreme rain event: it will be necessary to reduce the anthropogenic water infiltrations in the contaminated area, to reduce the risk of PFAS migration in soil and groundwater.

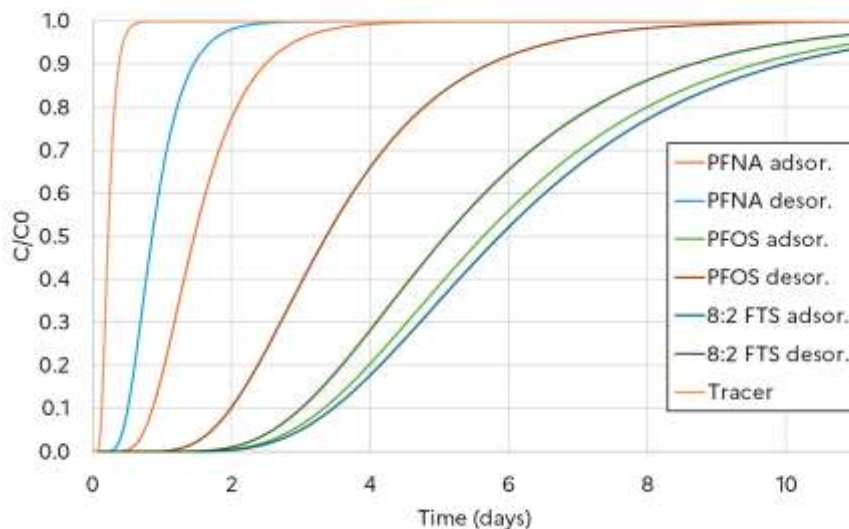


Figure 16: Simulated breakthrough curves of PFNA, PFOS, and 8:2 FTS with sorption and desorption partitioning coefficients (Besòs case study)

4.3 Conclusion on the groundwater risk assessment at the Besòs case study

For the **Besòs case study**, the **groundwater intrinsic vulnerability** fell within the upper range of the **moderate** classification. Various pollution sources are present in the Besòs case study, and in the frame of the UPWATER project, it has been decided to focus the study of the groundwater specific vulnerability on **PFAS** (per- and polyfluoroalkyl substances). Results from batch experiments indicated that **PFAS are mobile to very mobile substances** according to the UBA classification. **It can therefore be concluded that there is a high risk at this case study that PFAS reach groundwater.** The modeling indicated PFAS travel times in the range of 5 hours to 13 days. PFAS travel times are fast (less than 15 days) and leave few possibilities of remediation after a storm event: it will be necessary to reduce the anthropogenic water infiltrations in the contaminated area, to reduce the risk of PFAS migration in soils and groundwater.

5 Groundwater risk assessment in relation to the Athens case study

5.1 Intrinsic vulnerability

DRASTIC parameters and their corresponding ratings, applied for the Athens case study are presented in Table 16.

Table 16: DRASTIC parameters and corresponding ratings for the Athens case study

| Parameter | Range | Rating | Weight |
|------------------------|-------------------------|--------|--------|
| Depth to water | 1.5-4.5 | 9 | 5 |
| | 15-23 | 3 | |
| Net recharge | 50-100 | 3 | 4 |
| Aquifer media | Sand and gravel | 7 | 3 |
| | Karst limestone | 10 | |
| Soil media | Clay loam | 3 | 2 |
| | Thin or absent / Gravel | 10 | |
| Topography | < 2 | 10 | 1 |
| | > 18 | 1 | |
| Impact of vadose zone | Silt/clay | 1 | 5 |
| | Sand and gravel | 8 | |
| Hydraulic conductivity | 0.04 – 4 | 1 | 3 |
| | > 82 | 10 | |

In the Athens case study, the **depth to water** is generally between 3 and 19 m. In some areas, the depth to water can reach 52 m, but this is not a common value. Therefore, this value will not be taken into consideration in the frame of the DRASTIC analysis of the Athens case study, because this would lead to a lower rating for this parameter and therefore a lower DRASTIC index, which would not be representative of the area. These depths to water correspond to 4 DRASTIC ranges (1.5-4.5 m / 4.5-9 m / 9-15 m / 15-23 m), with a rating of 9, 7, 5, and 3, respectively.

The **net recharge** was calculated using the Microsoft Excel application ESPERE (Lanini et al., 2016). It includes several commonly used methods that are run simultaneously to estimate the recharge of an aquifer. The available data for this calculation were the daily precipitation and temperature for 2021 obtained from a weather station in Athens. In order to consider a safe scenario, it has been estimated in the model that all the rain will infiltrate. The mean net recharge calculated for 2021 for the Athens case study is 64.5 mm, with the Guttman and Zuckerman model (Guttman and Zuckerman, 1995). This value is in the 50 – 100 mm range of the DRASTIC R parameter, meaning a rating of 3.

In Athens, three different **aquifer media** can be found: “sand and gravel”, “clay and silt alternating with clayey gravel”, and “marl and calcareous siltstone”. The only aquifer media with a range in the DRASTIC method is “sand and gravel”, with a typical rating of 8. The range of the DRASTIC A parameter that could best describe “clay and silt alternating with clayey gravel” would be a range with a lower permeability than “sand and gravel”, making the groundwater less vulnerable to surface pollution. Therefore, a range with a lower rating would be a reasonable approximation for “clay and silt alternating with clayey gravel”. In the DRASTIC classification, a rating of 6 could be chosen for “massive limestone”. Nevertheless, this range proposed in the DRASTIC model seems inappropriate to describe the aquifer media in Athens. Therefore, to take this lower permeability for “clay and silt alternating with clayey gravel” into account, the range “sand and gravel” was chosen as well, but this time with a lower rating (7).

The aquifer media described as “marl and calcareous siltstone” corresponds to a medium with large grain sizes and openings in the aquifer, which could lead to a higher pollution potential than sand and gravel. Therefore, the range of the DRASTIC A parameter that could best describe “marl and calcareous siltstone” is a range with a higher permeability than “sand and gravel” and a higher rating. In the DRASTIC classification, higher ratings are available for “basalt” (rating of 9) and “karst limestone” (rating of 10). “Karst limestone”, with a typical rating of 10, could be a reasonable approximation for this type of aquifer media. The rating of the A parameter was therefore chosen between 7 and 10.

In Athens, the **soil media**, which refers to the uppermost portion of the unsaturated zone and the **impact of vadose zone**, corresponding to the material below the uppermost portion of the unsaturated zone and above the water table can be composed of different materials: “silty loam”, “clay loam”, “shrinking and/or aggregated clay” or “gravel”. For the soil media, these ranges correspond to a rating between 3 and 10. Therefore, two DRASTIC indexes were calculated: the first one with the lowest rating (3) and the second one with the highest rating (10), to evaluate the range of the groundwater vulnerability and consider a safe scenario. For the **impact of vadose zone** parameter, “silty loam”, “clay loam”, and “shrinking and/or aggregated clay” will correspond to the DRASTIC range “silt/clay” with a typical rating of 1. “Gravel” could be represented by the range “sand and gravel” with a typical rating of 8.

The **topography**, referring to the slope of the land surface, is highly variable. The maximum value is 88 %, which probably corresponds to hills. The 95th percentile is 26 %, meaning that only 5% of the measured slope values are above 26 %. At some locations, no slope is observed. Therefore, as the highest range of this DRASTIC parameter is > 18 with a rating of 1 and the lowest range is < 2 with a rating of 10, these two ratings will be considered for the DRASTIC index calculation for the Athens case study.

The **hydraulic conductivity** at the Athens case study is highly variable as well and was estimated between 10^{-8} and 10^{-1} m/s, i.e., between 8.64×10^{-4} and 8,640 m/d. This corresponds to ratings between 1 (0.04 – 4 m/d) and 10 (> 82 m/d).

Given that for some parameters, the variability among the Athens case study led to a range of ratings, two DRASTIC indexes were calculated: the first one with the lowest rating for all parameters (D_{\min}) and the second one with the highest rating (D_{\max}), to evaluate the range of the groundwater vulnerability and consider a safe scenario.

Therefore, for the Athens case study,

$$D_{\min} = 63$$

$$D_{\max} = 187$$

The DRASTIC index D_{\min} corresponds to a low vulnerability of the groundwater to surface pollution (DRASTIC index < 106). This index is representative of the locations with a high depth to water, a low-permeable soil material (saturated and unsaturated zones), a high slope, and a low hydraulic conductivity. On the contrary, the DRASTIC index D_{\max} corresponds to a high vulnerability of the groundwater to surface pollution (186 < DRASTIC index < 210). This value is in the lower range of the high vulnerability class. This index is representative of the locations with a low depth to water, a highly permeable soil material (saturated and unsaturated zones), a low slope, and a high hydraulic conductivity.

As the intrinsic vulnerability evaluation shows that groundwater at the Athens case study could be vulnerable to surface pollution, it seems relevant to assess the specific vulnerability associated with specific pollutants that can be found in the Athens case study in order to evaluate the risk for groundwater to be polluted by these specific pollutants.

5.2 Specific vulnerability

5.2.1 Pollutants considered in the frame of the groundwater risk assessment

Various pollution sources are present in the Athens case study. UPWATER groundwater monitoring campaigns showed that the Athens groundwater was highly polluted by PFAS, as well as caffeine and pharmaceuticals (see D4.3). For the same reasons as the ones presented for the Besòs case study (see chapter 4), it has been chosen to focus on PFAS in this case study for the groundwater specific vulnerability assessment. In addition, this will allow the application of the specific vulnerability assessment to another type of soil, with different physical and chemical characteristics, and to start the generalization of the conclusions for this pollutant family, for which there is a lack of data in literature concerning its fate and transport in soil and groundwater.

A specific vulnerability analysis was conducted to identify if these pollutants can lead to a risk of groundwater pollution at this site.

5.2.2 Material and methods

5.2.2.1 Soil sampling (NTUA)

Discussions were conducted between NTUA and Ineris in order to find the appropriate locations for sampling a soil that will be used for laboratory experiments to assess the groundwater specific vulnerability at this case study. The soil sampling campaign aimed to obtain PFAS-polluted soil to conduct release experiments.

At the Athens case study, 10 soil samples (S1 to S10) were taken by NTUA, according to the PFAS concentration ranges measured in groundwater. The main stormwater infiltration zones located upstream of the most polluted groundwater wells were prioritized, and the presence of activities that can use or generate PFAS was also considered. The location of these samples is presented in Figure 17. Given the geological map of the area, these samples were taken on fluvio-terrestrial deposits and are mainly composed of red clay and silt.

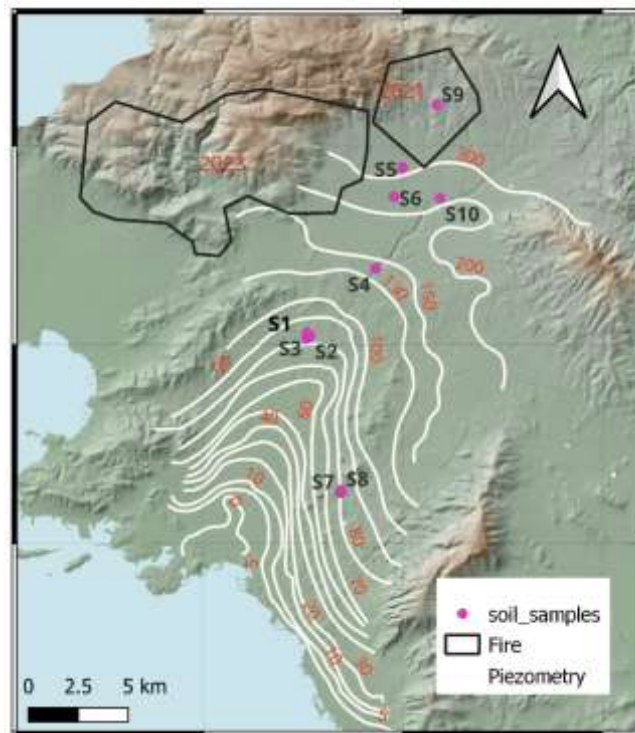


Figure 17: Soil sample location at the Athens case study

Before conducting any experiments, the samples were air-dried at room temperature and sieved at 2 mm.

5.2.2.2 PFAS analyses in soil samples (Ineris)

To verify the PFAS content of these 10 soil samples, a total of 22 PFAS were analyzed by Ineris in the fraction sieved at 2 mm (the 20 PFAS of the drinking water directive, as well as PFOSA and 10:2 FTS, see Table 8).

The concentrations of the 22 PFAS analyzed in the samples are presented in Table 17. PFAS content in these samples was low (between 0.4 and 7.7 $\mu\text{g}/\text{kg}$), showing that these samples are non-polluted with regard to soil PFAS background values found in literature (Tang et al., 2021; Brusseau et al., 2020; Zhang et al., 2019; Meng et al., 2018; Wang et al., 2018; Rankin et al., 2016; Strynar et al., 2012). This result was not expected given the sampling strategy applied. Nevertheless, as no PFAS-polluted soil was found for the Athens case study, it has been decided to conduct the groundwater risk assessment on a non-polluted soil. This is still relevant as sorption/desorption experiments on this soil will allow the calculation of sorption/desorption partitioning coefficients needed for the risk assessment.

Therefore, a composite soil sample was made with the samples showing the same texture and collected on the same geological layer. Samples S1, S2, S3, S4, S5, S6, S9, and S10 were mixed to obtain the soil sample on which all the experiments were done. This soil sample was named "CSA".

Table 17: PFAS content of the Athens soil samples S1 to S10 (µg/kg)

| Compound | S1 | S2 | S3 | S4 | S5 | S6 | S7 | S8 | S9 | S10 |
|---------------|------|------|------|------|------|------|------|------|------|------|
| PFBA | <0.1 | 0.1 | <0.1 | <0.1 | <0.1 | <0.1 | 0.4 | 0.3 | <0.1 | <0.1 |
| PFPeA | <0.1 | <0.1 | <0.1 | <0.1 | 0.5 | <0.1 | 0.2 | 0.3 | <0.1 | <0.1 |
| PFHxA | <0.1 | <0.1 | <0.1 | <0.1 | <0.1 | <0.1 | <0.1 | 0.2 | <0.1 | <0.1 |
| PFHpA | <0.1 | <0.1 | 0.1 | <0.1 | <0.1 | <0.1 | 0.2 | 0.3 | <0.1 | <0.1 |
| PFOA | 0.2 | 0.2 | 0.6 | 0.1 | <0.1 | 0.5 | 1.1 | 1.8 | 0.3 | 0.2 |
| PFNA | <0.1 | <0.1 | 0.4 | <0.1 | <0.1 | 0.1 | 0.5 | 0.2 | 0.2 | <0.1 |
| PFDA | <0.1 | 0.1 | 0.4 | <0.1 | <0.1 | <0.1 | 0.3 | 0.1 | <0.1 | <0.1 |
| PFUnDA | <0.1 | <0.1 | 0.1 | <0.1 | <0.1 | <0.1 | 0.1 | <0.1 | <0.1 | <0.1 |
| PFDoA | <0.1 | <0.1 | 0.2 | 0.1 | <0.1 | <0.1 | 0.2 | <0.1 | <0.1 | <0.1 |
| PFTTrDA | <0.1 | <0.1 | 0.1 | <0.1 | <0.1 | <0.1 | <0.1 | <0.1 | <0.1 | <0.1 |
| PFBS | <0.1 | <0.1 | <0.1 | <0.1 | <0.1 | <0.1 | <0.1 | <0.1 | <0.1 | <0.1 |
| PFPeS | <0.1 | <0.1 | <0.1 | <0.1 | <0.1 | <0.1 | <0.1 | <0.1 | <0.1 | <0.1 |
| PFHxS | <0.1 | <0.1 | <0.1 | <0.1 | <0.1 | 0.8 | <0.1 | <0.1 | <0.1 | <0.1 |
| PFHpS | <0.1 | <0.1 | <0.1 | <0.1 | <0.1 | <0.1 | <0.1 | <0.1 | <0.1 | <0.1 |
| PFOS | 0.3 | 0.2 | 4.1 | 0.3 | 0.2 | 6.3 | 1.9 | 1.8 | 0.7 | 0.2 |
| PFNS | <0.1 | <0.1 | <0.1 | <0.1 | <0.1 | <0.1 | <0.1 | <0.1 | <0.1 | <0.1 |
| PFDS | <0.1 | <0.1 | <0.1 | <0.1 | <0.1 | <0.1 | <0.1 | <0.1 | <0.1 | <0.1 |
| PFUnDS | <0.1 | <0.1 | <0.1 | <0.1 | <0.1 | <0.1 | <0.1 | <0.1 | <0.1 | <0.1 |
| PFDoDS | <0.1 | <0.1 | <0.1 | <0.1 | <0.1 | <0.1 | <0.1 | <0.1 | <0.1 | <0.1 |
| PFTTrDS | <0.1 | <0.1 | <0.1 | <0.1 | <0.1 | <0.1 | <0.1 | <0.1 | <0.1 | <0.1 |
| 10:2 FTS | <0.1 | 0.1 | 0.1 | <0.1 | <0.1 | <0.1 | <0.1 | <0.1 | <0.1 | <0.1 |
| PFOSA | <0.1 | <0.1 | <0.1 | <0.1 | <0.1 | <0.1 | <0.1 | <0.1 | <0.1 | <0.1 |
| Total 22 PFAS | 0.5 | 0.7 | 6.1 | 0.5 | 0.7 | 7.7 | 4.9 | 5 | 1.2 | 0.4 |

5.2.2.3 Soil physical and chemical characterization (Ineris)

A physical and chemical characterization was conducted by Ineris on the CSA sample. Results are presented in Table 18.

Table 18: Soil physical and chemical characteristics - CSA non-polluted soil

| Granulometry (g kg ⁻¹) | | | | | |
|---|----------------|---------------------------------------|-------------------------------|-----------------------|---------------------------|
| Parameter | Clay (< 2 µm) | Fine silt (2/20 µm) | Coarse silt (20/50 µm) | Fine sand (50/200 µm) | Coarse sand (200/2000 µm) |
| Value | 164 | 190 | 84 | 216 | 346 |
| Organic carbon and total nitrogen (g kg ⁻¹) | | | | | |
| Parameter | Organic carbon | Total nitrogen | Total carbon | C/N | Organic matter |
| Value | 30.5 | 2 | 60.1 | 15.5 | 52.7 |
| Parameter | pH (water) | Total limestone (g kg ⁻¹) | CEC (cmol+ kg ⁻¹) | | |
| Value | 8.2 | 247 | 19.2 | | |

This soil has a basic pH of 8.2. It is mainly composed of sand (56 wt.%). Among the sand, mainly coarse sand was observed (35 wt.%). This composition is very close to the one measured for the BCN soil sample. The CSA soil sample has an organic matter content of 5.3 %, whereas the BCN soil sample has an organic matter content of 0.9%. Therefore, a comparison of PFAS behavior in these 2 soils could allow us to assess the role of organic matter in PFAS sorption onto soils. Even if the soil organic matter is not the only soil constituent responsible for PFAS retention, a higher sorption is expected with the CSA soil sample than with the BCN soil sample.

However, with these characteristics concerning the granulometry, a low PFAS retention is still expected in this soil, meaning that a pollution entering the soil from the unsaturated zone will have a great potency to move toward groundwater and then, move far away from the pollution source. Nevertheless, as stated in chapter 3.2.2, PFAS sorption onto soil cannot be predicted from its organic matter content only, and soil mineral constituents will also play a role. Therefore, with a little data on this subject in literature, trying to predict PFAS transfer in the Athens soil could be a tough task, and uncertainty on the results could be high. That is why, in the frame of the groundwater risk assessment for the Athens case study, laboratory experiments were carried out in order to evaluate the transfer potential of PFAS. These experiments are described in the following section of this report.

5.2.2.4 PFAS sorption/desorption isotherms on CSA soil sample (Ineris)

PFAS sorption/desorption experiments were conducted by Ineris on the CSA soil sample. All experiments were conducted in triplicate in 50 mL polypropylene centrifuge tubes at a temperature of 21 ± 2 °C. The experimental procedure was the same as the one used for sorption/desorption isotherms conducted on the BCN soil sample and presented in chapter 4.2.2.5.

5.2.3 Results

5.2.3.1 PFAS sorption/desorption isotherms on CSA soil sample

The specific vulnerability of groundwater in this case study was assessed by working on a non-polluted soil. This situation is representative of the PFAS migration in a non-polluted soil, after being released from the pollution sources.

In the experiments concerning the CSA soil sample, it was possible to plot sorption isotherms for 4 PFAS out of the 30 PFAS analyzed in water, allowing to calculate a soil-water partitioning coefficient (K_D): PFOA, PFPeS, PFHxS, and PFHpS. These isotherms are presented in Figure 18. Error bars were calculated to consider a 95% confidence interval when two or three out of the three replicates showed consistency. If only one replicate was deemed consistent, the error bars were calculated to represent the global uncertainty. Sorption isotherms of these PFAS were found to be linear in the experimental conditions, following Equation 10.

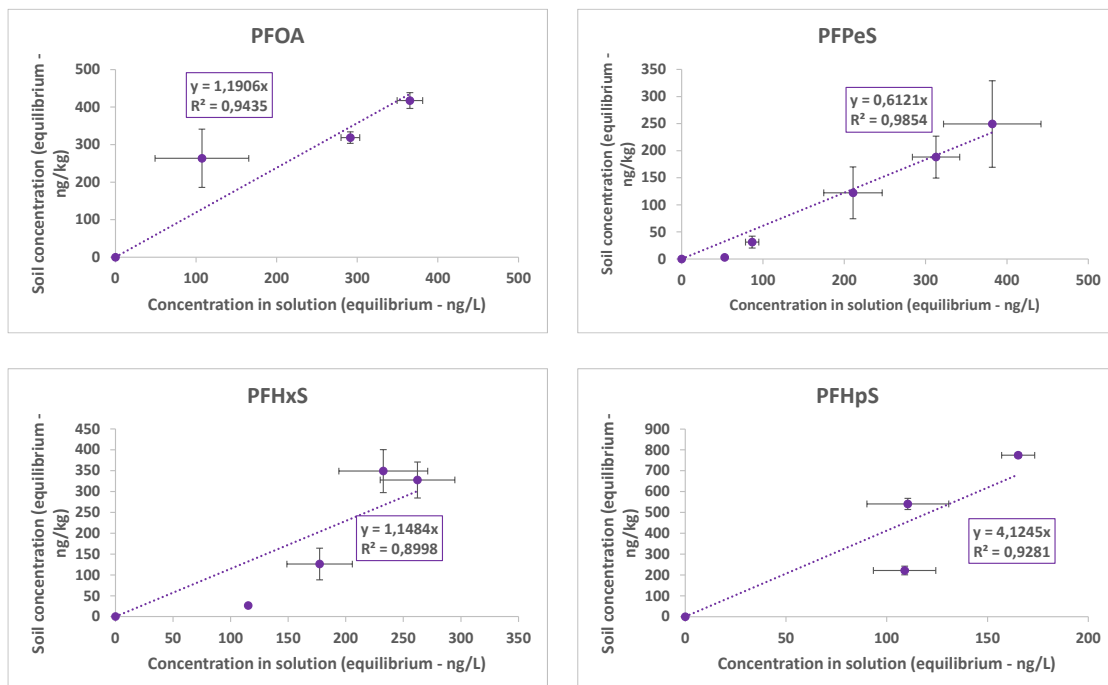


Figure 18: PFAS sorption isotherms on CSA soil sample

For 10 PFAS (PFBA, PFPeA, PFHxA, PFHpA, PFNA, PFBS, 4:2 FTS, 6:2 FTS, HFPO-DA, and ADONA), the plot of the isotherm was not possible because only 2 concentrations were consistent. Nevertheless, it was possible to calculate a K_D for these 10 molecules as well, using Equation 5 for each concentration. The mean value of the K_D calculated for each concentration was considered.

The other 16 PFAS were not quantified in solution after the sorption experiment, meaning that all the PFAS mass introduced in the soil-solution system was sorbed onto the soil. This does not mean that these PFAS will not be mobile at all in soils. In the experimental conditions, these PFAS were found to be less mobile than the others. With less soil or with a higher concentration of these PFAS in the soil-solution system, the sorption could be precisely quantified. These PFAS are PFOS, PFNS, PFDS, PFUnDS, PFDoDS, PFTrDS, PFDA, PFUnDA, PFDoDA, PFTrDA, PFTeDA, PFOA, PFOSA, 8:2 FTS, 10:2 FTS, and 9Cl-PF3ONS. They correspond to PFSA from 8 to 13 carbon atoms, PFCA from 10 to 14 and 18 carbon atoms, 2 FTS with 8 and 10 perfluorinated carbon atoms, a FASA with 8 carbon atoms, and a Cl-PFESA with 8 carbon atoms. These molecules are the ones with the longest carbon chain among the PFAS analyzed in these PFAS families. This is consistent with literature, indicating that long-chain PFAS have a greater affinity for the soil matrix than shorter-chain PFAS, due to the increased hydrophobicity of the longer carbon chains (Kleja et al., 2025).

The soil-water partitioning coefficients calculated for the Athens case study are presented in Table 19.

Table 19: Soil-water partitioning coefficients for the Athens case study

| PFAS | PFBA | PFPeA | PFHxA | PFHpA | PFOA | PFNA | PFBS |
|-----------|-------|-------|-------|---------|---------|---------|-------|
| KD (L/kg) | 0.91 | 0.15 | 0.07 | 0.21 | 1.19 | 4.27 | 0.40 |
| KOC | 30 | 5 | 2.1 | 7 | 39 | 140 | 13 |
| log KOC | 1.5 | 0.7 | 0.3 | 0.8 | 1.6 | 2.1 | 1.1 |
| PFAS | PFPeS | PFHxS | PFHpS | 4:2 FTS | 6:2 FTS | HFPO-DA | ADONA |
| KD (L/kg) | 0.61 | 1.15 | 4.12 | 0.24 | 0.88 | 0.68 | 0.44 |
| KOC | 20 | 38 | 135 | 8 | 29 | 22 | 14 |
| log KOC | 1.3 | 1.6 | 2.1 | 0.89 | 1.5 | 1.3 | 1.2 |

Regarding the uncertainties associated with the K_D calculation, it can be considered that K_D below 1L/kg are not significantly different, denoting very mobile compounds. This corresponds to PFCA containing up to 7 carbon atoms (PFBA, PFPeA, PFHxA, and PFHpA) and PFSA with up to 5 carbon atoms (PFBS, and PFPeS). This is confirmed by their log K_{OC} values, which are below 3, showing that these PFAS are very mobile in soil. As explained in chapter 3.2.3.1, log K_{OC} was used to rank the mobility of this PFAS according to the German environmental agency, UBA. Then, for the longer chain PFCA and PFSA, the K_D increased with an increasing carbon chain

length. This was observed for PFOA, PFNA, PFHxS, and PFHpS. Nevertheless, according to the UBA classification, they can still be considered as very mobile substances. The same trend was observed for 4:2 and 6:2 FTS, with a K_D increasing with the carbon chain length, denoting a higher sorption of longer chain FTS.

HFPO-DA and ADONA have a K_D of the same order of magnitude as the PFAS with the lower observed sorption, meaning that they are very mobile in soils. In particular, their K_D is even lower than the one calculated for the molecule they substitute (PFOA). This confirmed what was found for the Besòs case study, showing that substituents may not necessarily be a good alternative in terms of environmental behavior.

In addition, these results confirm that, for molecules with the same number of carbon atoms, PFSA sorption in soils is higher than PFCA sorption.

A comparison between the K_D obtained at the Besòs case study and the ones obtained at the Athens case study was made. The texture of these two soils was similar. They were mainly composed of sand with approximately the same amounts of clay and loam. The main difference between these two soils was their organic matter content. The BCN soil sample was composed of less than 1% of organic matter, whereas the CSA soil sample contained 5% of organic matter. For short-chain PFCA (PFBA, PFPeA, PFHxA, PFHpA), short-chain PFSA (PFBS, PFPeS), 4:2 FTS, 6:2 FTS, HFPO-DA, and ADONA, no significant differences were observed between the K_D calculated for the two soils. This result indicated that sorption of short-chain PFAS is not mainly driven by the organic matter content of the soil. Other soil components may be responsible for their retention. On the contrary, K_D calculated for long-chain PFCA (PFOA, PFNA), long-chain PFSA (PFHxS, PFHpS), 8:2 FTS, 9 Cl-PF3ONS, and PFOSA were higher for the CSA soil sample than for the BCN soil sample. This indicated that an increase in soil organic matter will lead to an increase in long-chain PFAS sorption. Therefore, soil organic matter was found to be the main soil component responsible for long-chain PFAS behavior.

The desorption experiments allowed the calculation of a desorption soil-water partitioning coefficient K_{Des} for 4 PFAS out of the 14 PFAS for which the retention onto the soil during the sorption experiments could be quantified (PFPeS, PFHxS, PFHpS, and PFNA). It was not possible to plot desorption isotherms because only 1 or 2 concentrations were consistent. K_{Des} for these 4 molecules were calculated using Equation 5 for each concentration. The mean value of the K_{Des} calculated for each concentration is presented in Table 20.

Table 20: Soil-water partitioning coefficients for the Athens case study

| PFAS | PFPeS | PFHxS | PFHpS | PFNA |
|------------------|-------|-------|-------|------|
| K_{Des} (L/kg) | 0.21 | 0.51 | 3.14 | 2.65 |

For the other 10 PFAS for which the retention onto the soil during the sorption experiments could be quantified (PFBA, PFPeA, PFHxA, PFHpA, PFOA, PFBS, 4:2 FTS, 6:2 FTS, HFPO-DA, and ADONA), it was not possible to calculate a K_{Des} for two reasons: concentrations were below the quantification limit, or when the molecule was quantified, initial and final concentrations were too close to allow a robust calculation.

The other 16 PFAS that were not quantified in solution after the sorption experiment (PFOS, PFNS, PFDS, PFUnDS, PFDoDS, PFTrDS, PFDA, PFUnDA, PFDoDA, PFTrDA, PFTeDA, PFODA, PFOSA, 8 :2 FTS, 10:2 FTS, and 9Cl-PF3ONS), were not quantified after the desorption experiment, denoting their stronger affinity for the soil matrix again.

Therefore, given the results of the intrinsic vulnerability analysis at this case study, showing that groundwater could be highly vulnerable to surface pollution at locations with a low depth to water, a highly permeable soil material (saturated and unsaturated zones), a low slope and a high hydraulic conductivity, combined with the results of the specific vulnerability, showing that PFAS are mobile to very mobile substances, **it can be considered that there is a high risk at this case study that PFAS reach groundwater.**

5.2.3.2 PFAS travel time modeling (Ineris)

The time needed for these pollutants to reach groundwater was calculated using the HYDRUS-1D model by Ineris. Parameters used to build the conceptual model were extracted from the UPWATER D3.7 report and were based on the intrinsic and specific vulnerability assessment presented in the previous paragraphs.

5.2.3.2.1 Specificity of the Athens case study

The specificities of the Athens case study are the presence of natural soil areas connected to potential rainfall infiltration locations. Contrary to the Besòs case study, in Athens, the soil was sampled in natural areas that are more representative of the possible rainfall infiltration in contaminated natural areas. The soil sample studied was a composite sample of different superficial soil samples with a high organic matter content (52.7 g/kg) and organic carbon content (30.5 g/kg). It was therefore necessary to define a soil column and a decrease in the organic content to model a more realistic PFAS sorption in the soil column profile. A discussion on the TOC decrease considered in the soil profile is proposed in the frame of a sensitivity analysis. A water infiltration of 62 mm was considered for the average scenario.

5.2.3.2.2 Intrinsic vulnerability parameters considered

➤ Soil column and water table depth

The soil horizons were described in the UPWATER D3.7 report and in the first part of this chapter. To be more specific in superficial layers, which are the first layers impacted by PFAS contamination in firefighting areas, they were divided into soil and subsoil, as was done in the UPWATER report D3.7.

The depth of the first aquifer varies greatly depending on the location within the Athens basin. The shallowest aquifer near areas with the highest potential PFAS contributions was measured at around 4.5 m below ground level. Shallower depths do exist (3 m), but they are less representative of the PFAS contribution areas, which are near the border of the Athens basin. The value of 4.5 m was therefore considered a reasonable upper limit for PFAS transfer in the soil column. This value is relatively conservative because transfers to existing aquifers are expected across the entire surface of the Athenian basin, and the area affected by these transfers extends significantly beyond the Quaternary deposits and affects the Neogene formation.

The choices (between case 1 and case 2) and assumptions made for the Athens conceptual model are presented in Figure 19. Case 2 was used because it was specific to the Athens case study.

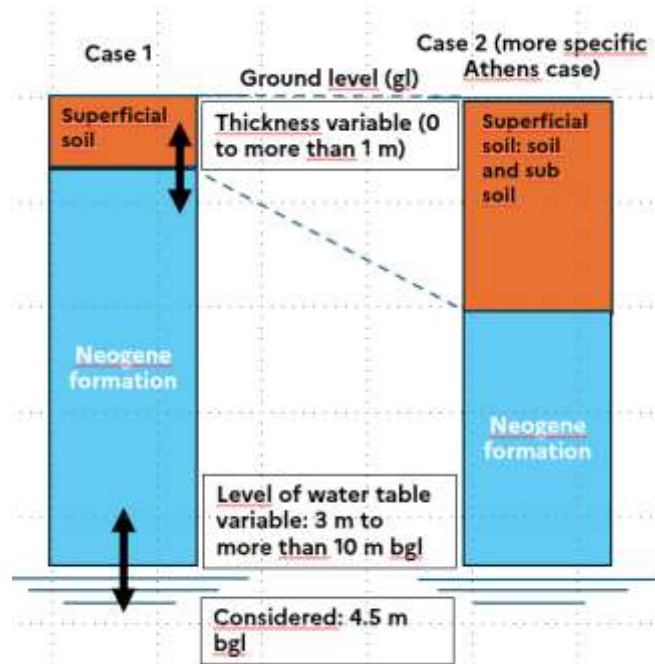


Figure 19: Parameters used for the Athens soil column and conceptual models

➤ Permeability and porosity of the soil column

A superficial aquifer is present in alluvial deposits of the Athenian plain. High horizontal permeabilities coming from the quaternary formation are not considered representative of transfers at the scale of the Athenian basin. Horizontal permeabilities obtained by calibrating the hydraulic model implemented as part of D3.7 vary greatly depending on the formations concerned (110 m/day for the Quaternary formation, 0.61 m/day for the Neogene formation). A relatively consistent assumption is to consider an anisotropy of 1 for the hydraulic conductivity and then a vertical permeability of the same value as the horizontal conductivity. A slightly higher permeability (0.864 m/day, or 10^{-5} m/s) was considered for the Neogene formation and the superficial soil derived from this formation to better match the assumption of worst-case conditions. This choice also represents a higher value (and worst-case condition) of permeability for the soil class considered (loam).

Infiltration reaches the annual recharge (62 mm) in only 1.75 hours with this unfavorable scenario.

The porosity was directly estimated from the saturated porosity of the soil modeled in the D 3.7 report. A value of 0.41 was chosen for the 0 - 2 m depth interval from the values of 0.42 and 0.40 used for the 0 - 30 cm and 0.3 - 2 m depth intervals in the study of the vadose zone in the D3.7 report. The value of 0.43 was also extracted from the 2 - 8 m interval in the D3.7 report and considered in the frame of the modeling for the 2 - 4.5 m depth interval.

5.2.3.2.3 Specific vulnerability parameters considered

Sorption of PFAS in the soil was determined to be linked with different solid phases of the soil, especially the organic phase. If a major contribution of the organic phase with high and medium content of organic matter is assumed, other phases of the soil (mineral phases and especially Fe/Mn oxy-hydroxide and other minerals providing surfaces involved in cation exchange) are also to be considered.

The soil analyzed by Ineris was sampled in natural areas by NTUA. The geology of the underlying soils is complex and comprises numerous units. A large part of these areas is occupied by recent alluvial deposits and Pleistocene deposits, as well as Neogene clastic and carbonate rocks.

The highest levels of Al, Fe, and Mn are found in the northern and western parts of the Athens basin (Argyraki and Kelepertzis, 2014). High spatial heterogeneity of these levels, therefore, suggests that PFAS adsorption, which is partly linked to these elements, will potentially be variable, especially in the deepest horizons.

In the frame of this study, a simplified assumption was made, considering that K_D was predominantly linked with the organic phase, which allows the use of the relation $K_D = K_{oc} \times f_{oc}$. This relation was used to model the decrease of sorption in the deepest part of the soil.

Sorption to the soil matrix was described with linear sorption isotherms coming from the results of batch experiments on the non-contaminated soil. K_D were derived from these experiments.

The organic matter content of the superficial soil (0 - 5 cm) coming from the Athens urban park (Chronopoulos et al., 1997) reached values ranging from 1.9 to 5.2% for calcareous soil. The soil sampled for the specific vulnerability study reaches the highest level (5.27%), confirming the topsoil affiliation of this composite sample. Therefore, the decrease of organic carbon observed on several points of the Athens basin in the EU Soil data set was used (Hiederer, 2013). Soil points that precisely matched the TOC value of the soil sampled in the frame of the UPWATER project in Athens were chosen, and the organic carbon decrease with depth was adjusted from this EU Soilgrid data. The topsoil was divided into 5 classes of TOC. The TOC of the Neogene formation was the same as the lower layer of the topsoil (Figure 20).

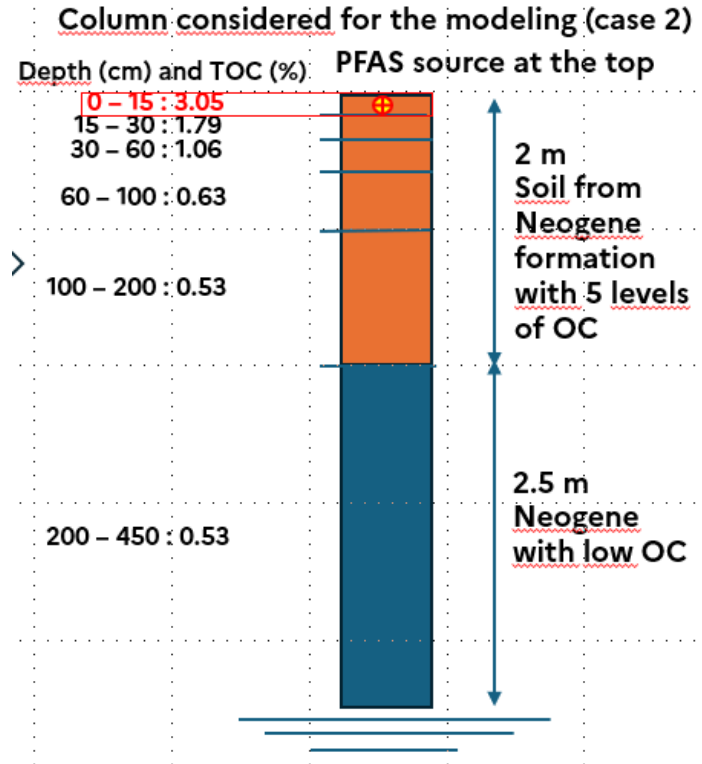


Figure 20: Conceptual model: decrease of the TOC with soil depth (Athens case study)

The specific K_D of each layer was derived from the K_D calculated after the batch experiments for 14 PFAS (see Table 19), using Equation 11.

$$K_{D \text{ layer}} = K_{oc} \times f_{oc \text{ layer}} \quad \text{Equation 11}$$

Factors affecting the decrease in K_D in the different soil layers are presented in Table 21.

Table 21: Factors affecting the decrease in K_D in the different soil layers

| Layer (cm) | depth 0 - 15 | 15 -30 | 30 -60 | 60 -100 | 100 -200 and 200 -450 |
|------------|--------------|--------|--------|---------|-----------------------|
| Factor | 1 | 0.59 | 0.35 | 0.2 | 0.17 |

The equivalent K_D used in modeling, considering the OC variation in the topsoil, are presented in Table 22.

Table 22: Equivalent K_D for the modeling (Athens case study)

| PFAS | PFBA | PFPeA | PFHxA | PFHpA | PFOA | PFNA | PFBS | PFPeS |
|--------------|-------|-------|---------|---------|---------|-------|---------------|-------|
| K_D (L/kg) | 0.21 | 0.03 | 0.02 | 0.05 | 0.27 | 0.97 | 0.09 | 0.14 |
| PFAS | PFHxS | PFHpS | 4:2 FTS | 6:2 FTS | HFPO-DA | ADONA | PFAS K_{D+} | |
| K_D (L/kg) | 0.26 | 0.93 | 0.05 | 0.20 | 0.15 | 0.10 | 1.72 | |

5.2.3.2.4 Results of the modeling phase

The breakthrough curves of the PFAS studied and of a non-reactive tracer are presented in Figure 21. In this figure, a breakthrough curve is named PFAS K_{D+} . This curve corresponds to PFAS that were introduced in the soil-solution system before the experiment but were below the quantification limit in the solutions after the sorption step. They were obtained by using a K_D calculated with the concentration equal to the quantification limit in solution and the corresponding concentration in the soil. This K_D was 7.6. This means that the travel time of these PFAS will be at least the one calculated with the “PFAS K_{D+} ” breakthrough curve.

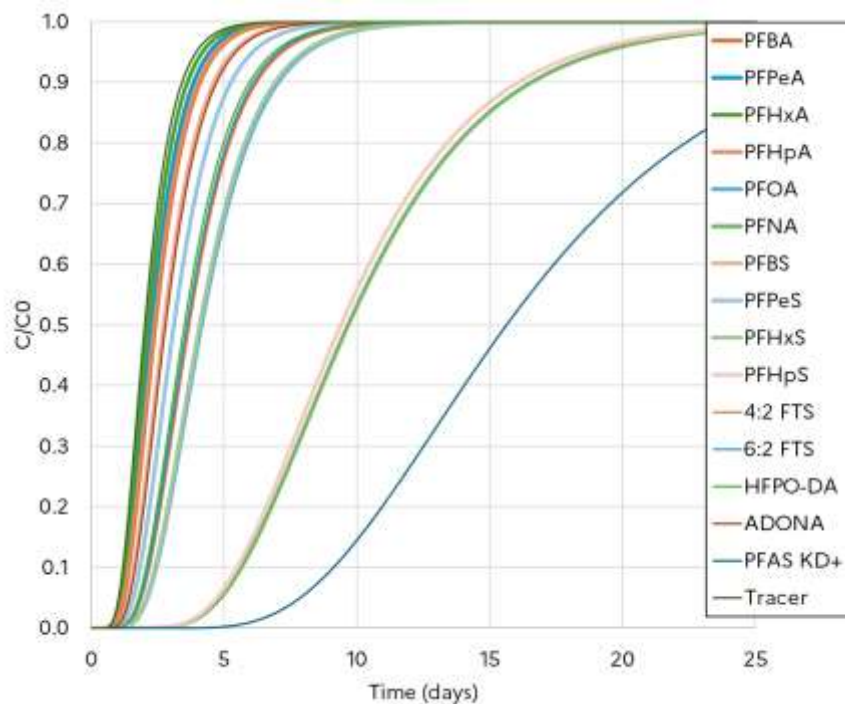


Figure 21: Simulated breakthrough curves of PFAS (Athens case study) - 6 layers

Due to the medium hydraulic conductivity and the length of the soil column (4.5m), the travel time for a non-reactive tracer under the unfavorable scenario was 2 days, while under the average scenario (considering annual precipitation), it exceeded one year. For PFAS, travel times ranged from 2 days to more than 15 days in the worst-case scenario. These travel times, along with the retardation factors, are presented in Table 23. Retardation factors covered a range from 1.1 to 4.7. They reached more than 7.7 for the PFAS that were not quantified in solution after the experiment. PFPeA, PFHxA, and PFHpA exhibited a tracer-like behaviour.

These travel times confirmed the high mobility of PFAS in this soil.

Table 23: Retardation factors and travel times of PFAS for the Athens case study

| PFAS | PFBA | PFPeA | PFHxA | PFHpA | PFOA | PFNA | PFBS | PFPeS |
|-----------------|-------|-------|---------|---------|---------|-------|----------|-------|
| R (-) | 1.8 | 1.1 | 1.1 | 1.2 | 2.1 | 4.8 | 1.4 | 1.5 |
| Travel time (d) | 3.6 | 2.2 | 2.2 | 2.4 | 4.2 | 9.6 | 2.8 | 3.0 |
| PFAS | PFHxS | PFHpS | 4:2 FTS | 6:2 FTS | HFPO-DA | ADONA | PFAS KD+ | |
| R (-) | 2.0 | 4.7 | 1.2 | 1.8 | 1.6 | 1.4 | 7.7 | |
| Travel time (d) | 4.0 | 9.4 | 2.4 | 3.6 | 3.2 | 2.8 | 15.4 | |

Infiltration of rainfall after a storm event and possibly anthropogenic sources are the main drivers of migration, due to the relatively large/medium hydraulic conductivity of superficial soil layers considered (10^{-5} m/s).

➤ Sensitivity analysis

In the frame of a sensitivity analysis, the organic matter fraction influence on the PFAS travel times was studied. This investigation was based on the hypothesis formed from batch experiments, suggesting that the soil organic matter content could influence the behaviour of PFAS in soils. For short-chain PFCA, short-chain PFSA, 4:2 FTS, 6:2 FTS, HFPO-DA, and ADONA, a non-significant influence of organic carbon was observed. However, for long-chain PFCA, long-chain PFSA, 8:2 FTS, 9 Cl-PF3ONS, and PFOSA, the soil organic matter had an impact on their sorption characteristics.

Therefore, in the frame of the Athens case study and with regard to the conceptual model based on the decrease of OC with increased soil depth, any changes in this parameter could alter the breakthrough order. Consequently, a second scenario was assessed, which involved a reduced evolution of K_D with respect to the f_{oc} for short-chain PFCA, short-chain PFSA, 4:2 FTS, 6:2 FTS, HFPO-DA, and ADONA. These PFAS are characterized by a sorption that is less significantly influenced by the OC content of the soil. For these PFAS, only 3 layers were considered in the topsoil, with K_D decreasing by a factor of 0.35. For these PFAS, the equivalent K_D considering this OC variation in the topsoil are presented in Table 24 (K_D S2). They are compared with the K_D used in the first scenario (K_D S1). These K_D values remain very low and are associated with mobile compounds.

Table 24: Equivalent K_D for the sensitivity analysis (Athens case study)

| PFAS | PFBA | PFPeA | PFHxA | PFHpA | PFBS | PFPeS | 4:2 FTS | 6:2 FTS | HFPO-DA | ADONA |
|-----------------|------|-------|-------|-------|------|-------|---------|---------|---------|-------|
| K_D S1 (L/kg) | 0.21 | 0.03 | 0.02 | 0.05 | 0.09 | 0.14 | 0.05 | 0.20 | 0.15 | 0.10 |
| K_D S2 (L/kg) | 0.39 | 0.06 | 0.03 | 0.09 | 0.17 | 0.26 | 0.10 | 0.38 | 0.29 | 0.19 |

This different behavior shows a different pattern for the breakthrough curves (Figure 22). Figure 22 shows a more pronounced separation of the breakthrough curves compared to Figure 21.

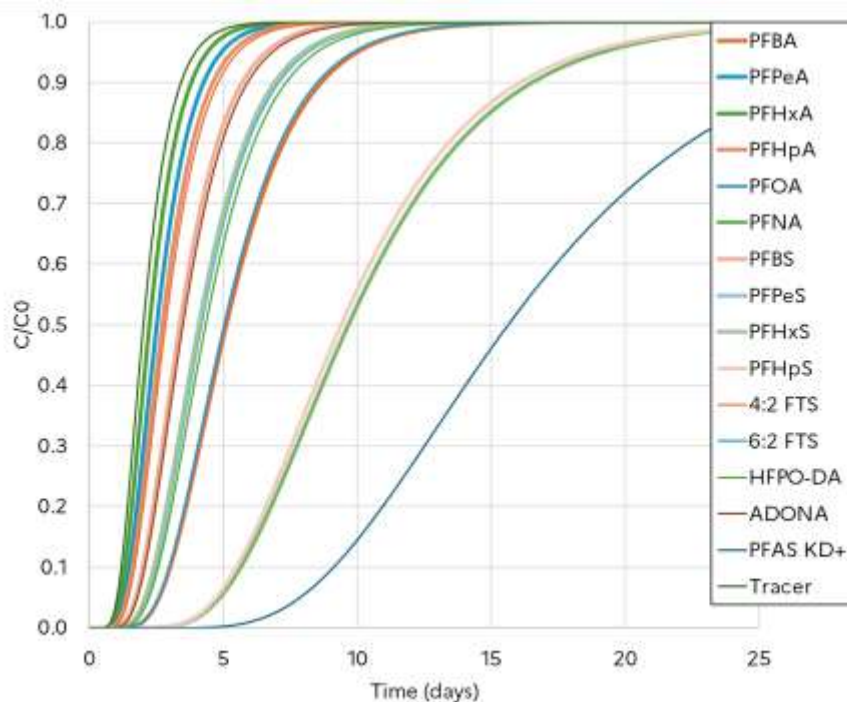


Figure 22: Breakthrough curves of PFAS (Athens case study - reduced influence of OC on some PFAS)

A comparison between the retardation factors of the 2 scenarios studied (worst-case conditions and sensitivity analysis with reduced influence of OC on some PFAS) is presented in Table 25.

R_{S1} corresponds to the retardation factors derived from the first scenario, while R_{S2} refers to the retardation factors from the sensitivity analysis. Travel times are presented as well in this table.

The retardation factors are therefore modified only for the PFAS for which the K_D was modified. A higher K_D value was used in these cases, leading to increased retardation factors. Nevertheless, these values are close to those calculated previously. As a result, travel times have increased by 0.4 to 1.5 days.

The modifications to the breakthrough order were minor and concerned 5 PFAS: PFHxS, HFPO-DA, PFOA, PFBA, and 6:2 FTS.

Nevertheless, these changes may lead to different PFAS fingerprints in groundwater samples collected at increasing distances from the PFAS source. Additional research is needed to confirm this potential shift towards a higher equivalent K_D value for soil columns and shorter-chain PFAS, which are less influenced by interactions with organic matter.

All these equivalent K_D values were very low (<1) except for the specific PFAS group “ K_{D+} ”, showing a high mobility of PFAS at this case study.

Table 25: Retardation factors and travel times of PFAS (Athens case study) - Sensitivity analysis

| PFAS | PFBA | PFPeA | PFHxA | PFHpA | PFOA | PFNA | PFBS | PFPeS |
|--------------------|-------|-------|---------|---------|---------|-------|---------------|-------|
| R_{S1} | 1.8 | 1.1 | 1.1 | 1.2 | 2.1 | 4.8 | 1.4 | 1.5 |
| Travel time S1 (d) | 3.6 | 2.2 | 2.2 | 2.4 | 4.2 | 9.6 | 2.8 | 3.0 |
| R_{S2} | 2.5 | 1.3 | 1.1 | 1.4 | 2.1 | 4.8 | 1.7 | 2.0 |
| Travel time S2 (d) | 5 | 2.6 | 2.2 | 2.8 | 4.2 | 9.6 | 3.4 | 4.0 |
| PFAS | PFHxS | PFHpS | 4:2 FTS | 6:2 FTS | HFPO-DA | ADONA | PFAS K_{D+} | |
| R_{S1} | 2.0 | 4.7 | 1.2 | 1.8 | 1.6 | 1.4 | 7.7 | |
| Travel time S1 (d) | 4.0 | 9.4 | 2.4 | 3.6 | 3.2 | 2.8 | 15.4 | |
| R_{S2} | 2.0 | 4.7 | 1.4 | 2.5 | 2.1 | 1.7 | 7.7 | |
| Travel time S2 (d) | 4.0 | 9.4 | 2.8 | 5.0 | 4.2 | 3.4 | 15.4 | |

A PFBS value of $1.7 \cdot 10^{-2}$ L/kg was used as a parameter in the transport model at the basin scale (D3.7). This value aligns with the equivalent K_D assessment made in this study when taking into account the deeper layer considered and the scale effect. The K_D of PFBS was $6.8 \cdot 10^{-2}$ L/kg in the deepest superficial layer, which is consistent with the assessment done at the basin scale in D3.7. This difference is also consistent with an upscaling between batch scale and field scale, as it was observed for the Stengården case study. Therefore, the K_D values of larger models, which incorporate more and deeper layers, reflect a scale effect. This effect can be particularly significant if hydraulic conditions result in different behavior (e.g., higher or lower pore velocities) compared to the first layers considered.

As in the Besòs case study, travel times to the first aquifer are low (less than 15 days). However, in this case, this situation occurs even in a natural area, with worst-case conditions. This highlights the need for particular attention to both natural and anthropogenic areas.

5.3 Conclusion on the groundwater risk assessment at the Athens case study

For the **Athens case study**, the **groundwater intrinsic vulnerability varied by location**. Various pollution sources are present in the Athens case study, and the groundwater specific vulnerability assessment focused on **PFAS** in this case study. Batch experiments yielded consistent results with those from the Besòs case study, indicating that PFAS are mobile to very mobile substances in this soil. Therefore, **there is a high risk that PFAS reach groundwater**. The modeling indicated PFAS travel times of 2 to 15 days. As in the Besòs case study, travel times to the first aquifer are short (less than 15 days). However, in Athens, this situation occurs even in a natural area, with worst-case conditions. This highlights the need for particular attention to both natural and anthropogenic areas.

6 Pollutant priority lists

6.1 Confirmation of current priority list (IDAEA, IWW-FO)

According to the monitoring results from the three case studies of the UPWATER project, several chemicals and groups of chemicals listed in the current priority list were confirmed as priority pollutants. The pollutants are presented in Table 26. In Stengården, no priority pollutants were found.

Table 26: UPWATER confirmation of Priority Compounds

| Chemical (Cas No) | Concern | Detection in UPWATER case studies |
|-------------------------------|--|--|
| PFOS (2795-39-3) | The lowest PNEC in freshwater is 0.072 µg/L. No PMT rating is available. | Athens: Detected in all wells in the first campaign at concentrations up to 3.5 µg/L. Detected in 27/33 wells in the second campaign at maximum concentrations of linear and branched PFOS of 2.3 and 0.1 µg/L, respectively. Besòs: Detected in all wells in 3/4 analysed CPS campaigns and in all but one well in the remaining campaign. Minimum concentrations ranged from 0.0034 to 0.0096 µg/L. Maximum concentrations ranged from 0.059 to 0.087 µg/L. |
| PFOA (335-67-1) | The lowest PNEC in freshwater is 0.178 µg/L. No PMT rating is available. | Athens: Detected in 84 - 94% of all wells in the two sampling campaigns at maximum concentrations of 0.055- 0.135 µg/L. The lowest concentrations ranged from 0.003 to 0.0115 µg/L. Besòs: Detected in all wells in 2/4 analysed CPS campaigns and 7/11 to 12/13 wells in the remaining two campaigns. Minimum concentrations ranged from 0.0021 to 0.0102 µg/L. Maximum concentrations ranged from 0.0184 to 0.0921 µg/L. |
| PFHxS (3871-99-6) | The lowest PNEC in freshwater is 0.15 µg/L. No PMT rating is available. | Athens: Detected in all wells of the first campaign with one well showing a very high concentration of 46.4 µg/L. Detected in 20/33 wells in the second campaign with max. concentrations of linear and branched PFHxS of 0.036 and 0.09 µg/L, respectively. Besòs: Detected in all wells of 3/4 CPS campaigns and in all but one well in the remaining campaign at concentrations ranging from 0.00019 to 0.0253 µg/L. |
| PFHxA (307-24-4) | The lowest PNEC in freshwater is 140 µg/L. No PMT rating is available. | Athens: Detected in 80 - 89% of all wells in the two sampling campaigns at maximum concentrations of 0.066- 0.316 µg/L. The lowest concentrations ranged from 0.0008 to 0.008 µg/L. |
| PFPeS (630402-22-1) | A PNEC and PMT rating is not available for PFPeS. | Athens: Detected in 50% of all wells in the first grab sampling campaign at concentrations ranging from 0.004 to 0.08 µg/L. |
| PFBS (29420-49-3) | The PNEC in freshwater is 0.45 µg/L. PMT compound ranked | Besòs: Detected in all wells in all campaigns at concentrations ranging from 0.0007 to 0.657 µg/L. |

| Chemical (Cas No) | Concern | Detection in UPWATER case studies |
|--------------------------------|---|---|
| | as 'very persistent, very mobile'. | |
| PFNA (375-95-1) | The lowest PNEC in freshwater is 1 µg/L. No PMT rating is available. | Athens: Detected in 73 - 74% of all wells in both sampling campaigns. Minimum concentrations ranged from 0.0009 to 0.001 µg/L. Maximum concentrations ranged from 0.016 to 0.03 µg/L. Besòs: Detected in all wells in the first CPS campaign and in 11/14 wells to 12/14 wells in the remaining three campaigns. Concentrations ranged from 0.00011 to 0.0233 µg/L. |
| PFBA (375-22-4) | The lowest PNEC in freshwater is 27.8 µg/L. No PMT rating is available. | Athens: Detected in all wells of the first grab sampling campaign at concentrations ranging from 0.04 to 0.74 µg/L. |
| Cadmium (7440-43-9) | The lowest PNEC in freshwater is 0.08 µg/L. Identified as a substance that tends to accumulate in sediment and/or biota. A PMT rating is not available. | Athens: Not detected in the first DGT sampling campaign but in 20 - 33% of the wells in the following campaigns. Maximum concentrations ranged from 0.03 to 1.2 µg/L and minimum concentrations ranged from 0.01 to 0.26 µg/L. Besòs: Detected in all wells in sampling campaigns 2 and 3, not detected in campaign 1. The lowest concentrations ranged from 0.01 to 1.2 µg/L and the highest concentrations ranged from 0.14-4.7 µg/L |
| Lead (7439-92-1) | The lowest PNEC in freshwater of 1.2 µg/L. Identified as a substance that tends to accumulate in sediment and/or biota. A PMT rating is not available. | Athens: Detected in all wells in the three analysed DGT sampling campaigns at minimum concentrations ranging from 0.01 to 0.03 µg/L and maximum concentrations ranging from 0.25 to 43.7 µg/L. Besòs: Detected in only 2/20 wells in the first campaign at concentrations ranging from 1.1-2.5 µg/L but in all wells in the two subsequent campaigns at concentrations ranging from 0.08-3.1 µg/L. |
| Mercury (7439-97-6) | Identified as a substance that tends to accumulate in sediment and/or biota. A PMT rating is not available, nor is the PNEC. | Besòs: Detected at concentrations ranging from 0.01-0.61 in all wells in 2/2 campaigns. |
| Nitrate (14797-55-8) | Nitrate is on the current priority list with a quality standard 50 mg/L. PMT rating or PNEC are not available. | Athens: Detected in all or close to all wells in all three sampling campaigns at concentrations ranging from 0.018 to 111 mg/L. Besòs: Detected in all or close to all wells in all three sampling campaigns at concentrations ranging from 0.1 to 87 mg/L. |

| Chemical (Cas No) | Concern | Detection in UPWATER case studies |
|--------------------------------------|---|--|
| Atrazine (1912-24-9) | Ranked as very persistent and very mobile and as persistent, mobile and toxic. The lowest PNEC in freshwater is 0.6 µg/L. The UBA PMT emission index for atrazine is medium. | Besòs: Detected in 15/21 wells in the first campaign but only in 2 - 5 wells in the next campaigns. Concentrations ranged from 0.002 to 0.005 µg/L. |
| Isoproturon (34123-59-6) | The lowest PNEC in freshwater of 0.3 µg/L. A PMT rating is not available. | Besòs: Detected in close to all wells in all three campaigns at maximum concentrations ranging from 0.035 - 0.063 µg/L. The lowest concentrations ranged from 0.0003 to 0.00104 µg/L. |
| Imidacloprid (138261-41-3) | The lowest PNEC in freshwater is 0.0068 µg/L. A PMT rating is not available. | Besòs: Detected in 71 - 85% of all wells, depending on sampling campaign, at concentrations ranging from 0.002 to 0.049 µg/L. |
| Ibuprofen (15687-27-1) | The lowest PNEC in freshwater is 0.011 µg/L. Ibuprofen is ranked as persistent and very mobile and as persistent, mobile and toxic. The UBA PMT emission index for ibuprofen is medium. | Besòs: Detected in 14/21 wells in the first campaign but only in 1 - 2 wells in the next campaigns. Concentrations ranged from 0.001 to 1.21 µg/L. |
| Bisphenol A (80-05-7) | The lowest PNEC in freshwater is 0.24 µg/L. A PMT rating is not available. | Besòs: Detected in 19/21 wells in the first UPWATER sampling campaign at concentrations up to 10.06 µg/L. Sampling campaign 2 and 3 measured both lower maximum concentrations (0.3 - 0.4 µg/L) and lower detection frequency (6 - 10/17 wells). The lowest concentrations ranged from 0.001-0.02 µg/L. |
| Diuron (330-54-1) | Diuron has a PMT rating and is 'very persistent very mobile'. The lowest PNEC in freshwater is 49 ng/L. The emission rating for diuron is 'very high'. | Besòs: Detected in all sampling campaigns in ¼ of the wells or more at concentrations ranging from 2 to 80 ng/L. |
| Diclofenac (15307-86-5) | The lowest PNEC in freshwater is 0.04 µg/L. A PMT | Besòs: Detected in all three campaigns in about ¾ of the wells. The lowest concentrations measured ranged from 0.006 to 0.009 µg/L. The highest concentrations ranged from 0.1-2.8 µg/L. |

| Chemical (Cas No) | Concern | Detection in UPWATER case studies |
|---------------------------------------|---|--|
| | rating is not available. | |
| Sulfamethoxazole (723-46-6) | The lowest PNEC in freshwater is 0.6 µg/L. A PMT rating is not available. | Besòs: Detected in all three sampling campaigns in ½ to ¾ of all wells with the lowest concentrations ranging from 0.0016 to 0.002 µg/L and the highest concentrations ranging from 0.03 to 0.058 µg/L. |
| Carbamazepine (298-46-4) | The lowest PNEC in freshwater is 2 µg/L. A PMT rating is not available. | Athens: Detected in 89% percent of all wells in the first campaign and in 58% in the second campaign at maximum concentrations of 0.165 - 0.223 µg/L. Minimum concentrations ranged from 0.0007 - 0.003 µg/L. Besòs: Detected in all three sampling campaigns in all or more than ¾ of all wells. The lowest concentrations range from 0.3 to 3 ng/L while the highest concentrations reached levels of 0.04 - 0.08 µg/L. |

6.2 Recommendation for uptake into the current priority list (IDAEA, IWW-FO)

A range of PMT compounds were quantified at high frequency and/or high concentration in the three case studies, suggesting that these compounds should be included in the priority list (see Table 27). We furthermore recommend all 53 PMT / very persistent, very mobile (vPvM) chemicals for uptake into the priority list that are included in the Substitute It Now (SIN) list (<https://sinlist.chemsec.org/>). The SIN list is a list of hazardous chemicals that pose a threat to human health and the environment and are used in a wide variety of articles, products, and manufacturing processes around the globe. It is based on the criteria defined within REACH, the EU chemicals legislation. UPWATER supports this recommended phasing out of particularly hazardous chemicals that threaten the environment, hence our recommendation to include these chemicals in the priority list. Four of the eight compounds we recommend overlap with the SIN list (benzotriazole, melamine, tris(chloropropyl) phosphate (TCCP), trifluoromethanesulfonic acid).

Results for the persistent virus HAdV differed between case studies, with Athens showing a low detection frequency of 18%, whereas the campaigns in the Besòs showed presence of this virus in 50% of all wells (in Stengården virus contamination is insignificant and was not monitored). An uptake into the priority list would be warranted if virus-infected groundwater were used for drinking water purposes. When used for irrigation and street cleaning purposes, the risk of infection is reduced.

Table 27: UPWATER recommendation to Priority list additions

| Chemical (Cas No) | Use | Concern | Detection in UPWATER case studies |
|--|---|--|--|
| Benzotriazole (95-14-7) | Industrial chemical used in lubricants and greases, washing & cleaning products, heat transfer fluids, anti-freeze products and coating products. In addition, manufacture of machinery and vehicles, fabricated metal products and plastic products) | Degrades slowly in the environment, transports easily in water and is hard to remove in water treatment plants, and toxic. PMT and vPvM. The UBA PMT emission index for benzotriazole is 'very high'. The lowest PNEC for freshwater is 97 µg/L. | Athens: Detected in 18 - 63% of all wells at maximum concentrations of 0.08 - 0.27 µg/L. The lowest concentrations ranged from 0.0027 - 0.006 µg/L. |
| Losartan (114798-26-4) | Pharmaceutical | Ranked as vPvM and PMT. The UBA PMT emission index for losartan is very high. The lowest PNEC in freshwater is 78 µg/L. | Besòs: Detected in 33 - 38% of all wells throughout the sampling campaigns at concentrations ranging from 0.0014 to 0.151 µg/L. |
| Tris(chloropropyl) phosphate (TCCP) (13674-84-5) | industrial chemical used in coating products, laboratory chemicals, leather treatment products, plastic and rubber products. | Ranked as very persistent and very mobile. The lowest PNEC in freshwater is 260 µg/L. The UBA PMT emission index for TCCP is medium. | Besòs: Detected in 11/21 wells in the first campaign and in 14 - 25% in the following campaigns. Minimum concentrations ranged from 0.065 µg/L to 0.136 µg/L. Maximum concentrations ranged from 0.16 µg/L to 5.37 µg/L. |
| 2,4-dichlorophenol (120-83-2) | pesticide metabolite, component in biocidal applications, general industrial intermediate, degradation of pharmaceuticals, etc.). | The PMT rating for 2,4-dichlorophenol is vPvM and PMT. The UBA PMT Reach Emission Index is low. | Stengården: Detected in 7/10 wells in sampling campaign 1 and in 5/9 wells in sampling campaign 2. The lowest concentrations ranged from 0.06 to 0.07 µg/L and the highest concentrations ranged from 0.33 to 0.44 µg/L. Besòs: Detected in 19 - 75% of all wells, depending on sampling campaign. The lowest concentrations ranged from 0.003 to 0.005 µg/L and the highest concentrations ranged from 0.10 to 4.81 µg/L, where the highest concentrations exceed the lowest PNEC in freshwater of 4.2 µg/L. |
| 4-chloro-2-methylphenol | pesticide (mecoprop) metabolite) | The PMT rating for 4-chloro-2-methylphenol is vPvM and | Stengården: Detected in 9/10 wells in sampling campaign 1 |

| Chemical (Cas No) | Use | Concern | Detection in UPWATER case studies |
|--|--|--|--|
| (1570-64-5) | | PMT. The lowest PNEC in freshwater is 2.57 µg/L. The UBA PMT Reach Emission Index is low. | and in 5/9 wells in sampling campaign 2. The lowest concentrations ranged from 0.04 to 0.4 µg/L and the highest concentrations ranged from 3.9 to 7.0 µg/L. |
| Metformin (657-24-9) | pharmaceutical | Metformin is rated PMT. The lowest PNEC in freshwater is 160 µg/L. The UBA PMT emission index for metformin is very high | Besòs: Detected in all sampling campaigns in ¾-½ of the wells with the lowest concentrations ranging from 0.001 to 0.005 µg/L and the highest concentrations ranging from 0.022 to 6.6 µg/L |
| Melamine (108-78-1) | industrial chemical | Melamine is rated vPvM. The lowest PNEC in freshwater is 360 µg/L. The UBA PMT Reach Emission index is 'very high'. | Besòs: Detected in all three campaigns in all wells. The lowest concentrations measured ranged from 6 to 118 ng/L, depending on the sampling campaign. The highest concentrations ranged from 2 to 3.9 µg/L |
| Trifluoromethane sulfonic acid (1493-13-5) | industrial chemical used in laboratory chemicals, paint, coating, air fresheners and fire fighting foam. | Trifluoromethane sulfonic acid is rated as vPvM. The UBA PMT Reach Emission index is 'very high'. The lowest PNEC in freshwater is 142.3 µg/L. | Besòs: Detected in all or close to all wells in the three sampling campaigns at concentrations ranging from 0.0026 to 0.7 µg/L. |

6.3 Recommendation for further research into chemical PMT properties (IDAEA, IWW-FO)

A range of chemicals were detected at high frequency and/or high concentration for which PMT data and, in some instances, PNEC data are currently lacking, see Table 28. PMT and missing PNEC data for these compounds should be determined urgently to better determine whether these compounds constitute an environmental threat.

Table 28: UPWATER recommendation to further investigation of persistence, mobility, and toxicity.

| Chemical (Cas No) | Use | Concern | Detection in UPWATER case studies |
|--|---------------------------|--|--|
| Acridone (578-95-0) | Industrial chemical | Lowest PNEC in freshwater: 0.39 µg/L. PMT data not available. | Besòs: Detected in all wells in the first campaign and in 38-50% in the following campaigns. Minimum concentrations ranged from 0.010 µg/L to 0.055 µg/L. Maximum concentrations ranged from 0.85 µg/L to 1.08 µg/L. |
| Valsartan (137862-53-4) | pharmaceutical | Lowest PNEC in freshwater: 560 µg/L. PMT data not available. | Besòs: Detected in all or close to all wells in the three sampling campaigns at concentrations ranging from 0.0087 to 0.68 µg/L. |
| Valsartan acid (164265-78-5) | pharmaceutical metabolite | Lowest PNEC in freshwater: 320 µg/L. PMT data not available. | Besòs: Detected in about ¼ of all wells in the three sampling campaigns at concentrations ranging from 0.005 to 0.78 µg/L. |
| Gabapentin (60142-96-3) | pharmaceutical | Lowest PNEC in freshwater: 1000 µg/L. PMT data not available. | Besòs: only measured in first campaign but was detected in 20 out of 21 wells at concentrations ranging from 0.002 to 2.5 µg/L. |
| Levetiracetam (102767-28-2) | pharmaceutical | Lowest PNEC in freshwater: 38 µg/L. PMT data not available. | Besòs: Detected in 50% of all wells in the first campaign at concentrations ranging from 0.002 to 9.99 µg/L. Was not measured in following campaigns. |
| Carbendazim (10505-21-7) | Pesticide and biocide | Carcinogenic, mutagenic and toxic to reproduction. Lowest PNEC in freshwater: 0.44 µg/L. PMT data not available. | Besòs: Detected in 17/21 wells in the first campaign at concentrations ranging from 0.007 to 2.12 µg/L. Could not be measured in following campaigns due to a method error. |
| Alprazolam (28981-97-7) | pharmaceutical | Lowest PNEC in freshwater: 0.077 µg/L. PMT data not available. | Besòs: Detected in all wells in the first campaign and in 75-79% in the following campaigns. Minimum concentrations ranged from 0.0014 µg/L to 0.0019 µg/L. Maximum concentrations ranged from 0.005 µg/L to 0.70 µg/L. |
| Lamotrigine (84057-84-1) | pharmaceutical | Lowest PNEC in freshwater: 8 µg/L. PMT data not available. | Athens: Detected in 63% of all wells in the first campaign at concentrations ranging from 0.004 to 0.11 µg/L. Was not measured in following campaign. |

| Chemical (Cas No) | Use | Concern | Detection in UPWATER case studies |
|---|--|--|--|
| Topiramate (97240-79-4) | pharmaceutical | Lowest PNEC in freshwater and PMT data not available. | Athens: Detected in 52% of all wells in the first campaign at concentrations ranging from 0.019 to 0.18 µg/L. Was not measured in following campaign. |
| Carbamazepin e-10,11-epoxide (36507-30-9) | pharmaceutical metabolite | Lowest PNEC in freshwater: 2.6 µg/L. PMT data not available. | Athens: Detected in 9/19 wells in the first sampling campaign at concentrations that range from 0.00094 to 0.0089 µg/L. Not measured in the second campaign. |
| Prometon (1610-18-0) | pesticide | Lowest PNEC in freshwater: 0.05 µg/L. PMT data not available. | Besòs: Detected in 11/21 wells in the first campaign at concentrations ranging from 0.002 to 0.57 µg/L. Could not be measured in following campaigns due to a method error. |
| Fipronil sulphide (120067-83-6) | pesticide metabolite | Lowest PNEC in freshwater: 0.012 µg/L. PMT data not available. | Besòs: Detected in 50% of all wells in all sampling campaigns, at concentrations ranging from 0.001 to 0.012 µg/L. |
| Bisphenol S (80-09-01) | Industrial chemical used in plastics, in epoxy glue, as an anticorrosive and in paper. | Lowest PNEC in freshwater: 12.88 µg/L. PMT rating not available. | Besòs: Detected in 57-95% of all wells, depending on sampling campaign. Concentrations ranged from 0.0001 to 0.26 µg/L. |
| Caffeine (58-08-2) | active ingredient in coffee and tea | Lowest PNEC in freshwater: 1.2 µg/L. PMT data not available. | Besòs: Detected in all wells in the first and third campaign, and 71% of all wells in the second campaign. Concentrations ranged from 0.003 to 0.064 µg/L. A PMT rating is not available. Athens: Detected in 89% of all wells in the first campaign at concentrations ranging from 0.003 to 0.063 µg/L. Detected in only 1 out of 33 wells in the second campaign. |
| Nicotine (58-08-2) | active ingredient in tobacco | Lowest PNEC in freshwater: 5.45 µg/L. PMT data not available. | Besòs: Detected in all wells in the first campaign and in 71-88% of all wells in the second and third campaign. Concentrations ranged from 0.0006 to 6.10 µg/L. A PMT rating is not available. Athens: Detected in 63% of all wells in the first campaign at concentrations ranging from 0.004 to 0.11 µg/L. Was not measured in following campaign. |
| Cotinine (486-56-6) | metabolite of nicotine | PNEC and PMT data not available. | Besòs: Detected in all wells in first campaign at 0.0003-0.5909 µg/L, and in the majority of the wells in the second and third campaigns with a |

| Chemical (Cas No) | Use | Concern | Detection in UPWATER case studies |
|---|----------------------|---|---|
| | | | maximum concentration of 0.0097 µg/L. Athens: Detected in all wells in the first grab sampling campaign at concentrations of 0.000834-0.00638 µg/L. |
| Cyclamate (139-05-9) | artificial sweetener | Lowest PNEC in freshwater: 18.5 µg/L . PMT data not available. | Besòs: Detected in 48-81% of all wells, depending on sampling campaign, at concentrations ranging from 0.003 to 2.96 µg/L. |
| Saccharin (81-07-2) | artificial sweetener | Lowest PNEC in freshwater: 12.88 µg/L. PMT data not available. | Besòs: Detected in 14-81% of all wells in the first two sampling campaigns. Not detected in the third campaign. Concentrations ranged from 0.0002 to 54.62 µg/L. |
| Acesulfame (33665-90-6) | artificial sweetener | Lowest PNEC in freshwater: 72.4 µg/L. PMT data not available. | Besòs: Detected in all wells in the first sampling campaign and 38-57% of all wells in the second and third sampling campaign. Minimum concentrations ranged from 0.0024 µg/L to 0.042 µg/L. Maximum concentrations ranged from 0.162 µg/L to 0.575 µg/L. |
| N,N-diethyl-metatoluamide (DEET) (134-62-3) | pesticide | Lowest PNEC in freshwater: 88 µg/L. PMT data not available. | Besòs: Detected in 64-100% of all wells, depending on sampling campaign, at concentrations ranging from 0.003 to 5.07 µg/L. Athens: Detected in 74% of all wells in the first campaign at concentrations ranging from 0.003 to 1.04 µg/L. A PMT rating is not available. |
| Simazine (122-34-9) | pesticide | Lowest PNEC in freshwater: 1 µg/L. PMT data not available. | Besòs: Detected in all or about ¾ of all wells in the three sampling campaigns at concentrations ranging from 0.0007 to 0.0298 µg/L. |
| Tebuconazole (107534-96-3) | pesticide | Lowest PNEC and PMT data in freshwater not available. | Besòs: Detected in all wells in the first campaign, and 29-43% of all wells in the two next campaigns. Concentrations ranged from 0.0006 to 0.22 µg/L. |
| Dichlorprop (120-36-5) | pesticide | Lowest PNEC in freshwater: 1 µg/L. PMT data not available. | Stengården: Detected in 7/10 wells in sampling campaign 1 and in 7/9 wells in sampling campaign 2. The lowest concentration measured was 0.02 µg/L and the highest concentrations ranged from 0.42-1.18 µg/L. |
| Mecoprop (93-65-2) | pesticide | Lowest PNEC in freshwater: 0.8 µg/L. PMT | Stengården: Detected in 9/10 wells in sampling campaign 1 and in 7/9 wells in sampling campaign 2. The lowest |

| Chemical (Cas No) | Use | Concern | Detection in UPWATER case studies |
|--|---|---|---|
| | | data not available. | concentrations ranged from 0.06 to 0.07 µg/L and the highest concentrations ranged from 2.7 to 3.5 µg/L. |
| 4-chlorophenol (106-48-9) | pesticide metabolite, component in biocidal applications, general industrial intermediate, degradation of pharmaceuticals | Lowest PNEC in freshwater: 2 µg/L. PMT data not available. | Stengården: Detected in 9/10 wells in sampling campaign 1 and in 6/9 wells in sampling campaign 2. The lowest concentrations ranged from 0.12 to 2.55 µg/L and the highest concentrations ranged from 7.9-11.9 µg/L. |
| 4-chlorophenoxypropionic acid (4-CPP) (3307-29-9) | pesticide metabolite | Lowest PNEC in freshwater: 11 µg/L. PMT data not available. | Stengården: Detected in 9/10 wells in sampling campaign 1 and in 5/9 wells in sampling campaign 2. The lowest concentrations ranged from 0.01 to 0.08 µg/L and the highest concentrations ranged from 0.12 to 6.96 µg/L. |
| 2-(2-chlorophenoxy)propionic acid (2-CPP) (25140-86-7) | pesticide metabolite | Lowest PNEC in freshwater: not available. PMT data not available. | Stengården: Detected in 9/10 wells in sampling campaign 1 and in 6/9 wells in sampling campaign 2. The lowest concentrations ranged from 0.06 to 0.72 µg/L and the highest concentrations ranged from 4.3-5.5 µg/L. |
| 2-(2-methylphenoxy)propanoic acid (2-MMP) (943-45-3) | pesticide metabolite | Lowest PNEC in freshwater: 28.3 µg/L. PMT data not available. | Stengården: Detected in 9/10 wells in sampling campaign 1 and in 6/9 wells in sampling campaign 2. The lowest concentrations ranged from 0.06 to 0.08 µg/L and the highest concentrations ranged from 0.24-0.28 µg/L. |
| Barium (7440-39-3) | heavy metal | Lowest PNEC in freshwater: 19 µg/L. PMT data not available. | Besòs: Detected in all wells in all sampling campaigns where the lowest concentrations ranged from 15 to 50 µg/L and the highest concentrations ranged from 99 to 110 µg/L. Athens: Detected in all wells in sampling campaign 1 at concentrations ranging from 4.18-13.38 µg/L. Not measured in subsequent campaigns. |
| Zinc (7440-66-5) | heavy metal | Lowest PNEC in freshwater: 7.8 µg/L. PMT data not available. | Besòs: Detected in all wells in all samplings campaigns at concentrations ranging from 3 to 94.9 µg/L. Athens: Detected in all wells in all three DGT sampling campaigns at concentrations ranging from 0.08 to 28.2 µg/L. |

| Chemical (Cas No) | Use | Concern | Detection in UPWATER case studies |
|---------------------------------|-------------|--|---|
| Manganese (7439-96-5) | heavy metal | Lowest PNEC in freshwater: 123 µg/L. PMT data not available. | Besòs: Detected in all wells in sampling campaigns 2 and 3, and in ¾ of them in campaign 1. The lowest concentrations ranged from 0.01 to 1.7 µg/L and the highest concentrations ranged from 367-630 µg/L. Athens: Detected in all wells in all three DGT sampling campaigns at concentrations ranging from 0.02 to 27.22 µg/L. |
| Nickel (7449-02-0) | heavy metal | Lowest PNEC in freshwater: 2 µg/L. PMT data not available. | Besòs: Detected in all wells in all sampling campaigns at concentrations ranging from 0.4 to 6.8 µg/L. Athens: Detected in all wells in all three DGT sampling campaigns at concentrations ranging from 0.04 to 5.4 µg/L. |
| Cobalt (7440-48-4) | heavy metal | Lowest PNEC in freshwater: 0.28 µg/L. PMT data not available. | Besòs: Detected in all wells in sampling campaigns 2 and 3, and in half of them in campaign 1. The lowest concentrations ranged from 0.08 to 0.8 µg/L and the highest concentrations ranged from 2.3 to 2.5 µg/L. Athens: Detected in 66-85% of all wells in the three DGT sampling campaigns. The lowest concentrations ranged from 0.01 to 0.02 µg/L and the highest concentrations ranged from 0.08 to 0.22 µg/L. |
| Copper (7440-50-8) | heavy metal | Lowest PNEC in freshwater: 1 µg/L. PMT data not available. | Besòs: Detected in all wells in sampling campaigns 2 and 3, and in half of them in campaign 1. The lowest concentrations ranged from 0.76 to 2.8 µg/L and the highest concentrations ranged from 6.7-9.8 µg/L. Athens: Detected in all wells in all three DGT sampling campaigns. The lowest concentrations ranged from 0.02 to 0.04 µg/L and the highest concentrations ranged from 3.0-5.1 µg/L. |
| Uranium (7440-61-1) | heavy metal | Lowest PNEC in freshwater: 0.015 µg/L. PMT data not available. | Athens: Detected in all wells in all three DGT sampling campaigns at concentrations ranging from 0.01 to 1.1 µg/L. |
| Chromium (7440-47-3) | heavy metal | Lowest PNEC in freshwater: 3.4 µg/L. PMT data not available. | Besòs: Detected in all wells in sampling campaigns 2 and 3, and in 1/4 of them in campaign 1. The lowest concentrations ranged from 0.2 to 20.9 |

| Chemical (Cas No) | Use | Concern | Detection in UPWATER case studies |
|----------------------|-----|---------|---|
| | | | <p>µg/L and the highest concentrations ranged from 10.0-16.4 µg/L.</p> <p>Athens: Detected in all wells in all three DGT campaigns at concentrations ranging from 0.02 to 0.66 µg/L.</p> |

6.4 Potential pollution sources (IDAEA, IWW-FO, AU)

Main pollution sources and stressors were identified in the frame of task 5.1 and presented in D5.1 (see Table 10 of D5.1 "Source/stressor list"). In this paragraph, some specific sources of pollutants identified in the frame of the UPWATER project are presented. These are examples, and precise identification should be completed with national databases, such as the ActiviPoll database in France (<https://ssp-infoterre.brgm.fr/fr/base-de-donnees/bd-activipoll>) and DVGW W-254 (2021); DVGW W-101 (2021) in Germany.

Heavy metals may be released from diffuse sources such as geogenic sources, losses of oil or lubricant from machines used in agriculture and horticulture, forestry and hunting, the mining industry, and military equipment, as well as pesticide or manure application in similar sectors. Point sources include leakage from landfill sites, biogas plants, and contaminated sites (DVGW W-254, 2021; DVGW W-101, 2021).

Nitrate originates from agricultural (especially manure spreading) and horticultural activities, and to a lesser degree from forestry and hunting.

Pharmaceuticals and their degradation products usually originate from wastewater either due to exfiltration from the sewer systems or infiltration of surface water with a high fraction of wastewater into groundwater (from storage containers, accidents related to the use of anaerobic digesters, leaking pipes), as well as the application of pharmaceuticals to fish ponds (DVGW W-254, 2021; DVGW W-101, 2021). Diffuse sources include patient and animal excretion (antibiotics) and agricultural runoff (antibiotics after manure spreading).

Industrial chemicals may originate from diffuse sources from the mining industry, such as drilling fluids and oil, cooling water, and lubricant losses from machines (DVGW W-254, 2021; DVGW W-101, 2021). Point sources include, amongst other sources, landfills, leaking sewage systems, and wastewater treatment plants, usage of (treated) wastewater for irrigation, improper disposal of chemical toilet water in campsites, and improper application of fertilizer and pesticides in sports facilities (DVGW W-254, 2021; DVGW W-101, 2021). Contaminants leaching from point sources such as derelict industrial sites and landfills include chlorinated solvents, chlorinated phenols, amines, PAHs, etc. The leakage of heating oil and facade drainage from residential buildings (DVGW W-254, 2021; DVGW W-101, 2021) may be considered diffuse or point source, depending on whether it is coming from a specific, identifiable location like a pipe, vent, or a single, contained spill point.

PFAS in particular originate primarily from landfills, fire drill sites, and direct industrial use (outphasing), but could also be from improper waste management.

Sweeteners, personal care compounds, and flame retardants typically stem from sewer leakage.

Current and derelict **pesticides and their degradation products** may stem from both diffuse sources (e.g., agriculture, horticulture, forestry, private gardens, golf courses, campsites, protection of infrastructures such as houses and railways) and point sources (e.g., dumpsites such as Stengården, accidental spills and leaks from pesticides storage sites) (DVGW W-254,

2021; DVGW W-101, 2021). Pesticides banned in agriculture often still find application in urban gardening. **Biocides** may leach from urban surfaces.

7 Identification of risk mitigation measures to meet targeted ecological environmental protection goals (IDAEA)

To meet the targeted environmental protection goals and mitigate the risk of exposure to hazardous chemicals, UPWATER recommends to:

- 1) Accelerate the uptake of chemicals recommended by UPWATER into the priority list (Table 27 plus 49 additional PMT/vPvM chemicals from the SIN List) and prohibit or, as a minimum, further restrict their use, to decrease environmental concentrations of these hazardous chemicals faster and promote their substitution with more environmentally friendly chemicals.
- 2) Identify, characterize, and manage the pollution sources
- 3) When the pollution sources cannot be identified and managed, implementation of mitigation measures between sources and sensitive targets (e.g., pollutant immobilization).
- 4) For example, when this is applicable in a site-specific point of view, encapsulate PFAS and other pollution via application of surface and penetrative sealants to paved firefighting training surfaces and airfields to minimize PFAS leaching to groundwater. Alternatively, PFAS may be absorbed by additives or otherwise chemically bound (e.g., Douglas et al., 2023).
- 5) Implement the treatment of polluted groundwater and surface water by advanced treatment urgently. Nature-based solutions are likely to work for biodegradable compounds, previously immobilized. For more recalcitrant compounds, additional treatments such as ion exchange or advanced oxidation will be needed.

8 Conclusion and perspectives

For the **Stengården case study**, the **groundwater intrinsic vulnerability** was assessed as **moderate**, indicating that the groundwater at the Stengården case study is moderately vulnerable to subsurface pollution (buried waste in the clay layer). At Stengården, the aquifer is primarily polluted by pesticides, specifically mecoprop (MCP) and dichlorprop (DCPP), along with their respective metabolites. The concentrations of these contaminants in groundwater significantly exceed the drinking water limits. Some of these contaminants can be found on the EU priority list (2,4-Dichlorophenol, 2-Chloro-2-methylphenol) due to their high mobility, persistence, and toxicity. The polluted water of the site is affecting groundwater several kilometers away, moving towards drinking water abstraction sites for the city of Copenhagen and the town of Roskilde. Therefore, **pesticides and their metabolites were the focus of the groundwater risk assessment** for this case study. Results of batch and column experiments indicated that all pesticides and pesticide metabolites studied in the frame of this project were **mobile to very mobile** substances according to the PMT (persistent, mobile, and toxic) classification by the German environmental agency, UBA. Therefore, given the results of the intrinsic vulnerability analysis in this case study, **there is a high risk that pesticides and pesticide metabolites reach groundwater beyond the actual site**. The modeling indicated pollutant travel times of 96 to 143 days to reach the first aquifer. This is verified as these compounds are actually detected in the monitoring wells. Nevertheless, these travel times from waste buried in the clay layer to the first aquifer, estimated under worst-case conditions, leave sufficient time to adjust remediation solutions in case of a storm (heavy rain) event (more pumping at the wells/hydraulic trap already in place to treat the pesticides in groundwater, for example).

For the **Besòs case study**, the **groundwater intrinsic vulnerability** fell within the upper range of the **moderate** classification, indicating that groundwater in Besòs could be vulnerable to surface pollution. Various pollution sources are present in the Besòs case study, and UPWATER could confirm the presence of a long list of EU-priority contaminants in the Besòs aquifer, with a range of them detected in all or close to all wells (e.g., isoproturon, diclofenac, PFAS, mercury). In the frame of the UPWATER project, the aim was to produce new and innovative knowledge by focusing the groundwater risk assessment on a family of emerging pollutants that have not yet been considered in previous studies but could contribute to the global environmental and health risk. This approach will further enable the improvement of groundwater risk assessment by considering a broader range of pollutants. Although it was not explicitly planned in this task of the project, it will enable carrying out a more comprehensive human health risk assessment in future studies. This will help to strengthen the understanding of groundwater pollution. Regarding industrial activities in the area, it has been decided to focus the study of the groundwater specific vulnerability on **PFAS** (per- and polyfluoroalkyl substances). This choice was also influenced by growing international concerns about these substances, due to their persistence in the environment, their toxicity, and their mobility in soils. In theory, this means that they can easily reach groundwater. Results from batch experiments indicated that **PFAS are mobile to very mobile substances** according to the UBA classification. Given the results of both the intrinsic vulnerability analysis and the specific vulnerability study, **it can be concluded that there is a high risk at this case study that PFAS reach groundwater**. The modeling indicated PFAS travel times in the range of 5 hours to 13 days. PFAS travel times are fast (less than 15 days) and leave few possibilities of remediation after a storm event: it will be necessary to reduce the anthropogenic water infiltrations in the contaminated area, to reduce the risk of PFAS migration in soils and groundwater.

For the **Athens case study**, the **groundwater intrinsic vulnerability varied by location**. Areas with a significant depth to the water table, low permeability in the soil (both saturated and unsaturated zones), steep slopes, and low hydraulic conductivity displayed **low vulnerability** to surface pollution. Conversely, locations with a shallow depth to the water table, high permeability in the soil (saturated and unsaturated zones), gentle slopes, and high hydraulic conductivity were found to be **highly vulnerable** to surface pollution. Various pollution sources are present in the Athens case study, and it appeared that the Athens groundwater was highly polluted by EU-priority list compounds such as PFAS, nitrate, lead, and carbamazepine. For the same reasons as the ones presented for the Besòs case study, the groundwater specific vulnerability assessment focused on **PFAS** in this case study. Batch experiments yielded consistent results with those from the Besòs case study, indicating that PFAS are mobile to very mobile substances in this soil. Therefore, based on the intrinsic vulnerability analysis and the specific vulnerability results from this case study, **there is a high risk that PFAS reach groundwater**. The modeling indicated PFAS travel times of 2 to 15 days. As in the Besòs case study, travel times to the first aquifer are short (less than 15 days). However, in Athens, this situation occurs even in a natural area, with unfavorable conditions. This highlights the need for particular attention to both natural and anthropogenic areas.

In addition, evaluating PFAS behaviour in two different soil types enhanced the understanding of their interactions with soils and groundwater. While the mobility of PFAS decreased as the carbon chain length increased, **long-chain PFAS can still be considered mobile in soils**. This means that they have the potential to form large pollution plumes in groundwater, which can reach sensitive targets, such as drinking water supply catchments. In addition, the results suggested that **soil organic matter may play a major role in the sorption of long-chain PFAS**, while the behaviour of short-chain PFAS appeared unaffected by a change in soil organic matter content. Other soil constituents may be responsible for their retention in soils. Complementary experiments are needed to further understand the main factors driving PFAS retention in soils, particularly in relation to their chemical structure.

Summing up the UPWATER monitoring activities in the case studies, we identify the need for uptake of eight further compounds into the EU priority list (benzotriazole, trifluoromethanesulfonic acid, melamine, metformin, 2-chloro-2-methylphenol, 2,4-dichlorophenol, losartan, and TCPP). Four of these eight compounds are on the *SIN list*, comprising high-use PMT/vPvM chemicals. We furthermore recommend all remaining 49 SIN list chemicals for uptake into the priority list, based on their especially high hazard to the environment.

Our results imply further strong restrictions on the use of PMT compounds, such as PFAS, to decrease environmental concentrations of these hazardous chemicals faster and promote their substitution with more environmentally friendly chemicals. The treatment of polluted groundwater by advanced treatment should proceed urgently to safeguard groundwater, environment, and human health. Nature-based solutions are likely to work for biodegradable compounds, but more recalcitrant compounds require additional treatments such as ion exchange or advanced oxidation.

9 References

- Ahrens, L., 2011. Polyfluoroalkyl compounds in the aquatic environment: a review of their occurrence and fate. *Journal of environmental monitoring* : JEM 13, 20-31.
- Ahrens, L., Norström, K., Viktor, T., Cousins, A.P., Josefsson, S., 2015. Stockholm Arlanda Airport as a source of per- and polyfluoroalkyl substances to water, sediment and fish. *Chemosphere* 129, 33-38.
- Albinet, M., Margat, J., 1970. Cartographie de la vulnérabilité à la pollution des nappes d'eau souterraine. *Bull. BRGM Paris* 2, ,3, 4, 13-22.
- Aller, L., Bennett, T., Lehr, J., Petty, R., Hackett, G., 1987. DRASTIC: Standardized system for evaluating groundwater pollution potential using hydrogeologic settings. *Journal of the Geological Society of India* 29,
- Argyaki, A., Kelepertzis, E., 2014. Urban soil geochemistry in Athens, Greece: The importance of local geology in controlling the distribution of potentially harmful trace elements. *Science of The Total Environment* 482-483, 366-377.
- Backe, W.J., Day, T.C., Field, J.A., 2013. Zwitterionic, Cationic, and Anionic Fluorinated Chemicals in Aqueous Film Forming Foam Formulations and Groundwater from U.S. Military Bases by Nonaqueous Large-Volume Injection HPLC-MS/MS. *Environmental Science & Technology* 47, 5226-5234.
- Baduel, C., Paxman, C.J., Mueller, J.F., 2015. Perfluoroalkyl substances in a firefighting training ground (FTG), distribution and potential future release. *Journal of Hazardous Materials* 296, 46-53.
- Bancheri, M., Coppola, A., Basile, A., 2021. A new transfer function model for the estimation of non-point-source solute travel times. *Journal of Hydrology* 598, 126157.
- Barna, R., Fernandez, A., Hlavackova, P., 2007. Assessment methodologies for copper and zinc mobility in a neutral synthetic soil: The influence of pH. *Colloids and Surfaces A: Physicochemical and Engineering Aspects* 306, 56-67.
- Barry, V., Winquist, A., Steenland, K., 2013. Perfluorooctanoic acid (PFOA) exposures and incident cancers among adults living near a chemical plant. *Environmental health perspectives* 121, 1313-1318.
- Battye, N., Patch, D., Koch, I., Monteith, R., Roberts, D., O'Connor, N., Kueper, B., Hulley, M., Weber, K., 2024. Mechanochemical degradation of per- and polyfluoroalkyl substances in soil using an industrial-scale horizontal ball mill with comparisons of key operational metrics. *Science of The Total Environment* 928, 172274.
- Bollmann, U.E., Fernández-Calviño, D., Brandt, K.K., Storgaard, M.S., Sanderson, H., Bester, K., 2017. Biocide Runoff from Building Facades: Degradation Kinetics in Soil. *Environmental Science & Technology* 51, 3694-3702.
- Brusseau, M., Anderson, R., Guo, B., 2020. PFAS concentrations in soils: Background levels versus contaminated sites. *Science of The Total Environment* 740, 140017.
- Buck, R.C., Franklin, J., Berger, U., Conder, J.M., Cousins, I.T., de Voogt, P., Jensen, A.A., Kannan, K., Mabury, S.A., van Leeuwen, S.P., 2011. Perfluoroalkyl and polyfluoroalkyl substances in the environment: Terminology, classification, and origins. *Integrated Environmental Assessment and Management* 7, 513-541.
- Campos Pereira, H., Ullberg, M., Kleja, D.B., Gustafsson, J.P., Ahrens, L., 2018. Sorption of perfluoroalkyl substances (PFASs) to an organic soil horizon – Effect of cation composition and pH. *Chemosphere* 207, 183-191.

Chronopoulos, J., Haidouti, C., Chronopoulou-Sereli, A., Massas, I., 1997. Variations in plant and soil lead and cadmium content in urban parks in Athens, Greece. *Science of The Total Environment* 196, 91-98.

Civita, M. (1994). Le carte della vulnerabilità degli acquiferi all'inquinamento. Teoria & pratica. Bologna, Pitagora.

Connell, L.D., Daele, G.v.d., 2003. A quantitative approach to aquifer vulnerability mapping. *Journal of Hydrology* 276, 71-88.

Corniello, A., Ducci, D., Napolitano, P. (1997). Comparison between parametric methods to evaluate aquifer pollution vulnerability using a GIS: an example in the 'Piana Campana', southern Italy.

Cousins, I.T., DeWitt, J.C., Glüge, J., Goldenman, G., Herzke, D., Lohmann, R., Miller, M., Ng, C.A., Scheringer, M., Vierke, L., Wang, Z., 2020. Strategies for grouping per- and polyfluoroalkyl substances (PFAS) to protect human and environmental health. *Environmental Science: Processes & Impacts* 22, 1444-1460.

Cui, D., Li, X., Quinete, N., 2020. Occurrence, fate, sources and toxicity of PFAS: What we know so far in Florida and major gaps. *TrAC Trends in Analytical Chemistry* 130, 115976.

Delolme, C., Hébrard-Labit, C., Spadini, L., Gaudet, J.-P., 2004. Experimental study and modeling of the transfer of zinc in a low reactive sand column in the presence of acetate. *J. Contam. Hydrol.* 70, 205-224.

Douglas, G.B., et al., *Sealants and Other Management Strategies for PFAS-Contaminated Concrete and Asphalt.* Current Pollution Reports, 2023. **9**(4): p. 603-622.

DVGW, 2021. *Technische Regel - Arbeitsblatt DVGW W 101 (A)*, Bonn: DVGW Deutscher Verein des Gas- und Wasserfaches e.V.

DVGW, 2021. *Technische Regel - Arbeitsblatt DVGW W 254 (A)*, Bonn: DVGE Deutscher Verein des Gas- und Wasserfaches e.V.

EC, 2022: Proposal for a Directive of the European Parliament and of the Council amending Directive 2000/60/EC establishing a framework for Community action in the field of water policy, Directive 2006/118/EC on the protection of groundwater against pollution and deterioration and Directive 2008/105/EC on environmental quality standards in the field of water policy. European Commission. Available at: <https://eur-lex.europa.eu/legal-content/EN/TXT/?uri=celex:52022PC0540>

Enell, A., Reichenberg, F., Warfvinge, P., Ewald, G., 2004. A column method for determination of leaching of polycyclic aromatic hydrocarbons from aged contaminated soil. *Chemosphere* 54, 707-715.

Filipovic, M., Woldegiorgis, A., Norström, K., Bibi, M., Lindberg, M., Österås, A.-H., 2015. Historical usage of aqueous film forming foam: A case study of the widespread distribution of perfluoroalkyl acids from a military airport to groundwater, lakes, soils and fish. *Chemosphere* 129, 39-45.

Finizio, A., Villa, S., 2002. Environmental risk assessment for pesticides: A tool for decision making. *Environmental Impact Assessment Review* 22, 235-248.

Frippiat, C.C., Holeyman, A.E., 2008. A comparative review of upscaling methods for solute transport in heterogeneous porous media. *Journal of Hydrology* 362, 150-176.

Frková, Z., Johansen, A., de Jonge, L.W., Olsen, P., Gosewinkel, U., Bester, K., 2016. Degradation and enantiomeric fractionation of mecoprop in soil previously exposed to phenoxy acid herbicides – New insights for bioremediation. *Science of The Total Environment* 569-570, 1457-1465.

- Fusco, F., Allocca, V., Coda, S., Cusano, D., Tufano, R., De Vita, P., 2020. Quantitative Assessment of Specific Vulnerability to Nitrate Pollution of Shallow Alluvial Aquifers by Process-Based and Empirical Approaches. *Water* 12, 269.
- Glover, C.M., Pazoki, F., Munoz, G., Sauvé, S., Liu, J., 2024. Applying the modified UV-activated TOP assay to complex matrices impacted by aqueous film-forming foams. *Science of The Total Environment* 924, 171292.
- Gogu, R.C., Dassargues, A., 2000. Current trends and future challenges in groundwater vulnerability assessment using overlay and index methods. *Environmental Geology* 39, 549-559.
- Guttman, J., Zuckerman, H. (1995). Flow model in the eastern basin of the Judea and Samaria hills. Tel Aviv, Israel, Tahal Consulting Engineers Ltd.
- Gyllenhammar, I., Berger, U., Sundström, M., McCleaf, P., Eurén, K., Eriksson, S., Ahlgren, S., Lignell, S., Aune, M., Kotova, N., Glynn, A., 2015. Influence of contaminated drinking water on perfluoroalkyl acid levels in human serum – A case study from Uppsala, Sweden. *Environmental Research* 140, 673-683.
- Hamid, H., Li, L.Y., Grace, J.R., 2020. Formation of perfluorocarboxylic acids from 6:2 fluorotelomer sulfonate (6:2 FTS) in landfill leachate: Role of microbial communities. *Environmental Pollution* 259, 113835.
- Herzke, D., Olsson, E., Posner, S., 2012. Perfluoroalkyl and polyfluoroalkyl substances (PFASs) in consumer products in Norway – A pilot study. *Chemosphere* 88, 980-987.
- Hiederer, R. (2013). Mapping Soil Properties for Europe -- - Spatial Representation of Soil Database Attributes.
- Houtz, E.F., Higgins, C.P., Field, J.A., Sedlak, D.L., 2013. Persistence of Perfluoroalkyl Acid Precursors in AFFF-Impacted Groundwater and Soil. *Environmental Science & Technology* 47, 8187-8195.
- Hubert, M., Arp, H.P.H., Hansen, M.C., Castro, G., Meyn, T., Asimakopoulos, A.G., Hale, S.E., 2023. Influence of grain size, organic carbon and organic matter residue content on the sorption of per- and polyfluoroalkyl substances in aqueous film forming foam contaminated soils - Implications for remediation using soil washing. *Science of The Total Environment* 875, 162668.
- Hunter Anderson, R., Adamson, D.T., Stroo, H.F., 2019. Partitioning of poly- and perfluoroalkyl substances from soil to groundwater within aqueous film-forming foam source zones. *Journal of Contaminant Hydrology* 220, 59-65.
- Kabiri, S., McLaughlin, M.J., 2021. Durability of sorption of per- and polyfluorinated alkyl substances in soils immobilized using common adsorbents: 2. Effects of repeated leaching, temperature extremes, ionic strength and competing ions. *Science of The Total Environment* 766, 144718.
- Kazakis, N., Voudouris, K.S., 2015. Groundwater vulnerability and pollution risk assessment of porous aquifers to nitrate: Modifying the DRASTIC method using quantitative parameters. *Journal of Hydrology* 525, 13-25.
- Kim, M., Kim, J., Hyun, S., 2012. Solubility of organic acids in various methanol and salt concentrations: The implication on organic acid sorption in a cosolvent system. *Chemosphere* 89, 262-268.
- Kleja, D.B., Campos-Pereira, H., Kikuchi-McIntosh, J., Pettersson, M., Golovko, O., Enell, A., 2025. Evaluation of Standardised (ISO) Leaching Tests for Assessing Leaching and Solid–Solution Partitioning of Perfluoroalkyl Substances (PFAS) in Soils. *Environments* 12, 179.
- Knight, E.R., Janik, L.J., Navarro, D.A., Kookana, R.S., McLaughlin, M.J., 2019. Predicting partitioning of radiolabelled 14C-PFOA in a range of soils using diffuse reflectance infrared spectroscopy. *Science of The Total Environment* 686, 505-513.

- Lanini, S., Caballero, Y., Seguin, J.-J., Maréchal, J.-C., 2016. ESPERE—A Multiple-Method Microsoft Excel Application for Estimating Aquifer Recharge. *Groundwater* 54, 155-156.
- Li, Y., Oliver, D.P., Kookana, R.S., 2018. A critical analysis of published data to discern the role of soil and sediment properties in determining sorption of per and polyfluoroalkyl substances (PFASs). *Science of The Total Environment* 628-629, 110-120.
- Liu, P., Zhu, D., Zhang, H., Shi, X., Sun, H., Dang, F., 2008. Sorption of polar and nonpolar aromatic compounds to four surface soils of eastern China. *Environmental Pollution* 156, 1053-1060.
- Lyakhlofi, S., Ouazzani, N., Hassani, L., Hebil, E.A.E. (1999). Impact de l'utilisation des eaux usées urbaines brutes sur la qualité de l'eau d'une nappe alluviale près de Marrakech (Maroc).
- Lyu, X., Liu, X., Wu, X., Sun, Y., Gao, B., Wu, J., 2020. Importance of Al/Fe oxyhydroxide coating and ionic strength in perfluorooctanoic acid (PFOA) transport in saturated porous media. *Water Research* 175, 115685.
- Machiwal, D., Jha, M.K., Singh, V.P., Mohan, C., 2018. Assessment and mapping of groundwater vulnerability to pollution: Current status and challenges. *Earth-Science Reviews* 185, 901-927.
- Mahmood-Ul-Hassan, M., Akhtar, M.S., Nabi, G., 2008. Boron and Zinc Transport Through Intact Columns of Calcareous Soils. *Pedosphere* 18, 524-532.
- Méndez, V., Holland, S., Bhardwaj, S., McDonald, J., Khan, S., O'Carroll, D., Pickford, R., Richards, S., O'Farrell, C., Coleman, N., Lee, M., Manefield, M.J., 2022. Aerobic biotransformation of 6:2 fluorotelomer sulfonate by *Dietzia aurantiaca* J3 under sulfur-limiting conditions. *Science of The Total Environment* 829, 154587.
- Meng, J., Wang, T., Song, S., Wang, P., Li, Q., Zhou, Y., Lu, Y., 2018. Tracing perfluoroalkyl substances (PFASs) in soils along the urbanizing coastal area of Bohai and Yellow Seas, China. *Environmental Pollution* 238, 404-412.
- Mesfin Tefera, Y., Gaskin, S., Mitchell, K., Springer, D., Mills, S., Pisaniello, D., 2022. Food grown on fire stations as a potential pathway for firefighters' exposure to per- and poly-fluoroalkyl substances (PFAS). *Environment International* 168, 107455.
- Milley, S.A., Koch, I., Fortin, P., Archer, J., Reynolds, D., Weber, K.P., 2018. Estimating the number of airports potentially contaminated with perfluoroalkyl and polyfluoroalkyl substances from aqueous film forming foam: A Canadian example. *Journal of Environmental Management* 222, 122-131.
- Moraru, C., Hannigan, R. (2018). Overview of Groundwater Vulnerability Assessment Methods. Analysis of Hydrogeochemical Vulnerability. C. Moraru and R. Hannigan. Cham, Springer International Publishing: 1-16.
- Naboulsi, A., Bouzid, T., Grich, A., Regti, A., El Himri, M., El Haddad, M., 2024. Understanding the column and batch adsorption mechanism of pesticide 2,4,5-T utilizing alginate-biomass hydrogel capsule: A computational and economic investigation. *International Journal of Biological Macromolecules* 275, 133762.
- National_Research_Council, 1993. Ground Water Vulnerability Assessment: Predicting Relative Contamination Potential Under Conditions of Uncertainty. The National Academies Press, Washington, DC
- Ochoa-Herrera, V., Field, J.A., Luna-Velasco, A., Sierra-Alvarez, R., 2016. Microbial toxicity and biodegradability of perfluorooctane sulfonate (PFOS) and shorter chain perfluoroalkyl and polyfluoroalkyl substances (PFASs). *Environmental Science: Processes & Impacts* 18, 1236-1246.
- OECD (2000). Guideline for the Testing of Chemicals No. 106: Adsorption–Desorption Using a Batch Equilibrium Method., Organisation for Economic Co-operation and Development.

- Ololade, I.A., Adeola, A.O., Oladoja, N.A., Ololade, O.O., Nwaolisa, S.U., Alabi, A.B., Ogungbe, I.V., 2018. In-situ modification of soil organic matter towards adsorption and desorption of phenol and its chlorinated derivatives. *Journal of Environmental Chemical Engineering* 6, 3485-3494.
- Overheu, N.D., Møller, M.G., Jepsen, T.S., Larsen, L.C., Thomsen, J., Tuxen, N. (2015). Tilvejebringelse af beslutnings-grundlag for den fremtidige af-værge på Stengårdens Losse-plads, ORBICON.
- Passarella, G., Masciale, R., Maggi, S., Vurro, M., Castrignanò, A. (2022). A Probabilistic Approach to Assess the Risk of Groundwater Quality Degradation. *Geospatial Technology for Human Well-Being and Health*. F. S. Faruque. Cham, Springer International Publishing: 379-401.
- Piwowarczyk, A.A., Holden, N.M., 2013. Phenoxyalkanoic acid herbicide sorption and the effect of co-application in a Haplic Cambisol with contrasting management. *Chemosphere* 90, 535-541.
- Rankin, K., Mabury, S.A., Jenkins, T.M., Washington, J.W., 2016. A North American and global survey of perfluoroalkyl substances in surface soils: Distribution patterns and mode of occurrence. *Chemosphere* 161, 333-341.
- Riise, G., Salbu, B., 1992. Mobility of dichlorprop in the soil-water system as a function of different environmental factors. I. A batch experiment. *Science of The Total Environment* 123-124, 399-409.
- Rodríguez-Cruz, M.S., Bælum, J., Shaw, L.J., Sørensen, S.R., Shi, S., Aspray, T., Jacobsen, C.S., Bending, G.D., 2010. Biodegradation of the herbicide mecoprop-p with soil depth and its relationship with class III tfdA genes. *Soil Biology and Biochemistry* 42, 32-39.
- Romero, E., Matallo, M.B., Peña, A., Sánchez-Rasero, F., Schmitt-Kopplin, P., Dios, G., 2001. Dissipation of racemic mecoprop and dichlorprop and their pure R-enantiomers in three calcareous soils with and without peat addition. *Environmental Pollution* 111, 209-215.
- Roskam, G.D., Comans, R.N.J., 2009. Availability and leaching of polycyclic aromatic hydrocarbons: Controlling processes and comparison of testing methods. *Waste Manage. (Oxford)* 29, 136-142.
- Schnebelen, N., Platel, J.P., Le Nindre, Y., Baudry, D. (2002). Gestion des Eaux Souterraines en Aquitaine - Année 5 - Etude Sectorielle ~ Protection de la nappe de l'Oligocène en région bordelaise - Nouvelles connaissances hydrogéologiques. Cartographie de la vulnérabilité aux pollutions, BRGM: 75.
- Shan, J., Xu, J., Zhou, W., Ji, L., Cui, Y., Guo, H., Ji, R., 2011. Enhancement of chlorophenol sorption on soil by geophagous earthworms (*Metaphire guillelmi*). *Chemosphere* 82, 156-162.
- Sharifan, H., Bagheri, M., Wang, D., Burken, J.G., Higgins, C.P., Liang, Y., Liu, J., Schaefer, C.E., Blotvogel, J., 2021. Fate and transport of per- and polyfluoroalkyl substances (PFASs) in the vadose zone. *Science of The Total Environment* 771, 145427.
- Shaw, D.M.J., Munoz, G., Bottos, E.M., Duy, S.V., Sauvé, S., Liu, J., Van Hamme, J.D., 2019. Degradation and defluorination of 6:2 fluorotelomer sulfonamidoalkyl betaine and 6:2 fluorotelomer sulfonate by *Gordonia* sp. strain NB4-1Y under sulfur-limiting conditions. *Science of The Total Environment* 647, 690-698.
- Shimabuku, K.K., Baumgardner, M.E., Bahr, R.B., Frojelin, N.R., Kennedy, A.M., Nolan, K.T., Stanton, N.E., 2023. Fluoride removal in batch and column systems using bonechar produced in a top-lit updraft drum gasifier and furnace. *Water Res.* 244, 120332.
- Sima, M.W., Jaffé, P.R., 2021. A critical review of modeling Poly- and Perfluoroalkyl Substances (PFAS) in the soil-water environment. *Science of The Total Environment* 757, 143793.
- Šimůnek, J., Angulo-Jaramillo, R., Schaap, M.G., Vandervaere, J.-P., Genuchten, M.T.v., 1998. Using an inverse method to estimate the hydraulic properties of crusted soils from tension-disc infiltrometer data. *Geoderma* 86, 61-81.

- Strynar, M.J., Lindstrom, A.B., Nakayama, S.F., Egeghy, P.P., Helfant, L.J., 2012. Pilot scale application of a method for the analysis of perfluorinated compounds in surface soils. *Chemosphere* 86, 252-257.
- Taghavi, N., Niven, R.K., Paull, D.J., Kramer, M., 2022. Groundwater vulnerability assessment: A review including new statistical and hybrid methods. *Science of The Total Environment* 822, 153486.
- Tang, L., Liu, X., Yang, G., Xia, J., Zhang, N., Wang, D., Deng, H., Mao, M., Li, X., Ni, B.-J., 2021. Spatial distribution, sources and risk assessment of perfluoroalkyl substances in surface soils of a representative densely urbanized and industrialized city of China. *CATENA* 198, 105059.
- Tubau, I., Vázquez-Suñé, E., Carrera, J., Valhondo, C., Criollo, R., 2017. Quantification of groundwater recharge in urban environments. *Science of The Total Environment* 592, 391-402.
- Turc, L., 1954. e bilan d'eau des sols: Relations entre les précipitations, l'évaporation et l'écoulement. *Annales Agronomiques* 5, 491-595.
- UBA (2019). Protecting the sources of our drinking water: The criteria for identifying persistent, mobile and toxic (PMT) substances and very persistent and very mobile (vPvM) substances under EU Regulation REACH (EC) No 1907/2006: 87.
- Uricchio, V.F., Giordano, R., Lopez, N., 2004. A fuzzy knowledge-based decision support system for groundwater pollution risk evaluation. *Journal of Environmental Management* 73, 189-197.
- Varnes, D.J., International Association of Engineering Geology Commission on, L., Other Mass Movements on, S. (1984). *Landslide hazard zonation : a review of principles and practice*. Paris, Unesco Paris.
- Vazquez-Sune, E. (2003). Urban groundwater. Barcelona city case study, UNIVERSITAT POLITÈCNICA DE CATALUNYA.
- Vázquez-Suñé, E., Ángel Marazuela, M., Velasco, V., Diviu, M., Pérez-Estaún, A., Álvarez-Marrón, J., 2016. A geological model for the management of subsurface data in the urban environment of Barcelona and surrounding area. *Solid Earth* 7, 1317-1329.
- Vrba, J., Zaporozec, A. (1994). Guidebook on mapping groundwater vulnerability. Hannover, H. Heise.
- Wang, Q., Zhao, Z., Ruan, Y., Li, J., Sun, H., Zhang, G., 2018. Occurrence and distribution of perfluorooctanoic acid (PFOA) and perfluorooctanesulfonic acid (PFOS) in natural forest soils: A nationwide study in China. *Science of The Total Environment* 645, 596-602.
- Wang, Y., Khan, N., Huang, D., Carroll, K.C., Brusseau, M.L., 2021. Transport of PFOS in aquifer sediment: Transport behavior and a distributed-sorption model. *Science of The Total Environment* 779, 146444.
- Winquist, A., Steenland, K., 2014a. Modeled PFOA exposure and coronary artery disease, hypertension, and high cholesterol in community and worker cohorts. *Environmental health perspectives* 122, 1299-1305.
- Winquist, A., Steenland, K., 2014b. Perfluorooctanoic acid exposure and thyroid disease in community and worker cohorts. *Epidemiology (Cambridge, Mass.)* 25, 255-264.
- Wu, S., Böhme, A., Ulrich, N., Chen, Z., Schäffer, A., Jahnke, A., 2025. The vertical migration of a pesticide mixture in sandy soil is strongly driven by their sorption behavior and can be altered by Polyethylene Microplastics. *Journal of Hazardous Materials* 494, 138511.
- Yan, P.-F., Dong, S., Manz, K.E., Woodcock, M.J., Liu, C., Mezzari, M.P., Abriola, L.M., Pennell, K.D., Cápiro, N.L., 2024. Aerobic biotransformation of 6:2 fluorotelomer sulfonate in soils from two aqueous film-forming foam (AFFF)-impacted sites. *Water Research* 249, 120941.
- Yang, L., Jin, M., Tong, C., Xie, S., 2013. Study of dynamic sorption and desorption of polycyclic aromatic hydrocarbons in silty-clay soil. *J. Hazard. Mater.* 244-245, 77-85.

Zhang, G., Pan, Z., Wu, Y., Shang, R., Zhou, X., Fan, Y., 2019. Distribution of Perfluorinated Compounds in Surface Water and Soil in Partial Areas of Shandong Province, China. Soil and Sediment Contamination: An International Journal 28, 502-512.

ANNEX 1 – DESCRIPTION OF THE INTRINSIC VULNERABILITY ASSESSMENT

A lot of methods have been published for groundwater intrinsic vulnerability assessment (GVA). **Overlay and index-based methods** (also called empirical or qualitative methods) are the first and most popular methods used for GVA (Moraru and Hannigan, 2018). These methods rely mostly on geological parameters. Scores or ratings are assigned to different parameters, providing by combination, a ranking of the aquifer vulnerability. Different methods have been developed for various types of aquifers. These methods are divided into **2 subgroups** (Gogu and Dassargues, 2000): hydrogeological complex and settings methods (**HCS methods**) and parametric system methods (**PS methods**). HCS methods imply a qualitative assessment of the vulnerability by linking hydrogeological, hydrographical, and morphological parameters that characterize the studied area. These methods are more suitable for large areas (Taghavi et al., 2022). PS methods are based on the selection of representative parameters for groundwater vulnerability assessment. The variation range of each parameter is divided into intervals to which specific values are assigned, reflecting the relative degree of sensitivity to pollution. Among the **PS methods**, the matrix systems (**MS**), the rating systems (**RS**), and the point count system models (**PCSM**) can be found. All PS methods rely on the same procedure. Representative parameters for groundwater vulnerability assessment are selected. The variation range of each parameter is divided into intervals assigned with specific values reflecting the relative degree of sensitivity to pollution. The **MS systems** rely on a restricted set of parameters, and the available methods are generally site-specific, developed for local, specific case studies. The degree of vulnerability is quantified by combining these parameters following several strategies specifically developed for each situation. The **RS systems** provide a fixed range of values for the relevant parameters used to assess groundwater vulnerability. Rating points are attributed to each interval, and the sum of rating points gives the evaluation. The rating systems are based upon the assumption of a generic pollutant. **PCSM** is also a rating parameter system. Additionally, a multiplier identified as a weight is assigned to each parameter to correctly reflect the relationship between the parameters. Rating parameters for each interval are multiplied accordingly with the weight factor, and the results are added to obtain the final score. The higher the score is, the greater the sensitivity of the area is.

Other methods can be used for GVA, such as **the process-based simulation methods**. These methods are based on the solution of conservation laws, including mass transport, heat transport, physics of solids, and constitutive relations to predict pollutant transport at both spatial and temporal scales (Machiwal et al., 2018). These methods were developed for GVA to take into account the hydrogeologic processes within the soil. However, the use of these methods has been limited due to their need for considerable field data, since they are not truly reliable when missing data needs to be estimated by indirect means.

Statistical methods are also used for GVA. They range from simple description statistics to complex regression analyses incorporating several predictor variables (Taghavi et al., 2022).

In the frame of the UPWATER project, **the DRASTIC method was selected** for assessing groundwater intrinsic vulnerability. This method was developed by the US EPA in 1985 (Aller et al., 1987). This method was selected in the frame of this project because it is now the most recognized method worldwide to assess groundwater intrinsic vulnerability (Taghavi et al., 2022; Kazakis and Voudouris, 2015) and it is mainly used at a small scale, which seems relevant as regard to the 3 case studies (Lyakhloufi et al., 1999). This is an index-based, parametric system and point count system method.

The DRASTIC method considers the following seven parameters: **D**epth to water, net **R**echarge, **A**quifer media, **S**oil media, **T**opography, **I**mpact of the vadose zone, and hydraulic **C**onductivity. Each parameter is classified either into ranges for continuous variables or into significant media types for thematic data, both having an impact on pollution potential. The typical rating range is from 1 to 10. Weight factors are used for each parameter to balance their importance. The final vulnerability index (D_i) is calculated as a weighted sum of the seven parameters and can be computed using the following equation:

$$D_i = \sum_{j=1}^7 W_j \times R_j$$

with D_i the DRASTIC index

W_j the weight factor for parameter j

R_j the rating for parameter j

The **D**epth to water refers to the depth of the water table. It determines the depth of material through which a pollutant has to travel before reaching the aquifer and, therefore, helps to determine the time needed to reach groundwater. There is a greater chance for attenuation to occur as the depth of the water table increases, because the travel time will be longer, and will allow adsorption, dispersion, degradation and other attenuation processes.

The net **R**echarge indicates the amount of water per unit area that penetrates the ground surface and reaches the water table. This recharge water may transfer pollutants vertically to the water table. Therefore, the greater the recharge, the greater the potential for pollution. Irrigation or artificial recharge may enhance net recharge and should be taken into account when evaluating this parameter.

Aquifer media refers to the consolidated or unconsolidated medium that serves as an aquifer. An aquifer is defined as a rock formation that will yield sufficient quantities of water for use (Aller et al., 1987). The larger the grain size and the more fractures or openings within the aquifer, the higher the permeability and the lower the attenuation capacity, consequently leading to a higher pollution potential.

Soil media refers to the uppermost portion of the unsaturated zone. It will have an impact on the amount of recharge that can infiltrate into the ground and, therefore, on the ability of a pollutant to move downward.

Topography refers to the slope and slope variability of the land surface. It will control the likelihood that a pollutant can run off or remain on the surface before infiltrating.

Impact of vadose zone refers to the attenuation characteristics of the material below the uppermost portion of the unsaturated zone and above the water table.

Hydraulic **C**onductivity refers to the ability of the aquifer to transmit water. Hydraulic conductivity is controlled by the amount and interconnection of void spaces within the aquifer, which may occur as a consequence of factors such as intergranular porosity, fracturing, and bedding planes.

These seven DRASTIC parameters have been assigned a relative weight ranging from 1 to 5, corresponding to the relative importance of each parameter with respect to the others, in terms of groundwater vulnerability. These weights are presented in Table 29.

Table 29: Weights assigned to DRASTIC parameters

| Parameter | Weight |
|---------------------------------------|--------|
| Depth to water | 5 |
| Net recharge | 4 |
| Aquifer media | 3 |
| Soil media | 2 |
| Topography | 1 |
| Impact of vadose zone | 5 |
| Hydraulic conductivity of the aquifer | 3 |

In addition, each DRASTIC parameter has been divided into ranges or significant media types that may have an impact on pollution potential. Each range for each DRASTIC parameter has been evaluated to assign a rating to it, varying between 1 and 10. The D, R, S, T, and C parameters have been assigned one value per range (see Table 30). The A and I parameters have been assigned a typical rating and a variable rating. The variable rating allows the user to choose either a typical value or to adjust the value based on more specific knowledge (see Table 31 and Table 32). In the frame of the UPWATER project, in order to be able to compare the DRASTIC ranking of the 3 case studies, the typical ratings were used.

In addition, the DRASTIC method provides two weight classifications, one for “normal” conditions and the other for conditions with intense agricultural activity. In the frame of the UPWATER project, the classification related to “normal” conditions was used. Even if pesticides will be considered at the Stengården case study, it will be inappropriate, given the use of the site (see chapter 0), to classify it as an intensive agricultural activity area.

Table 30: Ranges and ratings for the D, R, S, T, and C DRASTIC parameters

| Rating | D | R | S | T | C |
|--------|--------------------|------------------------|-------------------------------------|----------------------|------------------------------|
| | Depth to water (m) | Net recharge (mm/year) | Soil media | Topography (% slope) | Hydraulic conductivity (m/d) |
| 1 | > 31 | < 50 | Nonshrinking and nonaggregated clay | > 18 | 0.04 - 4 |
| 2 | 23 - 31 | | Muck | | 4 - 12 |
| 3 | 15 - 23 | 50 - 100 | Clay loam | 12 - 18 | |
| 4 | | | Silty loam | | 12 - 29 |
| 5 | 9 - 15 | | Loam | 6 - 12 | |
| 6 | | 100 - 180 | Sandy loam | | 29 - 41 |
| 7 | 4.5 - 9 | | Shrinking and/or aggregated clay | | |
| 8 | | 180 - 250 | Peat | | 41 - 82 |
| 9 | 1.5 - 4.5 | > 250 | Sand | 2 - 6 | |
| 10 | < 1.5 | | Thin or absent / Gravel | < 2 | > 82 |

The DRASTIC index provides a relative evaluation tool, allowing for the identification of areas that are more susceptible to groundwater pollution than others. Nevertheless, in order to facilitate the result interpretation, some users divided the final index into vulnerability classes (Cornielo et al., 1997). These authors have ranked vulnerability as low (index < 106), moderate (106<index<186), high (186<index<210) and very high (index>210), such as in another PSCM method, the SINTACS method, which was derived from the DRASTIC method by Italian hydrogeologists, to be adapted to a larger scale as regard to the hydrogeological diversity of Italy (Civita, 1994). This ranking of vulnerability classes was applied in the UPWATER project.

Table 31: Ranges and ratings for the A parameter

| Range | Rating | Typical rating |
|---|--------|----------------|
| Massive shale | 1 - 3 | 2 |
| Metamorphic/Igneous | 2 - 5 | 3 |
| Weathered Metamorphic/Igneous | 3 - 5 | 4 |
| Thin bedded sandstone, limestone, shale sequences | 5 - 9 | 6 |
| Massive sandstone | 4 - 9 | 6 |
| Massive limestone | 4 - 9 | 6 |
| Sand and gravel | 4 - 9 | 8 |
| Basalt | 2 - 10 | 9 |
| Karst limestone | 9 - 10 | 10 |

This first step of the groundwater risk assessment applied to each case study will therefore provide a first overview of the groundwater sensitivity to surface pollution based only on the intrinsic parameters of the soil, which is a general insight into its possibility to be polluted by any pollutants. Then, a specific groundwater risk assessment will be conducted, applied to a specific pollutant group, selected for each case study as regard to the compounds quantified in soil and in groundwater. This will correspond to the groundwater specific vulnerability assessment.

Table 32: Ranges and ratings for the I parameter

| Range | Rating | Typical rating |
|--|--------|----------------|
| Silt/clay | 1 - 2 | 1 |
| Shale | 2 - 5 | 3 |
| Limestone | 2 - 7 | 6 |
| Sandstone | 4 - 8 | 6 |
| Bedded limestone, sandstone shale | 4 - 8 | 6 |
| Sand and gravel with significant silt and clay | 4 - 8 | 6 |
| Metamorphic/igneous | 2 - 8 | 4 |
| Sand and gravel | 6 - 9 | 8 |
| Basalt | 2 - 10 | 9 |
| Karst limestone | 8 - 10 | 10 |

ANNEX 2 – INTRINSIC VULNERABILITY ASSESSMENT AT THE STENGÅRDEN CASE STUDY

DRASTIC parameters and their corresponding ratings, applied for the Stengården case study, are presented in Table 33.

Table 33: DRASTIC parameters and corresponding ratings for the Stengården case study

| Parameter | Range | Rating | Weight |
|------------------------|-------------------------------------|--------|--------|
| Depth to water | 15-23 | 3 | 5 |
| Net recharge | > 250 | 9 | 4 |
| | Impact assessment of this parameter | | |
| | 100 - 180 | 6 | |
| | 180 - 250 | 8 | |
| Aquifer media | Sand and gravel | 8 | 3 |
| Soil media | Sandy loam | 6 | 2 |
| Topography | <2 | 10 | 1 |
| Impact of vadose zone | Sand and gravel | 8 | 5 |
| Hydraulic conductivity | 4 - 12 | 2 | 3 |

In the Stengården case study, the **depth to water** is between 16 and 19 m. This corresponds to the DRASTIC range 15-23 m, with a rating of 3.

The **net recharge** was calculated using the Microsoft Excel application ESPERE (Lanini et al., 2016). It includes several commonly used methods that are run simultaneously to estimate the recharge of an aquifer. The available data for this calculation were the daily precipitation and temperature from 2009 to 2023, obtained from the weather station of Roskilde (10 km from the site). The slope of the land surface is close to 0, which is why we estimated that all the rain will infiltrate. Given these available data, two empirical methods could be used with the Microsoft Excel application ESPERE: the one proposed by Turc (Turc, 1954) and the one proposed by Guttman and Zuckerman (Guttman and Zuckerman, 1995). Both methods gave similar results. The mean net recharge calculated for 15 years (from 2009 to 2023) was 262 ± 84 mm/year, meaning a rating between 6 and 9, considering the uncertainty related to this value. The minimum net recharge was 117 mm, calculated for 2018, meaning a rating of 6. The maximum was 427 mm for 2023, meaning a rating of 9. In the frame of the UPWATER project, a rating of 9, which corresponds to the mean net recharge (262 mm), was used. Calculations were also done with the ratings of 6 and 8, in order to assess the impact of this parameter on the groundwater intrinsic vulnerability.

In Stengården, the **aquifer, soil, and unsaturated zone media** are composed of the same material, namely sandy loam. This range is only available for the **soil media** (S parameter) in the DRASTIC method

and corresponds to a rating of 6. The range of the DRASTIC A parameter, which could best describe the type of **aquifer media** present in the Stengården case study, is therefore “sand and gravel”, with a rating varying between 4 and 9. The larger the grain size and the more fractures or openings within the aquifer, the higher the permeability and the higher the rating, leading to a higher pollution potential. Therefore, a rating of 9 for this parameter means a medium with large pore size or fractures, mainly composed of gravel. On the other hand, a rating of 4 means that the medium is mainly composed of sand or fine material, with a small pore size. For the aquifer media in Stengården, the typical rating of 8 was therefore chosen, which is consistent with the soil granulometry analysis (see Table 2).

The **topography**, referring to the slope of the land surface, is close to 0 at Stengården. Therefore, the range of this parameter was chosen to <2 and the corresponding rating was 10.

The same range and the same rating for the **impact of vadose zone** parameter as for the aquifer media were chosen, i.e., “sand and gravel” with a rating of 8.

Given that the aquifer material observed on site is sandy loam, the **hydraulic conductivity** at the Stengården case study could be approached by the one calculated for sand and implemented in the hydrogeological model (see deliverable D4.1). This hydraulic conductivity is between 10^{-4} and 2.5×10^{-3} m/s, corresponding to 8.64 and 216 m/d, respectively. As the aquifer material is not pure sand, it would not be relevant to use the higher hydraulic conductivity in the DRASTIC index calculation. The lower value of 8.64 m/d seems more significant in this case. It corresponds to the DRASTIC range 4-12 m/d with a rating of 2.

With these ratings and weights of the different DRASTIC parameters, the calculated DRASTIC index for the Stengården case study is:

$$D = 143$$

In addition, two more DRASTIC indexes can be calculated to evaluate the impact of the net recharge on the value:

$$D_{100-180} = 131$$

$$D_{180-250} = 139$$

where $D_{100-180}$ is the DRASTIC index calculated with a net recharge between 100 and 180 mm/y, and $D_{180-250}$ is the DRASTIC index calculated with a net recharge between 180 and 250 mm/y.

The DRASTIC indexes calculated fall in the moderate vulnerability class. This first analysis shows that groundwater at the Stengården case study is moderately vulnerable to surface pollution. This will be further evaluated by assessing the specific groundwater vulnerability at this case study.

ANNEX 3 – INTRINSIC VULNERABILITY ASSESSMENT AT THE BESÒS CASE STUDY

DRASTIC parameters and their corresponding ratings, applied for the Besòs case study, are presented in Table 34.

In the area of the Besòs case study, the **depth to water** is between 3 and 15 m, which covers three ranges (1.5 – 4.5 m / 4.5 – 9 m / 9 – 15 m) and three DRASTIC ratings (9 / 7 / 5). Therefore, two DRASTIC indexes will be calculated with the minimum and maximum of these ratings. This will allow us to evaluate the weight of this parameter and to see if these different ratings for the depth to water will lead to different vulnerability classes.

The **net recharge** was extracted from the numerical flow and solute transport model of the Barcelona aquifers, used by the Catalan Water Authority for groundwater management purposes (Tubau et al., 2017; Vázquez-Suñé et al., 2016). It covers two DRASTIC ranges (180-250 mm/y and >250 mm/y), associated with a rating of 8 and 9, respectively.

In Besòs, the **aquifer media** is made of deltaic deposits (gravel, silts, and sands). The range of the DRASTIC A parameter, which could best describe the type of **aquifer media** present in the Besòs case study, is therefore “sand and gravel”, with a rating varying between 4 and 9 and a typical rating of 8. Given the geology, the typical rating of 8 can be considered as a conservative hypothesis when calculating the risk for groundwater to be reached by pollutants.

As the Besòs case study is located in an urban area, the **soil media** parameter, as defined by the DRASTIC method, is mainly made of non-permeable materials, such as concrete. These non-permeable zones lead to no or little water infiltration, meaning that a low rating should be attributed for the DRASTIC index calculation. For this parameter, a relevant rating could be 1, corresponding to the “nonshrinking and nonaggregated clay” range for this parameter.

The **topography**, referring to the slope of the land surface, is very smooth and usually less than 1% at Besòs. Therefore, the range of this parameter was chosen to <2 and the corresponding rating was 10.

In Besòs, the **vadose zone** is composed of sand, gravel, and clay. The range of the DRASTIC I parameter, which could best describe the type of vadose zone, is “Sand and gravel with significant silt and clay”, with a rating between 4 and 8. For this parameter, the typical rating of 6 was chosen for the same reason as for the choice of the typical rating for the aquifer media.

The **hydraulic conductivity** was extracted from the numerical flow and solute transport model of the Barcelona aquifers, used by Catalan Water Authority for groundwater management purposes (Tubau et al., 2017; Vázquez-Suñé et al., 2016). It covers two DRASTIC ranges (4-12 m/d and 12-29 m/d), associated with a rating of 2 and 4, respectively.

Table 34: DRASTIC parameters and corresponding ratings for the Besòs case study

| Parameter | Range | Rating | Weight |
|------------------------|--|--------|--------|
| Depth to water | 1.5 – 4.5 | 9 | 5 |
| | 9 – 15 | 5 | |
| Net recharge | 180-250 | 8 | 4 |
| | >250 | 9 | |
| Aquifer media | Sand and gravel | 8 | 3 |
| Soil media | Nonshrinking and nonaggregated clay | 1 | 2 |
| Topography | <2 | 10 | 1 |
| Impact of vadose zone | Sand and gravel with significant silt and clay | 6 | 5 |
| Hydraulic conductivity | 4-12 | 2 | 3 |
| | 12-29 | 4 | |

With these ratings and weights of the different DRASTIC parameters, two DRASTIC indexes were calculated: D_{min} , which is the minimum DRASTIC index calculated with the minimum rating for parameters with different ratings, and D_{max} , which is the maximum DRASTIC index calculated with the maximum rating for the same parameters.

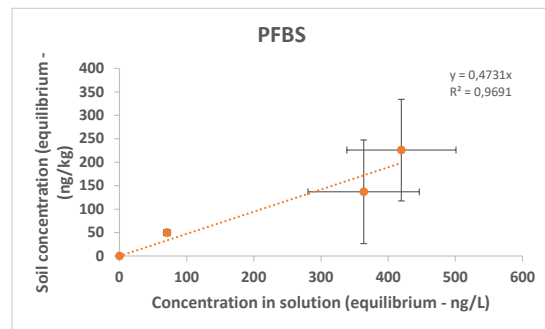
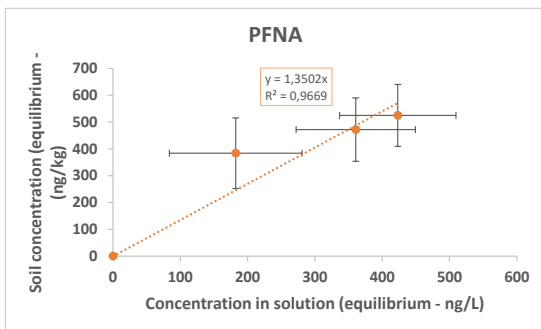
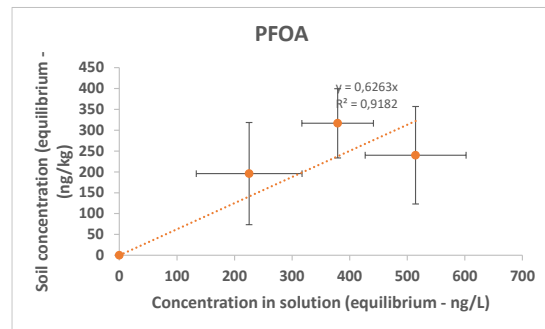
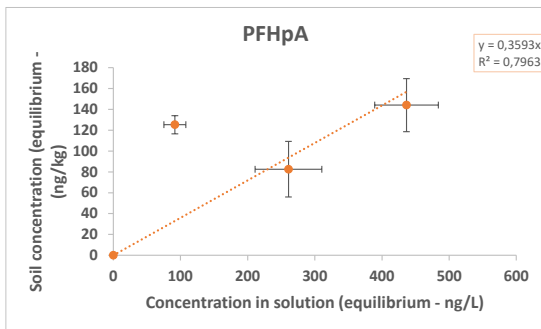
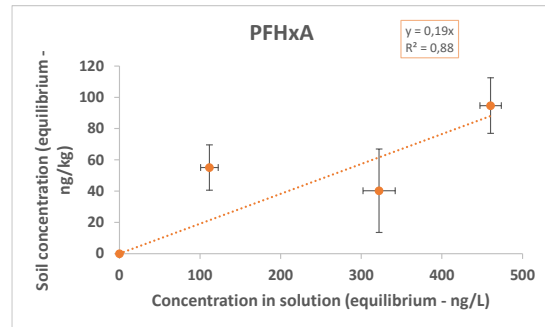
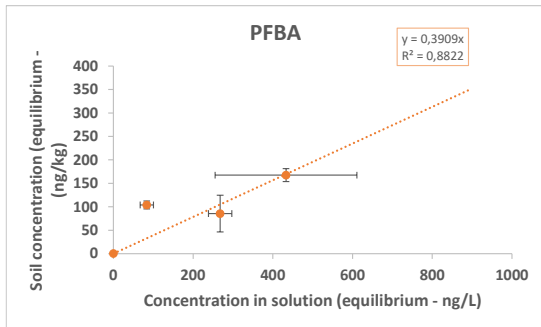
Therefore, for the Besòs case study,

$$D_{min} = 129$$

$$D_{max} = 159$$

These two DRASTIC indexes correspond to a moderate vulnerability (DRASTIC index between 106 and 186). If D_{max} is considered, this value is in the upper range of the moderate vulnerability class. As the intrinsic vulnerability evaluation shows that groundwater in the Besòs case study could be vulnerable to surface pollution, it seems relevant to assess the specific vulnerability associated with specific pollutants that can be found in the Besòs case study to evaluate the risk for groundwater to be polluted by these specific pollutants.

ANNEX 4 – SORPTION ISOTHERMS DERIVED FROM THE BCN SOIL SAMPLE



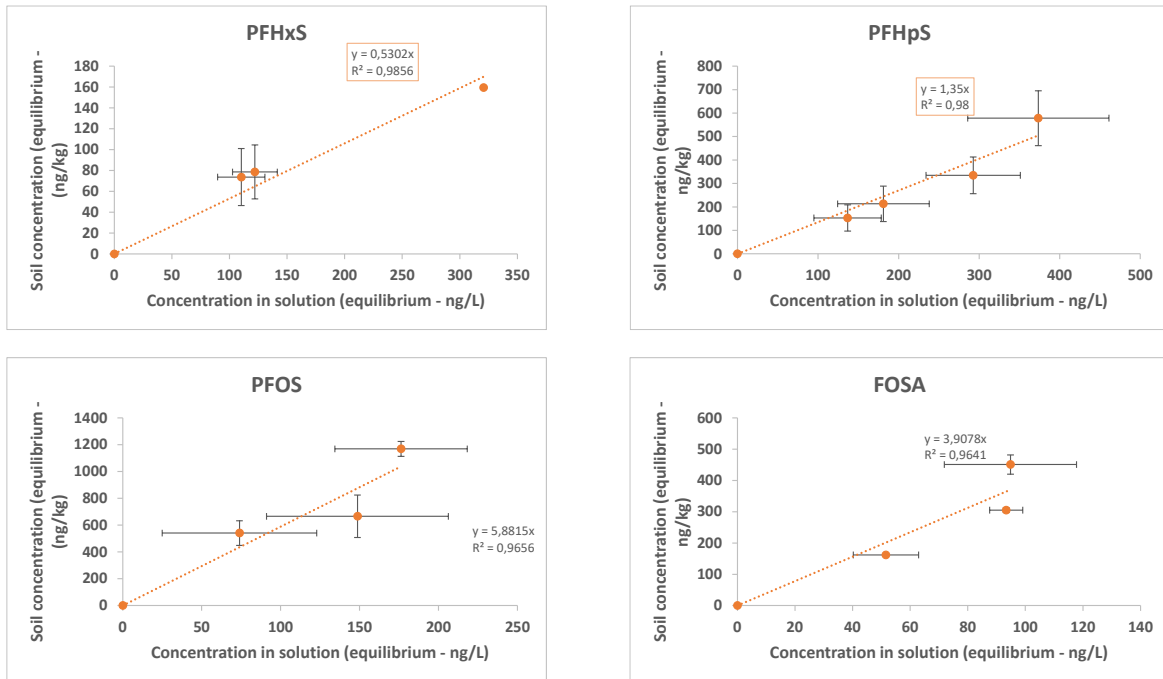


Figure 23: Sorption isotherms derived from the BCN soil sample

LIST OF FIGURES

| | |
|---|-----|
| Figure 1: Breakthrough curve of the studied pollutants (sorption/desorption of the mixed compound solution) | 22 |
| Figure 2: MCPP and DCPP breakthrough curves (sorption/desorption of the solution containing MCPP and DCPP)..... | 24 |
| Figure 3: Degradation of MCPP and DCPP | 25 |
| Figure 4: Conceptual model for pesticide transport modeling from pollution source to the first aquifer at the landfill scale (Stengården case study)..... | 27 |
| Figure 5: Simulated breakthrough curves for pesticides and pesticide metabolites (Stengården case study, K_D derived from column experiments) | 29 |
| Figure 6: Simulated breakthrough curves for pesticides and pesticide metabolites (Stengården case study, K_D derived from batch experiments) | 30 |
| Figure 7: Effect of degradation on the breakthrough curves of MCPP and DCPP (Stengården case study, K_D derived from column experiments) | 30 |
| Figure 8: Soil cross-section (sampling location of BCN soil sample in Sept. 2023)..... | 33 |
| Figure 9: Total PFAS concentrations in the three samples (S1-S3) of the Besòs soil..... | 37 |
| Figure 10: PFCA and PFSA concentrations in samples S1 and S2..... | 37 |
| Figure 11: PFAS families quantified in BCN-2 soil sample and concentrations of PFAS from the DWD .. | 40 |
| Figure 12: PFAS release from BCN-2 soil sample | 45 |
| Figure 13: PFAS sorption isotherms on BCN soil sample..... | 48 |
| Figure 14: Conceptual model for PFAS transport modeling from pollution source to the first aquifer (Besòs case study) | 51 |
| Figure 15: Simulated breakthrough curves of the PFAS studied (Besòs case Study - K_D from batch sorption) | 52 |
| Figure 16: Simulated breakthrough curves of PFNA, PFOS, and 8:2 FTS with sorption and desorption partitioning coefficients (Besòs case study) | 53 |
| Figure 17: Soil sample location at the Athens case study..... | 57 |
| Figure 18: PFAS sorption isotherms on CSA soil sample | 61 |
| Figure 19: Parameters used for the Athens soil column and conceptual models | 65 |
| Figure 20: Conceptual model: decrease of the TOC with soil depth (Athens case study)..... | 67 |
| Figure 21: Simulated breakthrough curves of PFAS (Athens case study) - 6 layers | 68 |
| Figure 22: Breakthrough curves of PFAS (Athens case study – reduced influence of OC on some PFAS) | 70 |
| Figure 23: Sorption isotherms derived from the BCN soil sample | 106 |

LIST OF TABLES

| | |
|---|----|
| Table 1: Pesticides and metabolites addressed in the frame of the UPWATER project – Stengården case study | 15 |
| Table 2: Soil physical and chemical characteristics – Stengården soil | 16 |
| Table 3: Soil-water partitioning coefficients (K_D) calculated after batch experiments | 20 |
| Table 4: Irreversibility of the sorption (sorption/desorption of the mixed compound solution) and comparison of K_D from batch and column experiments | 23 |
| Table 5: Comparison of the sorbed/desorbed mass of MCP and DCP in the frame of the 2 column experiments | 24 |
| Table 6: MCP and DCP half-lives under aerobic conditions | 26 |
| Table 7: Retardation factors and travel times for the pesticides and pesticide metabolites studied..... | 29 |
| Table 8: PFAS analysed in a first step in the Besòs soil samples | 35 |
| Table 9: PFAS content of the Besòs soil samples BCN, S1, S2, and S3 ($\mu\text{g}/\text{kg}$) | 36 |
| Table 10: Other PFAS measured in BCN-2 | 38 |
| Table 11: Soil physical and chemical characteristics | 42 |
| Table 12: Soil-water partitioning coefficients and soil organic carbon-water partitioning coefficients for PFAS released from the BCN-2 soil sample. | 46 |
| Table 13: Soil-water partitioning coefficients for the Besos case study | 48 |
| Table 14: Soil-water partitioning coefficients for the Besòs case study | 49 |
| Table 15: Retardation factors of the 18 PFAS studied in the Besòs case study..... | 52 |
| Table 16: DRASTIC parameters and corresponding ratings for the Athens case study..... | 54 |
| Table 17: PFAS content of the Athens soil samples S1 to S10 ($\mu\text{g}/\text{kg}$)..... | 59 |
| Table 18: Soil physical and chemical characteristics – CSA non-polluted soil | 60 |
| Table 19: Soil-water partitioning coefficients for the Athens case study | 62 |
| Table 20: Soil-water partitioning coefficients for the Athens case study | 63 |
| Table 21: Factors affecting the decrease in K_D in the different soil layers | 67 |
| Table 22: Equivalent K_D for the modeling (Athens case study)..... | 68 |
| Table 23: Retardation factors and travel times of PFAS for the Athens case study | 69 |
| Table 24: Equivalent K_D for the sensitivity analysis (Athens case study)..... | 70 |
| Table 25: Retardation factors and travel times of PFAS (Athens case study) – Sensitivity analysis..... | 71 |
| Table 26: UPWATER confirmation of Priority Compounds | 73 |
| Table 27: UPWATER recommendation to Priority list additions..... | 77 |
| Table 28: UPWATER recommendation to further investigation of persistence, mobility, and toxicity. | 79 |
| Table 29: Weights assigned to DRASTIC parameters..... | 97 |
| Table 30: Ranges and ratings for the D, R, S, T, and C DRASTIC parameters | 98 |

| | |
|--|-----|
| Table 31: Ranges and ratings for the A parameter | 99 |
| Table 32: Ranges and ratings for the I parameter..... | 100 |
| Table 33: DRASTIC parameters and corresponding ratings for the Stengården case study | 101 |
| Table 34: DRASTIC parameters and corresponding ratings for the Besòs case study | 104 |